The transcriptomic response of the cold-water coral *Desmophyllum dianthus* to experimental changes in pH

Sarina Niedzwiedz

Master Thesis

June 2021

Universität Bremen

ALFRED-WEGENER-INSTITUT
HELMHOLTZ-ZENTRUM FÜR POLAR-
UND MEERESFORSCHUNG

Title figure: *Desmophyllum dianthus* reef in the Chilean Comau fjord.

Photo by Thomas Heran, used with permission.

Title: The transcriptomic response of the cold-water corals *Desmophyllum dianthus* to experimental changes in pH

German title: Analyse der transkriptomischen Reaktion der Kaltwasserkoralle *Desmophyllum dianthus* auf experimentelle Änderungen des pH-Wertes

This study has been conducted at the Alfred Wegener Institute, Helmholtz Centre for Polar and Marine Research in Bremerhaven, Germany and the University of Bremen in Bremen, Germany.

Thesis Supervision: **Dr. Christoph Held**

Functional Ecology, Alfred Wegener Institute, Helmholtz Centre for Polar and Marine Research
Bremerhaven, Germany

Thesis Examiners:

First Examiner: **Prof. Dr. Björn Rost**

Marine BioGeoScience, Alfred Wegener Institute, Helmholtz Centre for Polar and Marine Research
Bremerhaven, Germany

Second Examiner: **Dr. Marlene Wall**

Experimental Benthic Ecology, Geomar, Helmholtz Centre for Ocean Research
Kiel, Germany

Bentho-Pelagic Processes, Alfred Wegener Institute, Helmholtz Centre for Polar and Marine Research
Bremerhaven, Germany

Table of contents

Zusammenfassung

Der pH-Wert des Meerwassers wird durch die Interaktion von verschiedenen physikalischen und biologischen Faktoren beeinflusst. Seit dem Beginn der Industrialisierung hat die steigende anthropogene Emission von Kohlenstoffdioxid (CO_2) einen zusätzlichen Einfluss auf den pH-Wert des Meerwassers, da atmosphärisches CO_2 mit Wassermolekülen reagieren kann. Bei dieser Reaktion werden Protonen frei, die zu einer Reduktion des pH Wertes führen (Ozeanversauerung; OA). Neben dem pH-Wert stellt die Aragonit Sättigung des Wassers einen biologisch relevanten Parameter zur Quantifizierung der OA dar, da er ein Maß für die „Leichtigkeit der Kalzifizierung" ist. Mit abnehmendem pH Wert, sinkt auch die Aragonit Sättigung des Wassers, wodurch kalzifizierende Organismen mehr Energie für die Bildung ihrer Kalzium Karbonat Strukturen aufwenden müssen. In kalten und tiefen Gewässern ist die Aragonit Sättigung aufgrund der erhöhten Löslichkeit von Aragonit besonders niedrig. Daher wurde lange davon ausgegangen, dass skleraktinische Kaltwasserkorallen (CWCs) zu den von der OA meist betroffenen Taxa gehören, da sich ein Großteil ihres Lebensraums auf Wassertemperaturen von 4–12 °C und Wassertiefen unter 50 m beschränkt. Allerdings kommen sie in einigen Bereichen des Ozeans in Aragonit ungesättigtem Wasser vor, was darauf hindeutet, dass sie in der Lage sind, die negativen Einflüsse von niedrigen Aragonit Sättigungswerten abzumildern. Ziel dieser Studie war es, Informationen über die Regulationen und Mechanismen zu gewinnen, die es der CWC *Desmophyllum dianthus* ermöglicht, unter niedrig pH Bedingungen zu überleben. Ein Verständnis dieser physiologischen und molekularen Prozesse wird dazu beitragen, die Entwicklung und zukünftige biogeographische Verbreitung von *D. dianthus* zu beurteilen.

Dazu wurden Korallen, die an einen pH-Wert von pH 8,0 akklimatisiert waren, zwei Wochen lang niedrigen pH-Bedingungen (pH 7,4) ausgesetzt, um ihre kurzfristige Anpassung an eine experimentelle Reduktion der pH-Bedingungen zu beurteilen. Danach wurde der pH-Wert für zwei Monate wieder auf pH 8,0 erhöht, um ihr Regenerationspotential zu ermitteln. Als Kontrolle dienten Korallen, die während des ganzen Versuches einem pH Wert von pH 8,0 ausgesetzt waren. Physiologische und transkriptomische Parameter wurden in verschiedenen Intervallen während des Experiments gemessen. Zusätzlich wurden die beobachteten Muster in der Genexpression mit Feldproben verglichen, die unter zwei verschiedenen pH-Bedingungen (pH 7,5; pH 7,8) gewachsen sind.

Die Ergebnisse dieser Studie deuten darauf hin, dass *D. dianthus* sehr tolerant gegenüber den hier untersuchten kurzfristigen Änderungen des Meerwasser-pH Werts ist. Während die Veränderungen des pH-Werts keinen signifikanten Einfluss auf die physiologischen Parameter hatten, deutete die dynamische Regulation des Transkriptoms auf ein phänotypisches Puffern ('phenotypic buffering') hin. Da weder eine pH-abhängige Veränderung der Kalzifizierungsraten, noch ein Unterschied in der Expression von Ionentransportern, die mit der Kalzifizierung assoziiert sind, festgestellt werden konnte,

wird davon ausgegangen wird, dass die veränderten pH Bedingungen keine negative Auswirkung auf die Kalzifizierung hatten. Allerdings wurde eine Herabregulierung von Genen, die für Zytoskeletelemente (Aktin und Tubulin) kodieren (Δ log2 fold change > 20), während der pH-Reduktion beobachtet. Dies könnte ein Indikator für eine Veränderung der Kristallstruktur des Kalzium Karbonat Skeletes sein. Die Atmungsraten zeigten keine pH-abhängigen signifikanten Änderungen, obwohl die mittlere Atmungsrate der Korallen während der pH-Reduktion (pH 7,4) im Vergleich zu der Kontrolle (pH 8,0) 15–38 % niedriger war. In Kombination mit einer allgemeinen Herab-Regulation der Genexpression nach der Reduktion des pH-Werts, deutet das auf eine metabolische Suppression als Kurzzeit-Reaktion hin. Dies wurde durch eine korrelierende niedrigere Expression (Δ log2 fold change > 20) von Genen, die zum Proteinsyntheseapparat gehören (Histone, ribosomale Untereinheiten und Elongationsfaktor), unterstützt. Nach dem Erhöhen des Nahrungsangebots während der Regeneration (pH 8,0), konnte eine starke Reaktion auf physiologischer (60–85 % höhere Kalzifizierungs-; 50–60 % höhere Atmungsraten) und transkriptomischer Ebene (1195 differentiell regulierte Transkripte) festgestellt werden. Dies könnte darauf hinweisen, dass die Nahrungsverfügbarkeit einen erheblichen Einfluss auf die Sensibilität von *D. dianthus* gegenüber niedirg-pH Bedingungen hat.

Vergleicht man die beobachteten Gen-Expressionsmuster des pH-Expositions-Experiments mit den der Feldproben, wurden in den Feldproben 38 % aller differentiell exprimierten Transkripte gefunden. Das zeigt, dass das Transkriptom von *D. dianthus* im Feld sehr variabel ist und stark von den vorherrschenden abiotischen Bedingungen beeinflusst wird. Stress- und Transkriptions-bezogene Gene (Metalloproteinasen und Zinkfinger) (Δ log2 fold change = 3,5) wurden verstärkt in den Proben gefunden, die unter niedrig pH Bedingungen (pH 7,5) im Feld gewachsen sind. Da die Feldproben jedoch von einer Vielzahl von variierenden Umweltfaktoren beeinflusst werden, ist die Zuordnung dieser Gene als pH-bezogene Reaktion schwierig.

Zusammenfassend wurde in dieser Studie gezeigt, dass *D. dianthu*s über umfassende Mechanismen verfügt, um kurzfristigen pH-Schwankungen zu widerstehen. Um Aussagen über die zukünftige Entwicklung von *D. dianthus* treffen zu können, muss die beobachtete metabolische Suppression und ihre langfristige Auswirkungen auf die Fitness der Korallen untersucht werden. Zusätzlich muss die starke Reaktion auf die Erhöhung des Nahrungsangebots beachtet werden, da der Ernährungszustand ein kritischer Faktor sein könnte, der die Empfindlichkeit der Korallen gegenüber niedrig-pH Bedingungen beeinflusst.

Summary

The seawater pH is influenced by the interaction of various natural physical and biological factors. Since the beginning of industrialisation, anthropogenic activities are also having a significant impact on the seawater pH, as the atmospheric increase of the carbon dioxide (CO_2) concentration led to an enrichment of the ocean with CO_2. The release of protons during the reaction of CO_2 with water molecules results in a declining pH (ocean acidification; OA). Apart from the seawater pH, the aragonite saturation state (Ω_{arag}) is commonly used to measure the OA, as it describes the 'easiness to calcify' and is therefore biologically relevant. With decreasing pH, the Ω_{arag} is also decreasing and calcifying organisms have to invest more energy to maintain their calcium carbonate structures, most prominently in cold and deep waters. Therefore, scleractinian cold-water corals (CWCs), such as the cosmopolitan species *Desmophyllum dianthus*, were thought to be among the taxa most threatened by OA, as they are mainly restricted to water temperatures between 4–12 °C and water depths below 50 m. However, their reported occurrence in aragonite under-saturated waters indicates that they are able to mitigate the negative impacts of the low Ω_{arag}. The aim of this study was to gain information on the regulations and mechanisms that allow the CWC *D. dianthus* to thrive under low-pH conditions. An understanding of the physiological and molecular processes affected by low-pH conditions will help to assess the development and future biogeographic distribution of *D. dianthus*.

Therefore, corals acclimated to pH 8.0 were exposed for two weeks to low-pH conditions (pH 7.4), to assess their short-term acclimation potential to an experimental reduction of the pH conditions. Afterwards, the pH was turned to pH 8.0 for two months, to determine their recovery potential. Corals being exposed to pH 8.0 during the whole experiment served as control. Physiological and transcriptomic response parameters were measured at various sampling times throughout the experiment. The observed gene expression patterns were compared to field samples that grew under two different pH conditions (pH 7.5; pH 7.8).

The results of this study suggest that *D. dianthus* is highly tolerant towards short-term changes in the seawater pH, in a range corresponding to the natural pH conditions. While no significant pH-dependent differences were detected on a physiological level, the dynamic regulation of the transcriptome indicates that the experimental pH-range was within the limits of phenotypic buffering. As a pH-dependent change was neither detected in the calcification rates nor in the expression of ion transporters, this suggests that the experimental changes of the seawater pH had no negative effect on calcification. However, the downregulation of genes coding for cytoskeletal elements (actin and tubulin) (Δ log2 fold change > 20) might be an indicator for a change in the crystal structure of the calcium carbonate skeleton. Further, no significant changes of the respiration rate during the two weeks of low-pH conditions could be observed, though the median respiration rate of the corals exposed to pH 7.4 was 15–38 % lower compared to the control. In combination with the immediate downregulation of genes after first reaching

pH 7.4, this may be an indicator for metabolic suppression under acute low-pH stress. This is supported by the downregulation of the expression of genes belonging to the protein synthesising apparatus (histones, ribosomal subunits and elongation factor) (Δ log2 fold change > 20). A change in the feeding regime during the recovery phase showed a strong regulation on both physiological (60–85 % higher calcification-; 50–60 % higher respiration rates) and transcriptomic (1195 differential regulated transcripts) level, indicating that the food availability influences the susceptibility of *D. dianthus* towards low-pH stress.

Comparing the observed gene expression patterns of the pH exposure experiment with field samples, 38 % of all differentially expressed transcripts were found in the field samples, suggesting that the transcriptome of *D. dianthus* is highly variable and strongly depends on the prevailing abiotic conditions. Stress- and transcription-related genes (metalloproteinase and zinc fingers) (Δ log2 fold change = 3.5) were found upregulated in those samples growing under pH 7.5 in the field. However, as the field samples were influenced by a multitude of fluctuating environmental factors, the assignment of these genes as a pH-related response is difficult.

In summary, this study demonstrated that *D. dianthus* has comprehensive mechanisms to withstand short-term pH fluctuations. To be able to draw conclusions about the development of *D. dianthus*, the observed metabolic suppression and its long-term effects on the corals fitness must be examined. In addition, the strong response towards the increased food supply must be noted, as the nutritional status may be influencing the corals sensitivity towards low-pH conditions.

Abbreviations

AIC	Akaike information criterion
ADP / ATP	Adenosine diphosphate / Adenosine triphosphate
ANOVA	Analysis of variance
ASH	Aragonite saturation horizon
BIC	Bayesian information criterion
BLAST	Basal local alignment search tool
BW	Buoyant weight
C	Carbon
Ca^{2+}	Calcium
cDNA	Complementary DNA, synthesized from single stranded RNA
CO_3^{2-}	Carbonate
CO_2	Carbon dioxide
Control group	Samples of the pH exposure experiment that experienced a constant pH = 8.0 during the whole experimental time
CSR	Cellular stress response
CWC	Cold water coral
D. dianthus	*Desmophyllum dianthus*
DEG	Differentially expressed genes
DGE analysis	Differential gene expression analysis
DIC	Dissolved inorganic carbon
DNA	Deoxyribonucleic acid
E_{deep}	Field samples from 300 m depth; pH = 7.5
$E_{shallow}$	Field samples from 20 m depth; pH = 7.8
GC content	Guanine-Cytosine content
GLS	Generalized least squares model
GO	Gene ontology
H^+	Proton
HCO_3^-	Bicarbonate
H_2CO_3	Carbonic acid
HSP	Heat shock protein
IPCC	Intergovernmental Panel on Climate Change
Log2 fold change	Measure, describing how much a quantity changes between two measurements
M1–15	Different RNA extraction methods, compared in the 'Method development'
n (statistics)	Number of replicates

N10–50	Statistical assembly quality parameter defining its contiguity
mRNA	Messenger RNA
OA	Ocean acidification
O_2	Oxygen
p (statistics)	Probability of rejecting the null hypothesis
pH	Negative decimal logarithm of the reciprocal of the hydrogen ion activity in a solution
RCP	Representative concentration pathways
RIN	RNA integrity number
RNA	Ribonucleic acid
RSB	RNA stabilisation buffer
RT	Room temperature
S_A	Salinity
SD	Standard deviation
SE	Standard error
$t_0 - t_6$	Molecular samplings during the pH exposure experiment
TA	Total alkalinity
Treatment group	Samples of the pH exposure experiment that experienced low-pH conditions pH = 7.4 for two weeks
Ω_{arag}	Aragonite saturation state
40S	Small ribosomal subunit
60S	Large ribosomal subunit

Glossary

Acclimation is the fast and reversible adjustment of gene expression patterns that modify the *phenotype* in response towards altered conditions. Thereby, a constant or increased *performance* is facilitated (Somero 2010).

Adaptation occurs over generations by *natural selection* of heritable *phenotypic* traits. It may lead to a shift in the *allele frequency* that changes the populations *tolerance limits* of an environmental factor (Donelson et al. 2019).

Allele frequency is the relative abundance of a gene variant (**allele**) in a population (Alberts et al. 2005).

Costs on a cellular level describe the amount of required cellular resources needed for defence and repair reactions counteracting cellular *stress* (Kültz 2005).

De novo **assembly** is a computational reconstruction of a longer sequence, using smaller sequence *reads*, without the use of a reference *transcriptome* (Wolf 2013).

Fitness is a measure of an individual's ability to survive and produce viable offspring in the prevailing environmental setting (Darwin 1859; Townsend et al. 2008).

Gene ontology is a dynamic and controlled vocabulary and classification of gene functions, which can be applied to all eukaryotes (Ashburner et al. 2000).

Genotype is the sum of *allele*-pair types of a diploid organism (Mahner and Kary 1997).

Intrinsic controls are regulations determined by inner cellular pathways (e.g. reproduction) (Kültz 2005). They can have an influence on the shape of the *reaction norm*.

Library is a collection of RNA or DNA fragments that is appropriate for sequencing (Wolf 2013).

Natural selection describes the force acting on heritable *phenotypic* traits of an individual, which are determining its *fitness*. It is the key driver of *adaptation* and evolution (Townsend et al. 2008).

Ocean acidification describes the reduction of the seawater pH, as a consequence to the rising atmospheric carbon dioxide concentrations, mainly due to anthropogenic activities (Doney et al. 2009).

Optimum is the environmental setting at which a *reaction norm* for a *phenotypic* trait expression reaches its maximum (Pörtner et al. 2005).

Orthologous genes are homologous genes of different species that evolved from the same ancestral gene and maintain a similar function (Thomas et al. 2012).

Performance is a measure of *phenotypic* expression of a fitness-related trait (Kingsolver and Huey 2003). A performance of zero marks the *tolerance limits* of an individual for an environmental factor.

Phenotype is the set of trait characteristics of an organism (Mahner and Kary 1997) that is influenced by the *genotype* and the environment.

Phenotypic buffering is a special case of *phenotypic plasticity*, describing the ability to maintain the same *performance* across a range of environmental conditions. It describes a *reaction norm* with zero slope (Reusch 2014).

Phenotypic plasticity is the ability of a single *genotype* to produce different *phenotypes* in response towards the environment (Fox et al. 2019).

Primary production is the synthesis of organic substances from inorganic substances (Bauer et al. 2013).

Reaction norm is a graph that describes the expected *phenotypic* trait expression (i.e. *performance*) of a *genotype* as a function of an environmental factor (Chevin et al. 2010).

Read is a short base-pair sequence of a RNA template inferred by sequencing (Wolf 2013).

Re-mineralization (=decomposition) is the conversion of organic to inorganic substances (Bauer et al. 2013).

Stress on a cellular level is inflicted by the environment and becomes apparent as the damage of macromolecules, the change of the cellular redox potential and/or the disturbance of cellular homeostases (Kültz 2005).

Tolerance range is the width of a *reaction norm*, which is determined by the *genotype* and can only be modified by *adaptation*. The **tolerance limits** describe a *performance* of zero (Chevin et al. 2010).

Total alkalinity after (Dickson 1981) is defined as the seawater's excess of proton acceptor over proton donors, with respect to zero level of protons.

Transcriptome is the entire ribonucleic acid produced by an organism, cell or tissue and can change depending on developmental stage, tissue or environmental conditions (DeBiasse and Kelly 2016).

1. Introduction

1.1 Carbonate chemistry in an acidifying ocean

The ocean's pH is determined by a complex interplay of various physical and biological factors, such as ocean mixing, temperature, pressure, biological production or calcification (Lauvset et al. 2020). Further, the seawater pH is directly influenced by the concentration of dissolved inorganic carbon (DIC) as water reacts with carbon dioxide (CO_2), forming the short-lived carbonic acid (H_2CO_3), which can react to bicarbonate (HCO_3^-) and carbonate (CO_3^{2-}). In each of these reactions one proton is released, lowering the seawater pH (Doney et al. 2009).

In pre-industrial times, the average seawater pH was at pH 8.2 (Zeebe 2012), with temporal and local differences, due to natural physical gradients and biological activities. Anthropogenic activities, such as the burning of fossil fuels and deforestation have led to a significant rise of the CO_2 concentration in the atmosphere (Doney and Schimel 2007). Overall, the atmospheric CO_2 concentration has risen by approx. 48 % from 280 ppm in preindustrial times to 419.05 ppm in April 2021 (CarbonTracker 2021). The fast increase of the atmospheric CO_2 partial pressure has established a gradient, with the ocean acting as sink (Sabine et al. 2004). Following the diffusive equilibrium between the atmosphere and the ocean, changes the seawater DIC concentration and the pH is a direct function of the anthropogenic released CO_2 to the atmosphere (Raven et al. 2005). From 1850–2018 the ocean has absorbed an estimated proportion of 25–30 % of the cumulative anthropogenic CO_2 emissions (Sabine et al. 2004; Friedlingstein et al. 2019; Hauck et al. 2020), which led to a freeing of protons and a decline of the seawater pH (Caldeira and Wickett 2003), referred to as ocean acidification (OA). Since 1980, an overall surface water pH decline of 0.017–0.027 pH units per decade was observed, which has led to a reduction of the seawater pH to a today's average of pH 8.1 (Zeebe 2012). Until the end of the century, the pH is likely to further drop up to 0.3 pH units, with local differences (IPCC 2019). The decreasing pH leads to a shift in the chemical balance between the carbonate species. Following the Bjerrum plot (Logan 2010), near future OA results in an increase of the HCO_3^- and a decrease of the CO_3^{2-} concentration (Zeebe and Wolf-Gladrow 2001) (**Figure 1**).
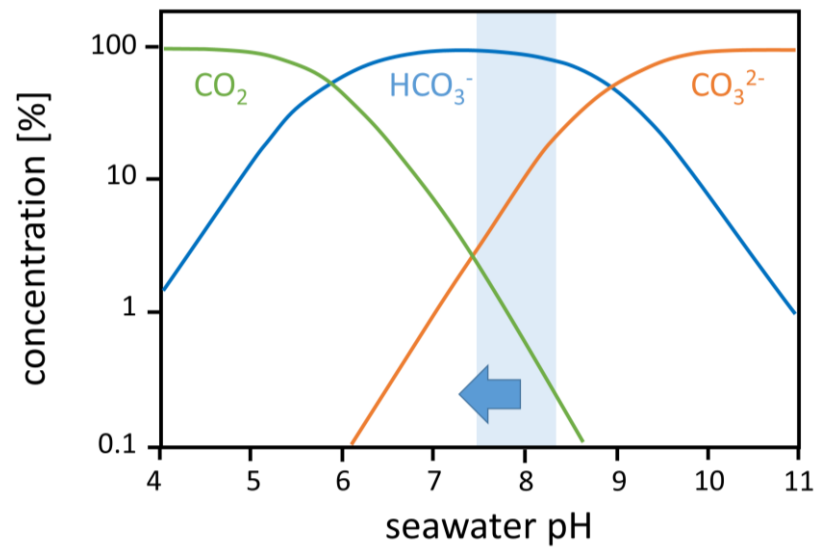
Figure 1: Bjerrum plot
The concentration [%] of carbon dioxide (green, CO_2), bicarbonate (blue, HCO_3^-) and carbonate (orange, CO_3^{2-}) along a logarithmic scale as a function of the seawater pH. The blue area marks the todays pH range of the ocean (pH 7.5–8.3 after Lauvset et al. (2020)). Blue arrow: development of seawater pH under ocean acidification scenarios.

Two important metrics of the OA are the seawater pH and the aragonite saturation state (Ω_{arag}) as both have an impact on biological processes. Besides calcite and vaterite, aragonite is an anhydrous form of CO_3^{2-}. Of these three anhydrous forms, calcite is the thermodynamically most and vaterite the least stable polymorph (Gopi et al. 2013). Due to the differences in stability, calcifying organisms use either calcite or aragonite to form their shells or skeletons. In the following, only the development of the aragonite concentration will be discussed, as aragonite is used by scleractinian corals (Stolarski et al. 2007).

The Ω_{arag} is the product of the actual concentrations of calcium (Ca^{2+}) and CO_3^{2-} in relation to the product of their concentrations at the chemical equilibrium (Jantzen et al. 2013) (**Equation 1**).

$$\Omega_{arag} = \frac{actual \ [Ca^{2+}] * [CO_3^{2-}]}{equilibrium \ [Ca^{2+}] * [CO_3^{2-}]}$$

Equation 1:
Aragonite saturation state

Accordingly, at $\Omega_{arag} = 1$ (aragonite saturation horizon; ASH), solid calcium carbonate ($CaCO_3$) does neither form nor dissolve. If $\Omega_{arag} < 1$, the dissolution of solid $CaCO_3$ is thermodynamically promoted, while if the $\Omega_{arag} > 1$, its precipitation is favoured (Atkinson and Cuet 2008).

Additionally to the atmospheric CO_2 partial pressure, water pressure and temperature are two important physical factors, influencing the ocean's pH and Ω_{arag}. At higher pressures, aragonite is becoming more

soluble. Therefore, a vertical Ω_{arag} gradient can be observed, declining with increasing depth (Zheng and Cao 2014).

Temperature is a further important physical driver on the oceans pH and Ω_{arag}. Regarding latitudinal differences, no clear gradient can be detected for pH, while the surface Ω_{arag} is ranging from ~3.7 in the tropics to ~1.4 in polar regions (Jiang et al. 2019). These patterns are the result of two processes. First, with decreasing seawater temperatures, the equilibrium between the carbon species is changing towards H_2CO_3 with less dissolved CO_3^{2-} in the seawater (**Figure 2a**). This is resulting in less free protons, an increasing seawater pH and a decreasing Ω_{arag}. Second, at lower seawater temperatures, the seawater can take up more CO_2 from the atmosphere (Portier and Rochelle 2005). Consequentially, more DIC is in the water, and the pH and Ω_{arag} are decreasing. These two processes have antagonistic effects on the seawater pH and are balancing each other almost out. Therefore, no latitudinal pH gradient can be seen. For Ω_{arag}, the two effects are additive, which can be seen as strong latitudinal gradient, with the Ω_{arag} decreasing towards colder water temperature at high latitudes (Jiang et al. 2019).

Summarizing the physical factors, influencing the oceans carbonate chemistry, the decreasing pH, high water pressure and cold temperatures are leading to a decline of the Ω_{arag}. In the past two centuries, this has already led to a shoaling of the ASH of up to 200 m, especially at higher latitudes (Feely et al. 2004).
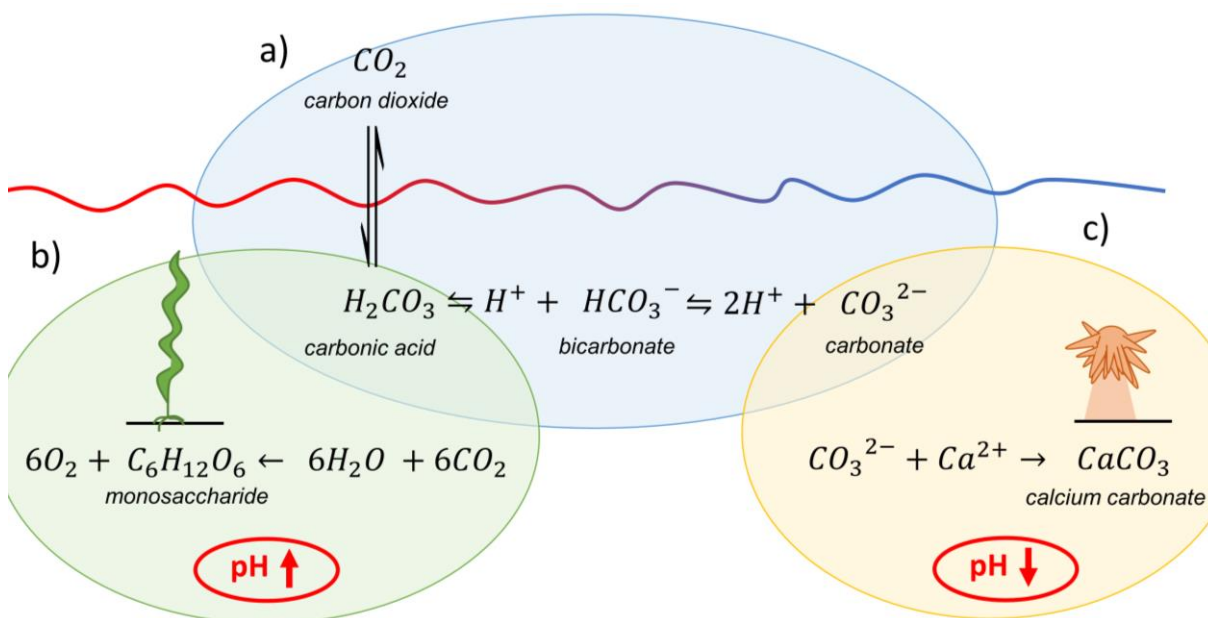
Figure 2: Carbonate chemistry of the seawater
a) Carbon dioxide (CO_2) dissolves in the seawater and forms carbonic acid (H_2CO_3), which can react further to bicarbonate (HCO_3^-) and carbonate (CO_3^{2-}), releasing a proton (H^+) in each reaction. The amount of CO_2 dissolving in the seawater depends on physical properties, e.g. the seawater temperature. **b)** Primary production ($C_6H_{12}O_6$ formation) binds DIC, which is increasing the seawater pH. **c)** Calcium carbonate ($CaCO_3$) formation reduces the total alkalinity of the seawater by binding carbonate (CO_3^{2-}), which is lowering the seawater pH.

Biological processes are also influencing the ocean's carbonate chemistry. They do not directly affect the pH, but rather the DIC concentration and total alkalinity (TA), which are causing chemical changes in the seawater, resulting in pH shifts (Lauvset et al. 2020).

Primary production decreases the DIC concentrations, as organic carbon is synthesised from inorganic carbon (**Figure 2b**). The reduction of DIC in the seawater results in an increase of the seawater pH. Consequential, during organic matter remineralization (e.g. respiration) the DIC concentration increases and the pH declines. The impact of remineralization on the natural seawater pH can be seen in the northern Indian and Pacific Ocean. As these water masses haven not been in contact with the atmosphere for ~1000 years (Zeebe 2012), they contain a high concentration of remineralised carbon and are acidic. The natural pH gradient due to organic matter formation and remineralization can be up to ~0.8 pH units (Lauvset et al. 2020).

The biogenic formation of calcium carbonate ($CaCO_3$) (calcification) also affects the DIC concentration by removing carbon from the seawater (**Figure 2c**). Additionally, by taking up CO_3^{2-}, the TA is affected, as CO_3^{2-} is a second level proton acceptor (two negative charges). Following the definition of TA after Dickson (1981), TA is defined as the concentration of proton acceptors over the concentration of proton donors under the constraint of electro-neutrality. The up-take of CO_3^{2-} leads to a decrease of proton acceptors in the seawater, resulting in a decline of the TA (Feely et al. 2004). This reduction of proton acceptors in the seawater during calcification leads to a decrease of the water's potential to buffer protons, resulting in a shift between the carbon species towards an increase of the H_2CO_3 and HCO_3^- concentrations and a decrease of the CO_3^{2-} concentration in the seawater. As the reduction in TA is twice as high as the reduction in DIC, the pH is decreasing during calcification (Zeebe and Wolf-Gladrow 2001; Feely et al. 2012). Consequential, the $CaCO_3$ dissolution increases the TA and, by enhancing the proton buffer capacity of the seawater, the pH (Feely et al. 2002).

1.2 Effects of ocean acidification on organisms

All of these processes affecting the seawater's carbonate chemistry have a severe impact on several biogeochemical cycles in the ocean. Generalizing their influence on marine organisms is difficult, as the impact is species-specific and varies regionally, due to differences of the environmental conditions.

To name some of the projected changes, Taucher et al. (2021) found, that OA leads to an altered carbon-nitrogen ratio of organisms. Thereby, the organic matter export and vertical nutrient fluxes are changed, affecting the efficiency of the biological pump in storing carbon in the deep sea. Carbon fixating organisms might benefit from higher CO_2 concentrations as they were reported to have higher carbon fixating rates (Doney et al. 2009). For calcifying organisms, such as calcifying plankton, benthic invertebrates (e.g. bivalves, echinoderms, crustacea, molluscs) or corals general negative impacts of OA were reported, such as reduced fertility or growth (Fabry et al. 2008).

1.3 The cold-water coral *Desmophyllum dianthus*

Scleractinian cold-water corals (CWCs) are occurring globally, being restricted to water temperatures between 4–12 °C. As they do not possess photosynthetic symbiotic algae (zooxanthellae), CWCs are not bound to the euphotic zone and mostly occur in water depths between 50–4000 m. Due to the low water temperatures and high pressure of their habitat, CWCs are already experiencing aragonite under saturation in large parts of their distribution range. CWCs act as ecosystem engineers in the deep-sea, by forming large-scale three-dimensional reefs. Thereby, CWCs provide shelter, feeding and nursery ground and serve as critical habitat for many fish species, supporting a high biodiversity (Orejas and Jiménez 2019). In a north-eastern Atlantic *Lophelia pertusa* reef, more than 1,300 associated species have been found (Roberts et al. 2006).

Desmophyllum dianthus (Esper, 1794) (Scleractinia) is a solitary scleractinian CWC species, belonging to the subclass of Hexacorallia. It is a cosmopolitan species, occurring in deep-waters between ~35–2,500 m though it has also been reported in shallower waters (Försterra and Häussermann 2003; Försterra et al. 2005). Primarily, it lives on hard substrate (e. g. rock walls or boulders), especially under overhangs with a slope exceeding 80 °. Its optimum temperature and salinity ranges are between 8–13 °C and $S_A = 28$–34 (Häussermann et al. 2009). Though being solitary, *D. dianthus* individuals can form pseudo-colonies with younger individuals growing on older ones (see picture on cover page). Thereby, they can form vast structures and reefs. Maximum densities of 1,500 individuals per square metre have been recorded (Försterra and Häussermann 2003). The calcareous skeletons of dead corals are being used by a multitude of sessile, endolithic and boring species, eventually causing a pseudo colony to break off and pile on the bottom. These piles serve again as habitat for a multitude of organisms and communities, which change significantly depending on the depth (Häussermann et al. 2009). Sherwood et al. (2008) investigated the trophic interactions of several CWC species. They showed that their diet is highly dependent on the species, ranging from phytodetritus and microzooplankton to degraded particulate organic matter and a primarily carnivorous diet.

The Chilean Comau fjord is a commonly used study site to investigate *D. dianthus*, as the species has been recorded in the entire fjord (Fillinger and Richter 2013). It is located at ~42 °S in an almost north-south disposition along 72,28 °W. It is 41 km long, 4.5 km wide, with a depth of about 600 m at its mouth, becoming shallower towards the head (Fillinger and Richter 2013). The fjord has two special geomorphic characteristics. Due to the north-south orientation, the fjord is relatively protected from winds and due to the absence of a sill at the fjord's mouth, the residence time of the deep water is shorter than in other fjords (Häussermann et al. 2009). Further, the fjord is characterized by a strong two-layer system. The depth of the surface water layer varies but is at approx. 15 m depth and shows pronounced seasonal changes, with temperatures ranging from 7 °C in September to 18.5 °C in January (Sánchez et al. 2011). Due to the high precipitation in the area of > 5000 mm per year, (Häussermann et al. 2009;

Schneider et al. 2016) and rivers discharge, the upper layer consists of brackish waters with changing salinities between S_A = 17.6–29. The biological production in the surface layer in the Comau fjord is dominated by strong latitudinal and seasonal patterns (Pantoja et al. 2011). A primary production of up to 6000 mg C m^{-2} d^{-1} in southern hemisphere spring was observed (Aracena et al. 2011), leading to a high rate of deep-sea export and carbon rich sedimentation.

The deep-water layer is dominated by sub-Antarctic water masses with more stable conditions. Mean temperatures and salinities range from 10–12 °C and S_A = 31–33 (Sánchez et al. 2011). Generally, nutrient concentrations are low in the surface layer and high in the sub-Antarctic deep waters (Iriarte et al. 2013, 2014).

A diverse pH regime was observed in the Comau fjord. Along a horizontal transect, pH differences between pH 7.51–8.1 were recorded. Regarding vertical changes, pH differences between pH 7.4 (250 m depth) and pH 8.3 (surface) were documented (Jantzen et al. 2013). Though the ASH is between 100 and 150 m in the fjord, high abundances of *D. dianthus* reefs below 150 m in aragonite undersaturated waters (Ω_{arag} = 0.5) were observed (Fillinger and Richter 2013; Jantzen et al. 2013).

This indicates that the biomineralisation of the calcareous skeleton underlies strong regulation mechanisms and the corals are actively retrieving the seawater's calcium carbonate (Moya et al. 2012; Carreiro-Silva et al. 2014). Anagnostou et al. (2012) suggest that the strong regulation is possible, due to the aragonite skeleton of CWCs not being in direct contact with the surrounding seawater. CWCs consist of four cell layers, divided in oral and aboral tissues with an ecto- and an endoderm each (**Figure 3**). The ectoderm is facing outside; the endoderm delimits a gastro-vascular cavity. The calcification process occurs at the calcioblastic ectoderm of the aboral tissue of the polyp. Specialized cells are secreting $CaCO_3$ into a biologically controlled environment (Allemand et al. 2004). For the aragonite crystallization, Ca^{2+} and DIC are required. The transport of charged particles across the four cell layers towards the calcification sites can either occur via diffusion between the cells or across the cell membranes, which requires energy and special carrier proteins or channels. The Ca^{2+} transport across the oral membrane was shown to be diffusional, along the concentration gradient (Jury et al. 2010). Its transport across the calcioblastic ectoderm however was shown to be active, and it is hypothesized that Ca^{2+} ions are exchanged with protons under the consumption of ATP. The exchange of Ca^{2+} ions with protons has the advantage of a reduction of the internal pH at the calcification sites, allowing or facilitating $CaCO_3$ precipitation (Hennige et al. 2014). However, the higher proton concentration in the ocean is (low seawater pH), the steeper the proton gradient between the calcifying medium and seawater has to be (Holcomb et al. 2014), as the chemical equilibrium of the seawater would favour a dissolution of the $CaCO_3$ skeleton. Pumping protons against a chemical equilibrium requires energy. Therefore, coral calcification is dependent on the surrounding seawater composition, despite occurring in a biologically controlled environment. While the seawater poses the only source for Ca^{2+}, the corals can derive the DIC for calcification either from the surrounding seawater, or from internal respiration.
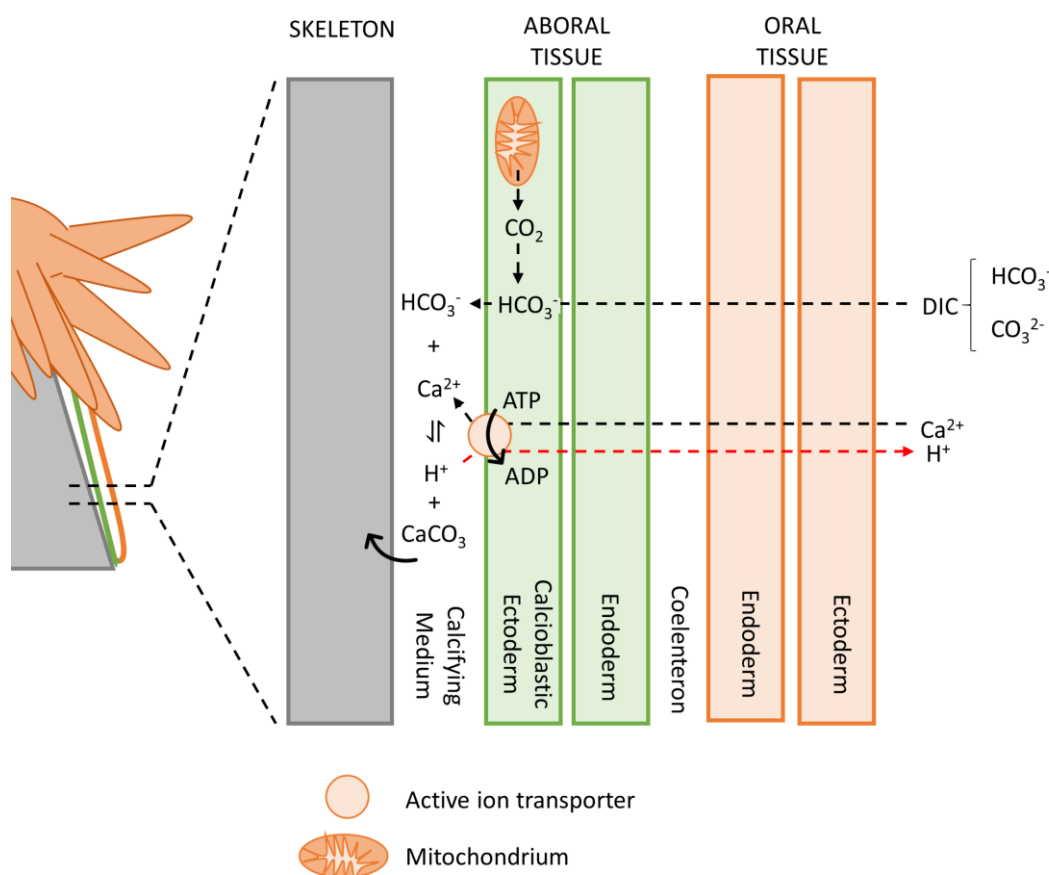
Figure 3: Model of the organization of calcification in cold-water corals
Cold-water corals consist of four cell layers, being divided into an aboral (green) and oral (orange) tissue. The oral ectoderm is facing outside, the calcioblastic ectoderm is facing the carbonate skeleton (grey), the oral and aboral endoderm are delimiting the coelenteron (gastro-vascular cavity). Calcification occurs at the calcioblastic ectoderm. For the calcification process, dissolved inorganic carbon (DIC; carbon dioxide: CO_2, bicarbonate: HCO_3^-, carbonate: CO_3^{2-}) and calcium ions (Ca^{2+}) are used. DIC can either be derived from the seawater or from respiration (mitochondria). Ca^{2+} is derived from the seawater, and transported actively (hydrolysis of ATP to ADP) to the calcification sites in exchange with protons. Modified after (Moya et al. 2012).

1.4 Transcriptomic responses to abiotic stress

As sessile organism *D. dianthus* cannot actively escape stressors. However, several protective mechanisms evolved that enable the species to survive environmental changes in their habitat up to a certain limit. Here, I want to shortly introduce the concepts of adaptation and phenotypic plasticity, as they are important to understand the ability of *D. dianthus* to respond to low-pH conditions (DeBiasse and Kelly 2016). All relevant definitions are summarized in the glossary.

The basis of adaptation are differences between individuals in their allele-pairs (genotype), which are resulting in different sets of trait characteristics (phenotypes) (Mahner and Kary 1997; Donelson et al. 2019). For instance, due to genetic differences, CWCs within a population have a slightly different tolerance towards low-pH conditions. By natural selection of phenotypes with a high performance at the prevailing conditions, the genotype can be altered over generations. Thereby, the local populations tolerance limits might adapt to their environment (Donelson et al. 2019). For example, if only CWCs

with a high performance at low-pH conditions survive and reproduce, the mean tolerance range of the population towards low-pH conditions will increase.

Within the genotype's tolerance limits, the phenotype can be modified in accordance with the environmental conditions (phenotypic plasticity) (Donelson et al. 2019; Fox et al. 2019) (**Figure 4**). The acclimation towards an altered condition (e.g. a change in pH; $pH_1 => pH_2$) is achieved by a fast and reversible modification of the gene expression pattern, which is expressed as a different phenotype, trying to maximise the performance ($P_1 => P_2$) (Kültz 2005; Deere and Chown 2006). The plastic modification in response towards an environmental factor allows the individual to mitigate the negative impacts of stressors and enables the survival in unfavourable environments. For example, within the pH tolerance limits of a CWC, it has the ability to alter its gene expression and regulate its internal pH (plasticity) to maintain calcification and growth (performance) even in low-pH conditions (Anagnostou et al. 2012). In an optimal environment, a phenotypic trait may reach its maximal performance (Pörtner et al. 2005). Moving towards the tolerance limits, the cellular stress level that is inflicted by the environmental factor increases. This may become evident in the damage of macromolecules, the change of the cellular redox potential and/or the disturbance of cellular homeostases (Kültz 2005). Therefore, maintaining performance at suboptimal conditions is costly, requiring cellular resources for defence and repair reactions against cellular damage. Therefore, the performance is not as high as at optimal environmental conditions. Close to the tolerance limits the inflicted damage cannot be counteracted and might cause apoptosis (Kültz 2005).
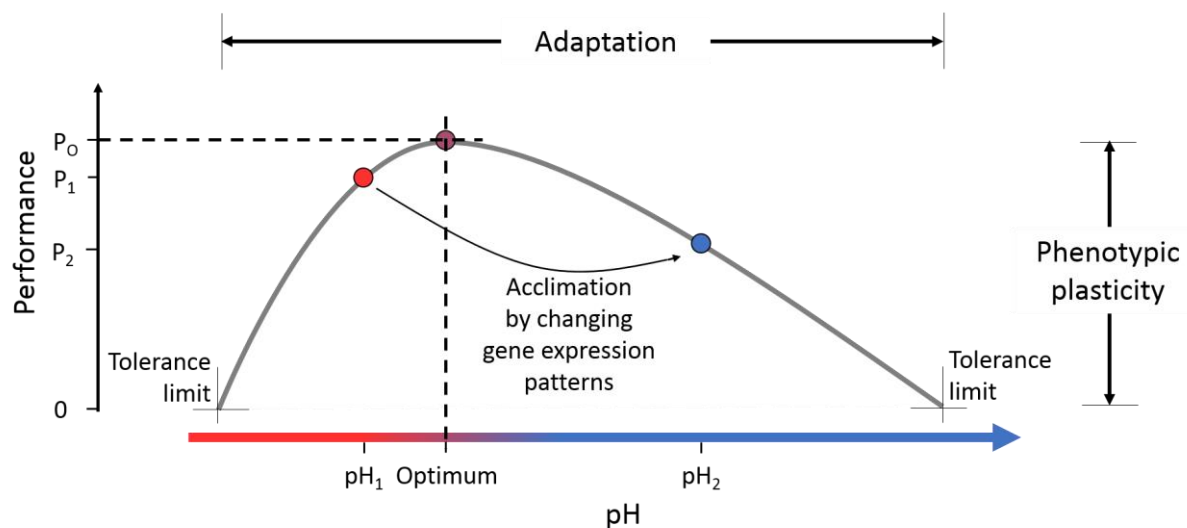
Figure 4: Schematic reaction norm
The phenotype of a single genotype is shown as a function of a trait performance (e.g. growth) over the seawater pH (environmental factor) (grey curve). The width of the reaction norm is determined by the adapted genotype and is limited by the tolerance limits. The optimum describes the environmental setting at which the performance reaches its maximum (P_O). An environmental change ($pH_1 => pH_2$) evokes an acclimation by changing the gene expression pattern, which is causing an adjustment of the phenotype, resulting in a change of performance ($P_1 => P_2$) as an expression of phenotypic plasticity.

A special case of phenotypic plasticity is phenotypic buffering. Within the limits of phenotypic buffering, no change in performance can be observed even though the environmental conditions have changed (Reusch 2014; Sunday et al. 2014). However, assuming that suboptimal conditions are increasing the cellular stress level, cellular costs to maintain performance are still increasing. This cannot be resolved with a physiological analysis.

The analysis of gene expression patterns can provide detailed insights into cellular regulations, mitigating the effects of environmental changes (DeBiasse and Kelly 2016), as the transcriptome represents the linking step between the intracellular signalling network that detects environmental changes and the physiological response (Kültz 2005). It thereby provides the possibility to resolve phenotypic buffering (Reusch 2014). The differential expression of protein-coding genes (i.e. the analysis of the messenger RNA; mRNA), is especially interesting, as their analysis can provide an understanding of the mechanisms and pathways that are targeted by an organism as response towards changing conditions. These regulations might help organisms to diminish the negative effects of stressors and allow them to thrive even in unfavourable environments.

1.5 Aim of this study and hypothesis

Considering only the ongoing geochemical processes of their actual distribution range, CWCs were thought to be one of the most threatened taxon by OA (Orr et al. 2005; Guinotte et al. 2006). The pH decline and future shallowing of the ASH have led to models that predict a potential habitat loss for CWC of up to 98 % until 2100 (IPCC 2019; Morato et al. 2020). Contrary to these predictions are the documentations of CWCs thriving in already aragonite undersaturated waters (Fillinger and Richter 2013; Jantzen et al. 2013). Additionally, there are studies finding no severe negative effect of an elevated CO_2 concentration on CWCs until the end of the century, as CWCs have the capacity to upregulate their internal pH at the calcification sites, inducing the $CaCO_3$ precipitation (Trotter et al. 2011; Form and Riebesell 2012; Maier et al. 2012; McCulloch et al. 2012a). This indicates that CWCs are tolerant towards pH changes, being able to mitigate the negative effects of the low-pH conditions.

However, Carreiro-Silva et al. (2014) showed an up-regulation of genes that are involved in cellular stress and immune defence after a six months low-pH experiment (pH 7.7) with *D. dianthus*. This indicates that there are physiological impacts of a decreasing seawater pH that are not becoming evident on an organismal level. Understanding the mechanisms and pathways that are regulated at low-pH conditions will help to model the future biogeographical distribution of CWCs.

The aim of this project is to assess the physiological mechanisms and regulatory pathways that enable the scleractinian cold-water coral *Desmophyllum dianthus* to thrive in aragonite undersaturated waters. Therefore, a pH exposure experiment (Control: pH 8.0 and Treatment: pH 7.4) was conducted. During the experiment the corals of the Treatment group were exposed for two weeks to low-pH conditions (pH

7.4), before the pH was increased to pH 8.0 for two months to assess their recovery potential. The gene expression profiles of the two groups will be compared at several time points during the experiment for a high temporal resolution of the cellular response.

Analysing the changes in the gene expression patterns of *D. dianthus*, requires the extraction of high-quality RNA from CWCs. Therefore, the first task of this thesis was to compare and optimize several methods to extract RNA of different coral species and single out the method with the highest RNA qualities. Additionally, three methods for molecular sampling (liquid nitrogen, RNA stabilisation buffer, biopsy) were compared, assessing different sampling possibilities for future experiments.

I.   Thereby, the RNA quality was expected to be highest after a sampling in liquid nitrogen. Further, it was analysed whether the presence of $CaCO_3$ in the samples had a negative effect on the RNA quality. Therefore, three cellular disintegration methods (Proteinase K digestion, ceramic beads, RNA lysis buffer) with different destructive impacts on the $CaCO_3$ skeleton were compared.

II.   The RNA quality was hypothesised to be highest after a proteinase K digestion, as the concentration of $CaCO_3$ in solution was assumed to be smallest.

The calcification and respiration rate of the corals in the pH exposure experiment were evaluated, to analyse the transcriptomic responses in the context of physiological measurements. Regarding the physiological analysis of the pH exposure experiment,

III.   the calcification rate was hypothesized to decrease and the respiration rate to increase under experimentally reduced pH 7.4 compared to the Control group at pH 8.0.

To be able to analyse the differential gene expression, a comprehensive reference transcriptome for *D. dianthus* was generated that was as complete as possible. Therefore, all available samples were used to generate a *de novo* reference transcriptome to include a wide range of organismal responses. The analysis of the gene expression patterns was guided by the following hypothesis.

IV.   The number of differentially expressed genes was expected to increase directly after exposure to the experimentally reduced pH but return to the expression levels of the Control group within the recovery phase.

V.   The expression of genes that are involved in cellular stress and biomineralisation were hypothesized to be upregulated under reduced pH 7.4 (Treatment group) compared to the Control group.

The gene expression profiles that were observed in the pH exposure experiment was compared with *D. dianthus* individuals that were sampled in the Chilean Comau fjord at two different pH conditions ($E_{shallow}$: pH 7.8 and E_{deep}: pH 7.5) to assess, whether the measured reactions were comparable to field conditions.

VI.   Thereby, the number of differentially expressed genes as response to low-pH conditions was expected to be higher of the field samples than of the pH exposure experiment samples.

2. Material and Methods

2.1 Method development: RNA extraction from cold-water corals

In total 15 different RNA extraction methods were compared, testing combinations of five coral species (three tropical; two CWC species), three extraction kits (Qiagen RNAeasy Mini; Zymo Quick RNA Mini Prep; Zymo Direct Zol RNA Mini Prep), three sampling methods (liquid nitrogen; RNA stabilisation buffer; biopsy) and three methods for cellular disintegration (Proteinase K digestion; ceramic beads; RNA lysis buffer). An overview of all methods can be seen in **Table 1**.

The quality of the RNA extraction methods (M1–M15) was assessed by evaluating three categories: the feasibility of the method, the total RNA yield (peQLab Biotechnologie GmbH NanoDrop ND-1000 Spectrophotometer) and the RNA integrity (LabChip GX Touch Nucleic Acid Analyzer). To be able to compare the results, points were assigned for each evaluation criterion and added up for the respective method (**Table 1**). The feasibility was divided in three categories, with 3 marking the best feasibility. The replicate mean RNA yield was classified into four categories: 1: 0–50 ng RNA/µl, 2: 50–100 ng RNA/µl, 3: 100–200 ng RNA/µl, 4: >200 ng RNA/µl. The RNA integrity was assessed of five methods (M10–15) by the replicate mean of the RIN (RNA integrity number) value. The possible RIN values range from 1 to 10, with 1 being most degraded and 10 being most intact RNA (Mueller et al. 2016).

Best results with an overall score of 12.6 (Feasibility: 2, RNA yield: 157.46±42.6 ng µl^{-1} and RNA quality: RIN = 7.6±0.86) were obtained by the following procedure (M14):

a) Snap freeze *D. dianthus* directly after sampling in liquid nitrogen and store the samples at -80 °C until further processing.

b) Mortar frozen samples to a fine powder in liquid nitrogen, using a liquid nitrogen-cooled mortar to prevent the material from thawing.

c) Transfer ~100 mg of the powdered coral sample into RNA Shield ©Zymo and extract the RNA directly or store the samples at -80 °C until RNA extraction. The calcium carbonate was not removed from the samples before RNA extractions, but pelleted and discarded in the first step of the RNA extraction.

d) Extract RNA using the "Zymo Quick RNA MINI Prep Plus" Kit, following the enclosed protocol. Modifications were as follows:

- No proteinase K digestion of the samples before adding the RNA Lysis Buffer
- Incubation of the samples in the RNA Lysis Buffer for five minutes at room temperature (RT)
- Incubation of the DNase 1 Mix for 60 min at RT
- RNA elution in 30 µl DNase/RNase free water, followed by an incubation for five minutes at RT

Table 1: Method development
The table shows an overview of all 15 different methods (M1–M15) that were compared in the course of the method development, giving details about the used species, sample type, number of replicates, sampling method, the cellular disintegration and the used RNA extraction kit. The quality of each respective method was assessed by scoring the feasibility (max.: 3), the mean RNA yield [ng µl^{-1}] (max.: 4) and the mean RIN value (max.: 10) and summing up their results. Best results were obtained by M14 (marked in red). *NA*: measurement not available.

Method	Species	Sample type	*n*	Tool to obtain samples	Sampling method	Cellular disintegration	Extraction Kit	Results			
								Feasi-bility	Mean RNA yield [ng µl^{-1}]	Mean RIN value	Sum
M1	*Caryophyllia huinayensis*	whole recruits	2	tweezer	liquid nitrogen	on vortex with ceramic beads	Qiagen RNAeasy Mini	3	**1** (48.7±1.6)	*NA*	(4)
M2		whole recruits	2	tweezer	liquid nitrogen	Proteinase K digestion for 3h at 55 °C, 350 rpm	Zymo Quick RNA Mini Prep	2	**3** (122.6±83)	*NA*	(5)
M3		whole recruits	2	tweezer	RSB – Qiagen RNAlater	on vortex with ceramic beads	Qiagen RNAeasy Mini	3	**2** (76.9±6.8)	*NA*	(5)
M4		whole recruits	2	tweezer	RSB – Zymo Shield	Proteinase K digestion for 3h at 55 °C, 350 rpm	Zymo Quick RNA Mini Prep	2	**1** (46±4.67)	*NA*	(3)
M5	*Montipora sp.*	coral fragment	2	pincher	liquid nitrogen	on vortex with ceramic beads	Qiagen RNAeasy Mini	3	**1** (30.4±20.6)	*NA*	(4)
M6	*Stylopora sp.*	coral fragment	2	pincher	liquid nitrogen	Proteinase K digestion for 3h at 55 °C, 350 rpm	Zymo Quick RNA Mini Prep	2	**4** (201.5±13.1)	*NA*	(6)
M7		coral fragment	2	pincher	RSB – Qiagen RNAlater	on vortex with ceramic beads	Qiagen RNAeasy Mini	3	**2** (57.8±63.5)	*NA*	(5)
M8	*Seriatropora sp.*	coral fragment	2	pincher	RSB – Zymo Shield	Proteinase K digestion for 3h at 55 °C, 350 rpm	Zymo Quick RNA Mini Prep	2	**3** (110.7±21.3)	*NA*	(5)

Table 1: Method development – continued

Method	Species	Sample	*n*	Tool to obtain samples	Preservation of sample	Cellular disintegration	Extraction Kit	Results			
								Feasi-bility	Mean RNA yield [ng µl^{-1}]	Mean RIN value	Sum
M9		Tentacles (biopsies)	2	tweezer	RSB – Zymo Shield	Proteinase K digestion for 3h at 55 °C, 350 rpm	Zymo Quick RNA Mini Prep Plus	2	**1** (9.92±0.02)	*NA*	(3)
M10		coral fragment	4	hammer and chisel	liquid nitrogen	Proteinase K digestion for 3h at 55 °C, 350 rpm	Zymo Quick RNA Mini Prep	2	**3** (185.9±86.4)	**2.75**	**7.75**
M11		fine powder	2	nitrogen-cooled mortar	liquid nitrogen; stored in Zymo Shield on -80°C	Proteinase K digestion for 3h at 55 °C, 350 rpm	Zymo Quick RNA Mini Prep Plus	2	**4** (327.1±06.4)	**2.3**	**8.3**
M12	*Desmophyllum dianthus*	coarse powder	2	nitrogen-cooled mortar	liquid nitrogen; stored in Zymo Shield on -80°C	Proteinase K digestion for 3h at 55 °C, 350 rpm	Zymo Quick RNA Mini Prep Plus	2	**4** (212.9±111)	**2.25**	**8.25**
M13		coral fragment	2	nitrogen-cooled mortar	liquid nitrogen; stored in Zymo Shield on -80°C	Proteinase K digestion for 3h at 55 °C, 350 rpm	Zymo Quick RNA Mini Prep Plus	2	**4** (267.2±77.8)	**2.2**	**8.2**
M14		**fine powder**	**6**	**nitrogen-cooled mortar**	**liquid nitrogen; stored in Zymo Shield on -80°C**	**no proteinase K digestion; incubation in RNA lysis buffer for 5min at RT**	**Zymo Quick RNA Mini Prep Plus**	**2**	**3** (157.5±42.6)	**7.6**	**12.6**
M15		fine powder	6	nitrogen-cooled mortar	liquid nitrogen; stored in Zymo Shield on -80°C	no proteinase K digestion; incubation in RNA TRI Reagent for 5min at RT	Zymo Direct Zol RNA Mini Prep	1	**3** (157.3±35.2)	**7.06**	**11.1**

2.2 Sampling

2.2.1 pH exposure experiment

Desmophyllum dianthus individuals for the pH exposure experiment were collected by scientific divers and with a ROV (MARISCOPE, Commander2) between 2014 and 2017 in the Chilean Comau and Piti Palena fjord (**Figure 5**).
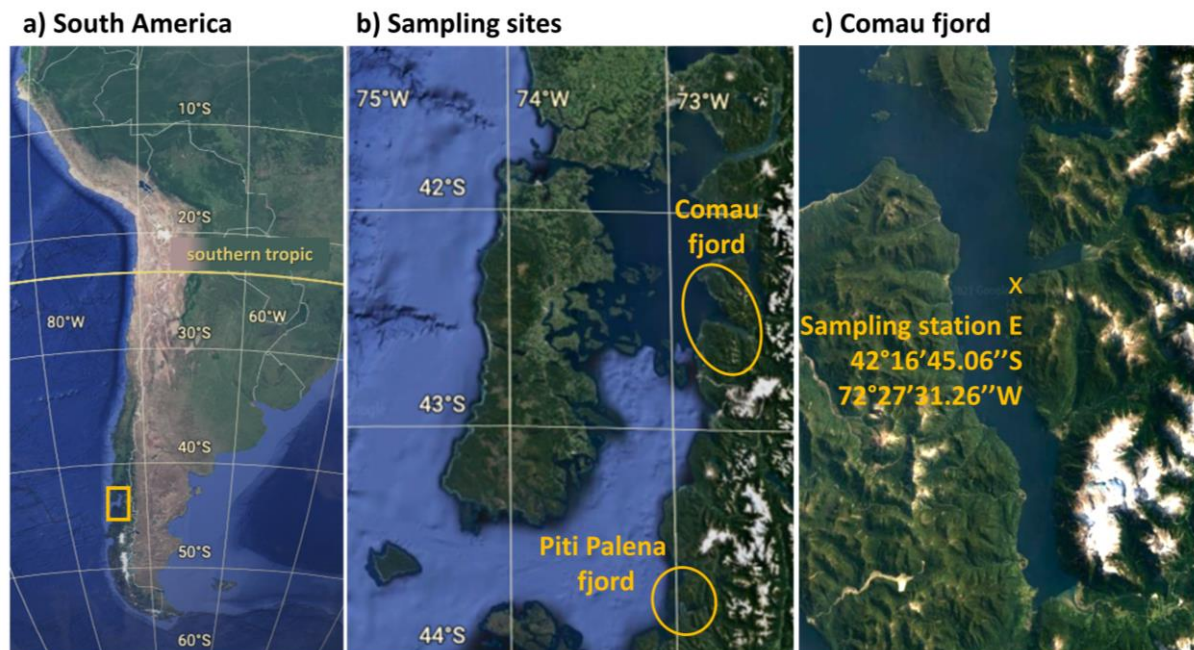
Figure 5: Sampling sites
a) South America, with the sampling area (Comau and Piti Palena fjord) marked with a yellow rectangle in Chile. **b)** Overview map of the Chilean Comau and Piti Palena fjord. **c)** Sampling station E with coordinates in the Chilean Comau fjord shows the sampling station of the field samples. Maps modified after: (Earth 2021).

The living corals were transported by plane at 10 °C in plastic bags, containing seawater and a 100 % oxygen atmosphere. The transport from Chile to the thermostatically controlled facilities of the Alfred Wegener Institute, Helmholtz Centre for Polar and Marine Research (Bremerhaven, Germany) lasted approx. two days. The corals were kept at collection site ambient conditions (11.5 °C, pH 8.0, $S_A = 31.5$) and fed three times a week *ad libitum*, for at least two years after sampling.

2.2.2 Field samples

During a sampling campaign of the PACOC project in 2017, *Desmophyllum dianthus* individuals were collected by scientific divers and with a ROV (MARISCOPE, Commander2) at different sites along a pH gradient in the Chilean Comau fjord. A natural pH difference of 0.3 pH units was recorded in different depths at sampling station E (42°16'45.06''S, 72°27'31.26''W) (**Figure 5c**), with pH 7.8 at 20 m ($E_{shallow}$) and pH 7.5 at 300 m (E_{deep}). Four individuals were sampled at both depths. The corals were snap-frozen in liquid nitrogen directly after sampling and stored on -80 °C until further analysis.

2.3 pH exposure experiment

Before the start of the experiment, skeletal parts of the corals that were not covered with tissue were removed (submerged Dremel equipped with a diamond blade: DREMEL Europe, Breda, Netherlands). Afterwards the individuals were glued on polyethylene screws (Preis Easy Glue Underwater: Preis AquaristikKG, Bayerfeld, Germany) to be able to handle the corals for physiological measurements. Afterwards, the corals recovered for at least 24 h before the start of the experiment.

The pH exposure experiment, including the monitoring of the abiotic and physiological parameters, was conducted by M. Sc. Kristina Beck from May to September 2019. The data were statistically analysed and interpreted in the course of this thesis.

2.3.1 Experimental design and carbonate system manipulation

The pH exposure experiment ran for 99 days and consisted of a Control and a Treatment group (**Figure 6**). The Control group experienced stable pH conditions at pH 8.0 throughout the experimental time. The pH of the Treatment group remained stable at pH 8.0 until day 16, before it was lowered artificially to pH 7.4 within 24 hours in gradual steps of 0.2 pH units. The seawater's pH was reduced within 24 h by diluting the water with acidic (pH 4.5) artificial seawater until pH 7.4 was reached. Low-pH conditions lasted two weeks (day 18–31). For the last two months of the experiment (day 33–99), the pH was increased within 24 hours to pH 8.0. The artificial increase of the pH was achieved by outgassing of CO_2 from the water until pH 8.0 was reached.

During the first two months of the experiment, the polyps were fed individually three times a week with one dead krill *Euphausia pacifica* using tweezers. In the last month of the experiment, the corals were fed *ad libitum* (affects only the sampling on day 99). During feeding, the circulation system was shut off for two to three hours.
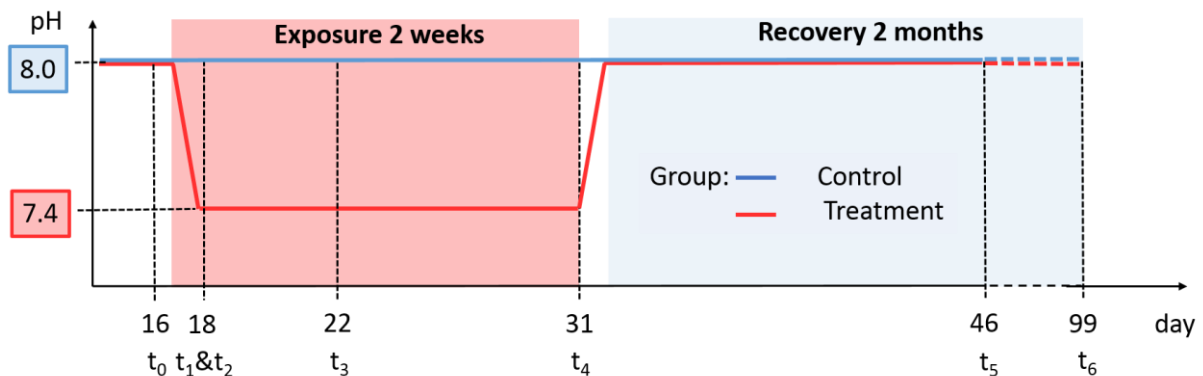
Figure 6: Schematic experimental design
The pH exposure experiment run for 99 day and consisted of a Control (blue) and a Treatment (red) group. The Control group experienced a constant pH = 8.0 during the whole experimental time. The Treatment group was exposed to pH = 7.4 for two weeks (day 18–31). Afterwards the seawaters pH of the Treatment group was increased to pH 8.0 for two months during the recovery phase. The pH de- and increase was performed within 24 h. $t_0 – t_6$ mark molecular sampling times.

For the Control and the Treatment group a recirculating aquarium system was set up, containing artificial seawater (Dupla Marin Premium Reef Salt, Germany). Each aquarium system (150 L in total) consisted of two replicate tanks (35 L each), which contained the corals. The replicate tanks were connected by a technical tank (80 L). Temperature and pH were monitored every 15 min in the replicate tanks and adjusted within the technical tank by a digital IKS control system (iks aqauastar, iks ComputerSystem GmbH, Germany). Additionally, the temperature and pH was recorded five times a week, using a WTW pH electrode (WTW pH 3310), which was calibrated once a week. The pH was measured in NBS scale. The salinity (WTW Cond 3210), and oxygen content (YSI PrpoODO; calibrated once before the start of the experiment with 100 % saturated water) were also monitored. All water tanks were kept in darkness within a temperature-controlled room, set to 10 °C. Twice a week, 50 L of the water were replaced with freshly prepared artificial seawater.

2.3.2 Physiological parameters

Calcification rate. The calcification rate of five corals ($n = 5$) was determined at five times during the experiment on day 1, 16, 31, 46 and 99 of the Control and the Treatment group. The buoyant weight (BW) was used instead of the alkalinity anomaly method (Chisholm and Gattuso 1991), as problems in the DIC analysis occurred during the pH exposure experiment (Müller 2019). The BW of a coral was determined by placing them on a watch glass, which was suspended in a water-filled weighing chamber. The watch glass with the coral was attached to a balance mounted on a frame on top of the weighing chamber (Spencer Davies 1989). The weight of the skeleton can be calculated by dividing the measured BW by the seawater-coral-density ratio after subtracting it from one (**Equation 2**). The calcification rate per day was determined by dividing the delta BW of a coral ($t_{x+1} - t_x$) through the BW on t_x multiplied with the time between the two measurements. The result was multiplied with 100 to calculate the calcification rate per day in percent (**Equation 3**).

$$Weight\ of\ skeleton\ [mg]$$
$$= \frac{bouyant\ weight\ coral\ [mg]}{1 - \left(seawater\ density\ [mg\ cm^{-3}] \middle/ coral\ density\ [mg\ cm^{-3}]\right)}$$

Equation 2:
Buoyant weight
(Spencer Davies 1989)

$$Calcification\ rate\ [\%\ d^{-1}]$$
$$= \frac{\Delta BW\ [g]\ (t_{x+1} - t_x)}{BW\ [g]\ t_x * exposure\ time\ [d]} * 100$$

Equation 3:
Calcification rate

Respiration rate. The respiration rate of five corals ($n = 5$) was measured on day 16, 18, 22, 32, 46 and 99 of the Control and the Treatment group. The oxygen consumption was measured within closed 0.8 ml incubation chambers (Schott bottles). Before the start of the incubations, the corals and screws were cleaned with a soft brush to remove organisms that were attached to the screws and bare skeletal parts. For the measurements, the corals were screwed upside-down into the Schott bottle lid in accordance with their natural downward orientation. One additional chamber without coral served as blank to measure background respiration, e.g. of bacteria. The incubation chambers were completely submerged in a temperature-controlled water bath on a magnetic stirring plate. Magnetic stirrers inside the incubation chambers ensured a homogenic oxygen concentration inside the chamber. The temperature was measured every 10 s inside the water bath by TidbiT Loggers (data not shown). The oxygen consumption was measured at the beginning of the incubations and at the end after 8–15 h using an YSI ProODQ oxygen meter. To calculate the respiration rate, the consumed amount of oxygen by the corals was corrected for the background respiration, multiplied with the incubation volume and divided by the incubation time multiplied with the tissue surface of the coral. The result was multiplied with 24 h to calculate the respiration rate per day (**Equation 4**). The corals tissue surface was modelled, by fitting a truncated cone into the coral and calculating its surface.

$$Respiration\ rate\ [^{\mu mol}/_{d\ cm^2}]$$

Equation 4:
Respiration rate

$$= \frac{(O_{2\ Start} - O_{2\ End} - O_{2\ Background\ respiration})\ [\mu mol\ l^{-1}] * incubation\ volume\ [l]}{incubation\ time\ [h] * tissue\ surface\ [cm^2]} * 24\ h$$

Statistics. All statistical analyses of the physiological data were run in RStudio (Version 1.3.1093). A generalized least squares model was fitted on the calcification and respiration rate, using the "gls" function of the R package "nlme" (Pinheiro et al. 2020). For repeated measures analysis of variance of the calcification and respiration rate (time series), the day of the experiment and pH treatment were modelled as additive fixed effects. A compound symmetry structure was integrated into the model, specifying the time covariate (day of the experiment) and the repeatedly measured corals as grouping factor. The model's fit on the data was assessed by comparing the AIC and BIC of different models and determining the residuals' variance structure of each model. The normality of residuals (Shapiro-Wilk test, $p > 0.05$) and homoscedasticity (Levene's test, $p > 0.05$) of the data were tested. Analysis of variance (ANOVA) was tested on the model by using the "anova" function, to assess the influence of the fixed effects. Pairwise comparisons were performed, using the "emmeans" function of the R package "emmeans" (Lenth 2021) to calculated the degrees of freedom and Tukey adjustment of the *p*-value.

2.4 Molecular analysis

During the pH exposure experiment, five corals of both the Control and the Treatment group were sampled at all seven time points (**Table 2**). The corals were snap-frozen in liquid nitrogen directly after sampling and stored at -80 °C until analysis. Individuals of the pH exposure experiment used for molecular analysis were not used for physiological analysis to avoid the results being biased by the handling stress.

Of each field sampling station ($E_{shallow}$ and E_{deep}), four corals were analysed.

Table 2: Molecular sampling
The table specifies the time points of the pH exposure experiment at which *Desmophyllum dianthus* individuals were sampled for molecular analysis ($n = 5$).

Day of the experiment	Time point	Description of the time point
16	t_0	24 hours before pH reduction of the Treatment group to pH 7.4
18	t_1	2 hours after the Treatment group reached pH 7.4
18	t_2	24 hours after the Treatment group reached pH 7.4
22	t_3	5 days after the Treatment group reached pH 7.4
31	t_4	2 weeks after the Treatment group reached pH 7.4
46	t_5	2 weeks after the Treatment group re-reached pH 8.0
99	t_6	2 months after the Treatment group re-reached pH 8.0

2.4.1 RNA extraction

pH exposure experiment. The RNA extraction method of the pH exposure experiment samples followed the method development (see section 2.1). Before the total RNA was extracted, all snap-frozen corals were ground to a fine powder, using a liquid nitrogen mortar to prevent the material from thawing and the RNA from degradation. The powder was transferred in Zymo Shield and stored on -80 °C until extraction. The total RNA was extracted from each individual following the instructions of the "Zymo Quick RNA Mini Prep Plus"-Kit (R1057). Modifications were as referred to in section 2.1. RNA contamination and yield were determined using a NanoDrop (peQLab Biotechnologie GmbH NanoDrop ND-1000 Spectrophoteter), evaluating the 260 nm/280 nm and 260 nm/230 nm spectrometric ratios. RNA integrity was analysed, evaluating the RIN values of the LabChip (LabChip GX Touch Nucleic Acid Analyzer).

Field samples. The RNA of the field samples was extracted by Dr. Marlene Wall. The snap-frozen tissue samples were disrupted, using lysis tubes with ceramic beads (bead-mill, 2 x 30 sec 30 Hz, Qiagen TissueLyser II, Germany). Afterwards, the samples were centrifuged for 3 min at 1,500 rcf and the clear supernatant was processed as described in the protocol of the "Qiagen AllPrep DNA/RNA column

extraction Kit". Deviating from the protocol, a second on-column washing step was included and the RNA was eluted in two steps. RNA contamination and concentration were determined by evaluation the A260 nm/280 nm and A260 nm/230 nm spectrometric ratios of the samples. The RNA integrity was not assessed.

2.4.2 cDNA library preparation and sequencing

The cDNA library preparation, sequencing and bioinformatic analyses of the pH exposure experiment and the field samples were consistently conducted as follows.

High quality RNA samples were diluted to a total RNA content of 1000 ng per sample. The cDNA library was prepared, following the instructions of the "Illumina TrueSeq Stranded mRNA Sample Preparation" guide. First, the mRNA was purified from the total RNA and fragmented before being transcribed into cDNA. Afterwards, the cDNA was modified by adenylating the respective 3' ends and ligating sample-specific adapters (RNA Adapter Plate, 96plex (RAP)). Each workflow was split into two days, stopping after the synthesis of the second cDNA strand (first "safe stopping point" of the protocol), storing the samples on -20 °C. All in-line controls reagents were used. The quality and concentration of all cDNA libraries were determined, using a LabChip (LabChip GX Touch Nucleic Acid Analyzer).

Before pooling, all libraries were diluted to 10 nM. To remove the primer peak from the pool an additional washing step was included as follows: add 560 µl of clean NGS beads to 700 µl pool (ratio sample:beads 1:0.8); mix thoroughly; incubate 15 min at room temperature (RT) on bench; incubate 5 min at RT on magnetic rack; discard 1260 µl supernatant; wash two times with 1 ml 80 % ethanol; let pellet air-dry for 25 min; remove from magnetic stand; add 352 µl Resuspension buffer; mix thoroughly; incubate 3 min at RT; transfer 340 µl into a clean tube.

The pooled cDNA library was sequenced with the Illumina "NextSeq 2000", following the "NextSeq 2000 Sequencing System Guide". The optional 2 % PhiX control was added to the pool.

2.5 Bioinformatic pipeline

The bioinformatic analyses were carried out on a high performance computing system (Cray CS400) at the Alfred Wegener Institute, Helmholtz Centre for Polar and Marine Research. All scripts used for bioinformatics analysis are available in the supplement section 7.1. **Figure 7** shows an overview of the conducted bioinformatic pipeline, used for the data analysis.
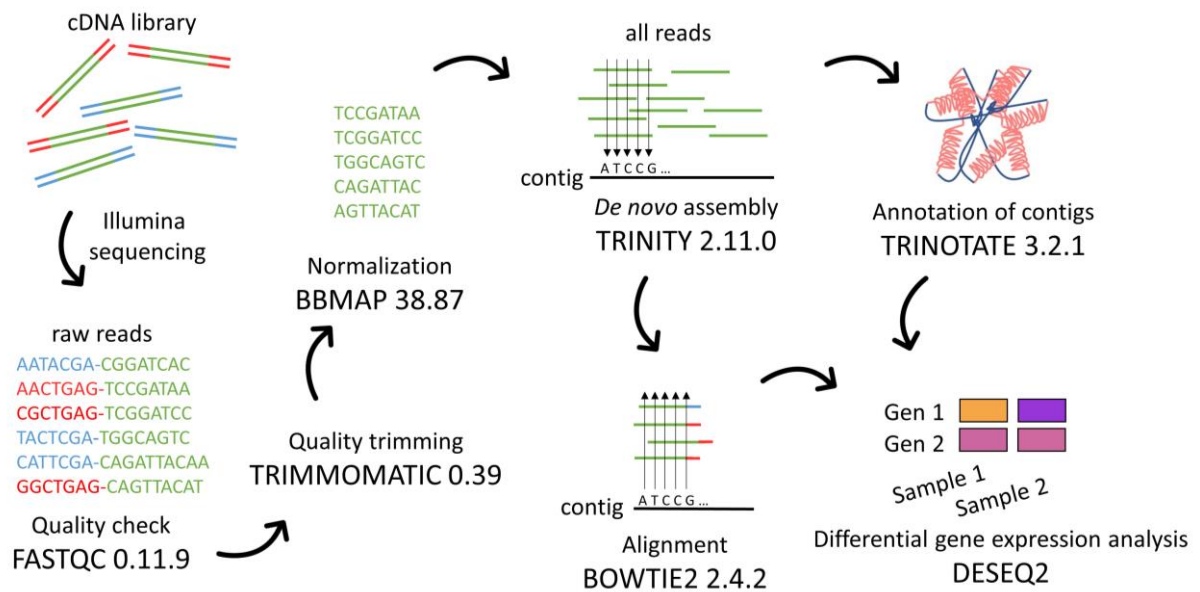
Figure 7: Bioinformatic pipeline
After the cDNA library was sequenced, the paired-end reads were quality checked using FastQC v0.11.9 (Andrew 2010). The reads were quality trimmed, using Trimmomatic v0.39 with default setting (Bolger et al. 2014) and normalized (BBMap, v38.87; (Bushnell 2014)). The *de novo* assembly was constructed with Trinity, v2.11.0 (Haas et al. 2013). The assembly was annotated using Trinotate v3.2.1 (Bryant et al. 2017). The reads were mapped onto the *de novo* assembly by Bowtie2 v2.4.2 (Langmead and Salzberg 2012) and the differential gene expression analysis was assessed using the R package DESeq2 (Love et al. 2014).

After sequencing, the paired-end reads were demultiplexed and quality checked using FastQC v0.11.9 (Andrew 2010). Adapter clipping and quality trimming were performed using Trimmomatic v0.39 (Bolger et al. 2014) with default setting. All reads were normalized using bbnorm.sh from the BBtools suite v38.87 (Bushnell 2014) with an average depth of 100x and a minimum depth of 5x before they were *de novo* assembled using the Trinity genome independent transcriptome assembler v2.11.0 (Haas et al. 2013) with the option for strand specificity (--SS_lib_type RF). The completeness of the *de novo* transcriptome was assessed with Busco v4.1.4 (Seppy et al. 2019) by comparing it with the metazoan database and analysing the content of expected genes.

Transcripts with a length of < 300 bp were discarded for further analyses. The annotation of the *de novo* transcriptome was performed using the Trinotate functional annotation suite v3.2.1 (Bryant et al. 2017). The annotation included a homology search (BLASTX and BLASTP) against the UniProt Swiss-Prot database. Further annotation information like entries from the Kyoto Encyclopaedia of Genes and

Genomes (KEGG) and the assignment of Gene Ontology (GO) terms were retrieved from a database. The read representation of the assembly was assessed using Bowtie2 v2.4.2 (Langmead and Salzberg 2012).

For the differential expression analysis, reads of all samples were aligned separately onto the *de novo* transcriptome using Bowtie2 v2.4.2. Relative transcript abundance was quantified using salmon v1.3.0 (Patro et al. 2017) and differential gene expression was assessed with the R package DESeq2 (Love et al. 2014). Regarding the differential gene expression analysis, differences in the expression level were regarded as statistically significant at a *p*-value of $p < 0.001$ and a log fold change of two. The 'control'-samples served as reference for expression differences in the 'low-pH'-samples (**Table 3**).

Table 3: Differential gene expression analysis
The table shows the considered comparisons for the differential gene expression. The 'control-samples' thereby served as reference for the 'low-pH samples'.

Dataset	Sampling time	day	Low-pH samples	*n*	vs	Control-samples	*n*
pH exposure experiment	t_0	16	Treatment t_0	5	↔	Control t_0	4
	t_1	18	Treatment t_1	4	↔	Control t_1	5
	t_2	18	Treatment t_2	5	↔	Control t_2	5
	t_3	22	Treatment t_3	5	↔	Control t_3	5
	t_4	32	Treatment t_4	4	↔	Control t_4	5
	t_5	46	Treatment t_5	4	↔	Control t_5	5
	t_6	99	Treatment t_6	4	↔	Control t_6	5
Field samples	-	-	E_{deep}	4	↔	$E_{shallow}$	4

3. Results

3.1 Method development: RNA extraction from cold-water corals

Table 1 shows the description and scoring of each tested method (M1–M15). The spectrometric ratios of each method is available in the **Supplementary table 1.**

Comparing the different sampling methods for molecular analysis, the mean RNA yield of those samples that were snap-frozen in liquid nitrogen was 2.5 times higher than after putting the samples into RNA stabilisation buffer (RSB) (**Table 4**). The spectrometric absorption ratios 260 nm/280 nm and 260 nm/230 nm were closest to the respective target values after the liquid nitrogen sampling. The RNA yield and spectrometric ratios of coral biopsies revealed to be worst of the three methods. The RIN values were not determined.

Regarding the cellular disintegration methods, the mean RNA yield was highest after proteinase K digestion and lowest after the treatment with ceramic beads (**Table 4**). The spectrometric absorption ratios 260 nm/280 nm and 260 nm/230 nm were close to the target values for all cellular disintegration methods, with the exception of the 260 nm/230 nm ratio after the treatment with ceramic beads (0.56±0.23). The RIN value was twice as high after cellular disintegration with lysis buffer than after a proteinase K digestion.

Table 4: Method comparisons
The table shows the mean RNA yield [ng µl^{-1}] ± SD, the mean spectrometric absorption ratios ± SD (260 nm/280 nm and 260 nm/230 nm) and the mean RIN value ± SD of different sampling methods (liquid nitrogen, RNA stabilising buffer (RSB) and biopsies) and cellular disruption methods (proteinase K digestion, ceramic beads and lysis buffer) prior to the RNA extraction.

Methods		Description	RNA yield [ng µl^{-1}]	260/280 (aim: 2.0)	260/230 (aim: 1.8–2.2)	RIN
Sampling method	M1, M2, M5, M6, M10–15	Liquid nitrogen	171.1±90.7	2.17±0.1	1.72±0.73	*NA*
	M1, M2, M5, M6	RSB	72.8±28.3	2.05±0.27	1.01±0.43	*NA*
	M9	Biopsy	9.9±0.2	1.68±0.2	0.6±0.1	*NA*
Cellular disinte-gration	M2, M4, M6, M8–13	Proteinase K digestion	164.9±102	2.04±0.02	1.71±0.06	3.16±1.77
	M1, M3, M5, M7	Ceramic beads	53.4±19.4	2.23±0.05	0.56±0.23	*NA*
	M14, M15	Lysis buffer	157.4±0.14	2.14±0.09	2.08±0.19	7.36±0.43

3.2 Abiotic parameters

pH exposure experiment. The temperature, salinity and the oxygen concentration of the Control and the Treatment group remained stable at collection site ambient conditions (~11.5 °C; ~S_A = 31.6; ~8.94 mg O_2 L^{-1}; **Table 5**) throughout the experimental time, as did the mean pH of the Control group (pH 7.98±0.07). In the Treatment group the mean pH remained stable before, during and after the low-pH treatment (7.91±0.06; 7.33±0.08; 8.01±0.06). The aim of this experiment was a pH difference of 0.6 pH units over two weeks (day 17–32), which was achieved (Δ pH = 0.561±0.067). Before and after the low-pH treatment the Δ pH between the two groups was below 0.08 pH units (**Figure 8**, **Table 5**).

Table 5: Abiotic parameters during the pH exposure experiment
The table shows the mean temperature [°C] ± SD, mean salinity [PSU] ± SD, mean oxygen concentration [mg L^{-1}] ± SD and mean pH [NBS scale] ± SD of the Control and the Treatment group throughout the pH exposure experiment. Mean Δ pH ± SD: absolute pH difference between the Control and the Treatment group before, during and after the low-pH treatment (pH 7.4).

Parameter	Control group	Treatment group		
		Before low-pH day 1–17	**During low-pH** day 17–32	**After low-pH** day 32–99
Temperature [°C]	11.4±0.2	11.5±0.2		
Salinity [PSU]	31.58±0.13	31.60±0.13		
Oxygen [mg L^{-1}]	8.94±0.15	8.93±0.17		
pH [NBS scale]	7.98±0.07	7.91±0.06	7.33±0.08	8.01±0.06
Δ pH [NBS scale]	–	0.034±0.039	0.561±0.067	0.007±0.040
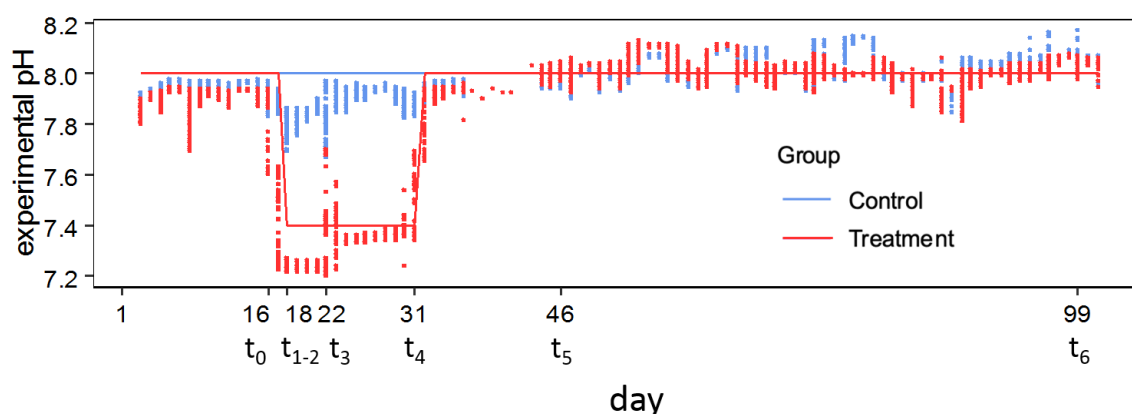
Figure 8: Experimental pH
The plot shows the pH conditions during the experimental time (day) of the Control group (blue) and the Treatment group (red). The solid lines show the aimed pH value of the respective group, while the dots shows the actual pH measurements [NBS scale], monitored every 15 min by the digital IKS control system. From day 36–44 the IKS system was not operable and pH measurements were completed by daily pH measurements, using WTW pH electrodes. t_0 – t_6 mark days of molecular samplings.

Field samples. In summer 2017, the abiotic parameters of the PACOC sampling stations $E_{shallow}$ and E_{deep} were as follows: $E_{shallow}$: depth 20 m, pH 7.8, temperature 12.2 °C; E_{deep}: depth 300 m, pH 7.5, temperature 11.2 °C. Accordingly, the pH difference between the two stations was 0.3 pH units during the sampling time. A long-term monitoring of the abiotic conditions of the sampling site is not available.

3.3 Physiological measurements

Calcification rate. The calcification rate [% d^{-1}] was affected by the fixed parameter of Day ($p < 0.001$), while the pH treatment (Group) had no significant impact (**Table 6**). An increase in the calcification rate was seen throughout the experimental time, with the calcification rate being significantly higher on day 99 (t_6) compared to day 16 (t_0). On day 31(t_4), the calcification rate of the Treatment group was trending lower compared to the Control group. However, no significant difference between the Control and the Treatment group was detected (**Figure 9**).
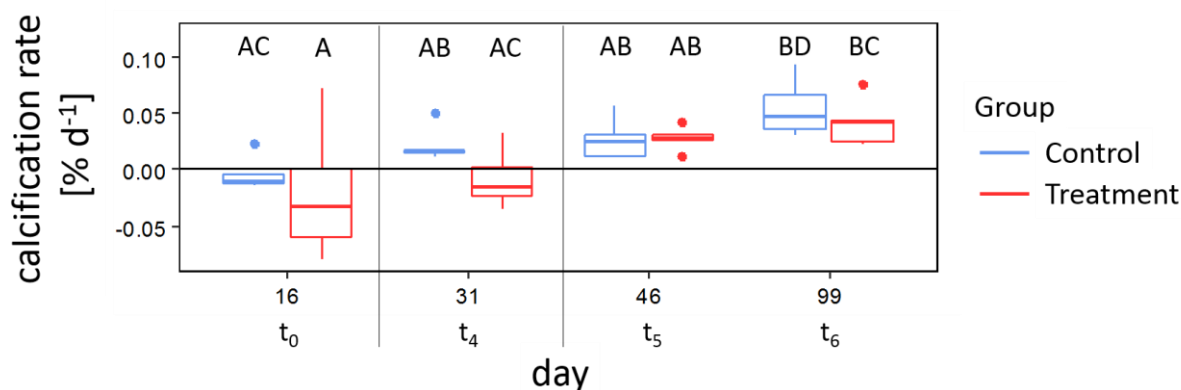
Figure 9: Calcification rate
Calcification rate [% d^{-1}] of *Desmophyllum dianthus* of the Control (blue) and Treatment group (red) was plotted against experimental days. $t_0 - t_6$ mark days of molecular samplings. Different capital letters indicate significant differences between groups (*n* = 5; two-way ANOVA with post hoc Tukey test; *p* < 0.05). Black horizontal line marks 0 % $CaCO_3$ aggregation. Black vertical lines: start and the end of the low-pH treatment (pH 7.4) of the Treatment group. Boxplots: box: quartiles; horizontal bar within the box: median; whiskers: minimum and maximum measurement; dots: outliers.

Respiration rate. The coral's respiration rate was clearly distinguishable from microbial background respiration (0.01 ± 0.01 mg h^{-1}, data not shown) and only affected by the fixed parameter of Day ($p < 0.0001$). Compared to day 16, the respiration rate was 56–64 % higher on day 99 in both groups, being significantly higher to all previous measurements. The fixed parameter of Group had no impact on the respiration rate ($p > 0.05$). The median respiration rate of the Treatment group on day 18–32 was trending lower compared to the Control group (**Table 6**, **Figure 10**).
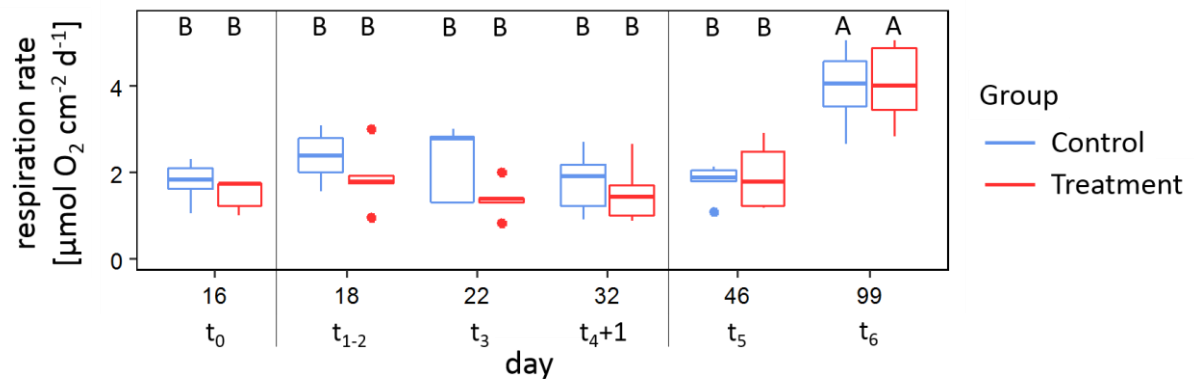
Figure 10: Respiration rate
The respiration rate [μmol O$_2$ cm^{-2} d^{-1}] of the *Desmophyllum dianthus* of the Control (blue) and Treatment group (red) was plotted against experimental days. $t_0 - t_6$ mark days of molecular samplings. Different capital letters indicate significant differences between groups ($n = 5$; two-way ANOVA with post hoc Tukey test; $p < 0.05$). Black vertical lines within pH exposure experiment: start and the end of the low-pH treatment (pH 7.4) of the Treatment group. Boxplots: box: quartiles; horizontal bar within the box: median; whiskers: minimum and maximum measurement; dots: outliers.

Table 6: Statistical results
Results of the analysis of variance (two-way ANOVA) to assess the effect of the fixed parameters Day and Group on the variability of the calcification rate [% d^{-1}] and respiration rate [μmol O$_2$ cm^{-2} d^{-1}] of *Desmophyllum dianthus* in the pH exposure experiment.

Parameter	numDF	F-value	*p*-Value
Calcification rate			
Day	3	12.99	**< 0.0001**
Group	1	1.509	0.23
Respiration rate			
Day	5	24.11	**< 0.0001**
Group	1	1.13	0.67

Note: The calcification and respiration rate were tested against the additive effects of day and group. numDF: numerator degrees of freedom. Statistically significant values ($p < 0.05$) are marked in bold.

3.4 Molecular sample quality

RNA. The mean RNA concentration of all samples was 183.97±65.7 ng µl^{-1} (**Figure 11a**). Four samples had a total RNA yield below 1000 ng, with 774 ng being the lowest yield. The analysis of the spectrometric ratios of the sample's absorption at 230, 260 and 280 nm, showed that the samples were free of contaminants, with the mean 260 nm/280 nm ratio of all samples being 2.13±0.03 (target value: 2.0) and the 260 nm/230 nm value being 2.05±0.16 (target value: 1.8–2.0) (**Supplementary table 1**). The mean RNA integrity number (RIN value) of the pH exposure experiment samples was 6.99±0.94 (max. value: 10) (**Figure 11b**). The RIN value of the field samples was not determined.

cDNA. The mean generated cDNA yield of all samples was 147.16±44.07 nM (**Figure 11c**). Two samples had a cDNA yield below 10 nM. The DNA integrity number (DIN) could not be dtermined as it can only be generated of genomic DNA.

Reads. On average 15,062,518±1,465,311 raw-reads were processed per sample, summing up to a total of ~2.197 billion raw-reads. The reads length ranged between 35–151 base pairs, with a mean GC (guanine-cytosine) content of 43.5±0.4 %. After the data were quality trimmed (see section 2.5) the paired samples consisted of an average of 14,327,580±1,643,244 reads per sample, summing up to a total of ~2.196 billion reads. The reads length ranged between 36–151 base pairs, with a mean GC content of 43.3±0.4 % (**Supplementary table 2**).

Reference transcriptome and annotation. The *de-novo* assembly of *Desmophyllum dianthus* was compiled from 74 cDNA libraries, containing ~2.196 billion paired-end Illumina reads. After contigs with a size of < 300 bp were discarded, the reference transcriptome consisted of 1,429,568 contigs with a mean size of 785 bp and N50 of 958 bases. The reference transcriptome had a mean GC content of 40.81 %. The comparison of the reference transcriptome with the metazoan BUSCO database revealed that 0.6 % of the conserved genes were missing. 99.1 % of complete BUSCO matches were found. In total, GO terms were assigned to 252,905 transcripts (**Supplementary table 3**).
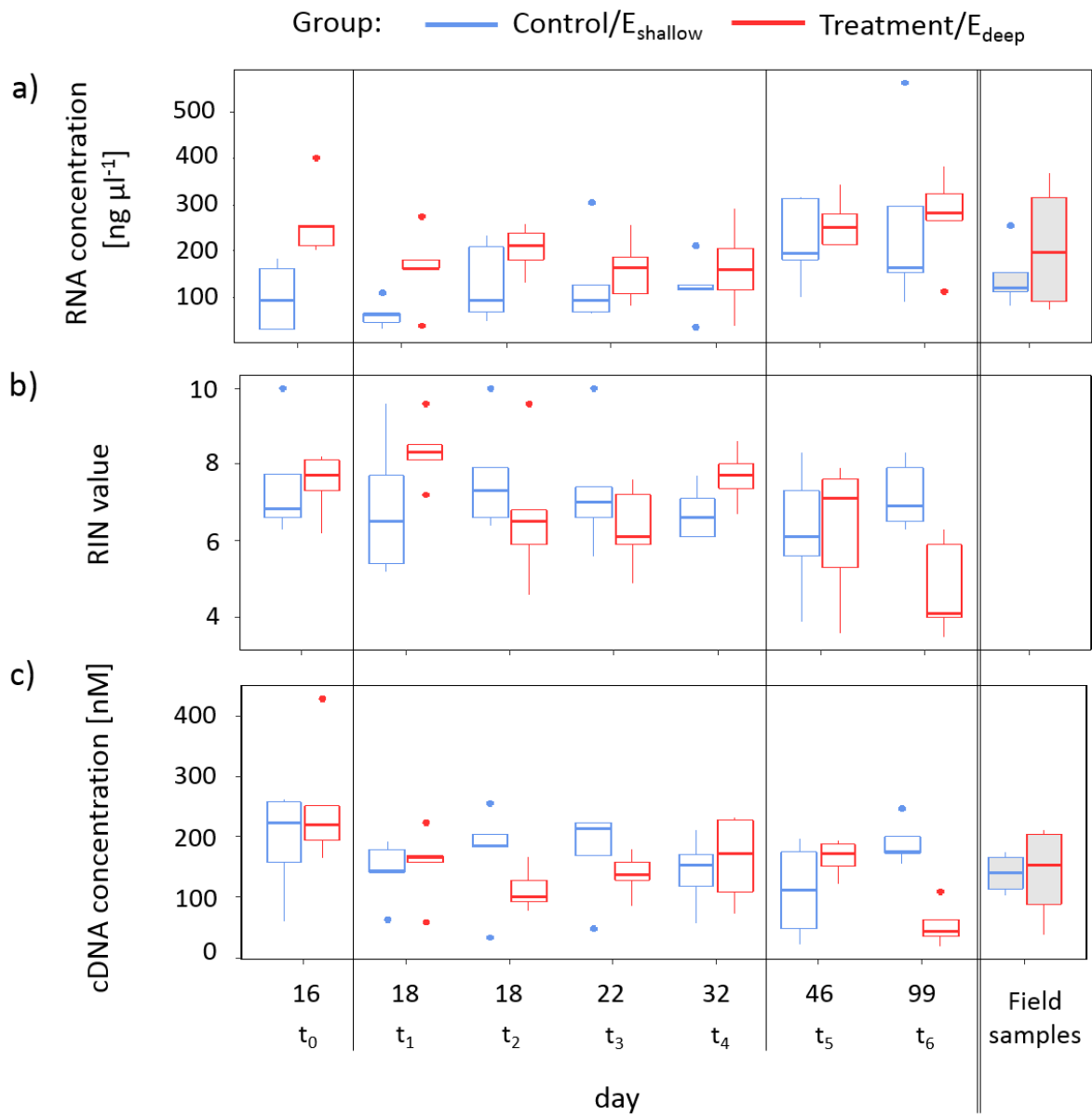
Figure 11: Molecular sample quality

The **a)** RNA yield [ng µl^{-1}], **b)** RNA integrity numbers (RIN) and **c)** cDNA yield [nM] of the pH exposure experiment (white boxplots n=4–5) and field samples (grey bloxplots n=4) were plotted of each treatment (blue frame: Control/E$_{shallow}$; red frame: Treatment/E$_{deep}$) of all sampling times (t_0–t_6: pH exposure experiment; t: field samples). Black vertical lines within pH exposure experiment: start and the end of the low-pH treatment (pH 7.4) of the Treatment group. Double black vertical line: separation of the pH exposure experiment from field samples. Boxplots: box: quartiles; horizontal bar within the box: median; whiskers: minimum and maximum measurement; dots: outliers.

3.5 Differentially expressed genes

Comparing the number of differentially expressed genes (DEGs) of the low-pH samples with their control (**Table 3**), 6331 regulations were found in total. Of all regulations, 20.4 % were annotated (**Figure 12**).

In the pH exposure experiment, the number of DEGs ranged between 300 and 360 from $t_0 - t_3$, while it ranged between 600 and 1200 DEGs at the least three sampling times of the experiment (t_4–t_6). Two hours after the pH decrease (t_1), the number of upregulated genes almost halved compared to the gene expression before the low-pH conditions (t_0), while the number of downregulated genes increased by ~45 %. During the low-pH treatment (t_1–t_4) the number of upregulated genes increased steadily, while the number of downregulated genes decreased until five days after the pH-lowering event (t_1–t_3). After two weeks of pH 7.4 treatment (t_4), the number of downregulated genes was two to four times as higher as in the first week of low-pH treatment (t_1–t_3). Comparing the number of regulated genes before (t_0) and two weeks after the low-pH conditions (t_5), the number of upregulated genes stayed within the same magnitude, while the number of downregulated genes was ~2.8 times higher on t_5. On t_6 the number of up- and downregulated genes was highest of all considered sampling times.

Of all regulations found in the pH exposure experiment and the field samples, ~38 % were found in the field samples, with as many up- as downregulated genes.
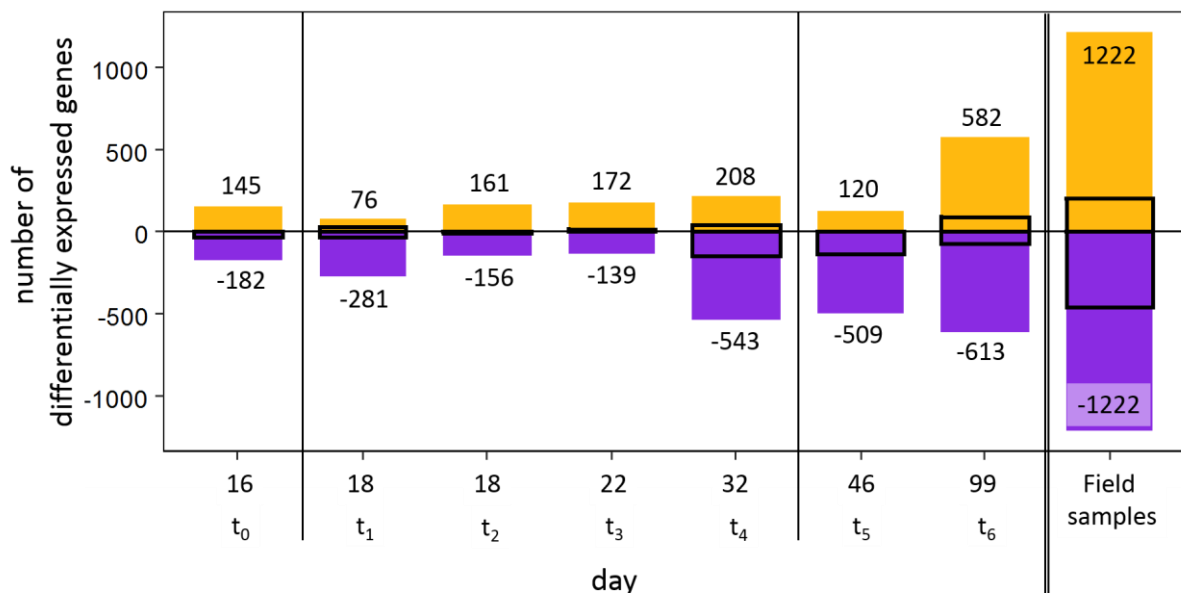
Figure 12: Differential gene expression patterns
Transcripts of all sampling times of the pH exposure experiment (t_0–t_6) and the field samples whose expression level changed significantly (adjusted $p > 0.001$) are indicated as follows: upregulated genes: yellow; downregulated genes: purple. Total number of transcripts of each category are indicated above or below the corresponding bars. Portion of annotated transcripts are marked with a black frame within the corresponding bars. Black vertical lines within pH exposure experiment: start and the end of the low-pH treatment (pH 7.4) of the Treatment group. Double black vertical line: separation of the pH exposure experiment from field samples.

3.6 pH exposure experiment vs. field samples

In total, 6,331 transcripts were regulated in the pH exposure experiment and the field samples, with 2,686 up- and 3,645 downregulations. Thereby, 18 transcripts were mutually upregulated and 34 mutually downregulated, accounting for a proportion of ~0.82 % (**Figure 13**).
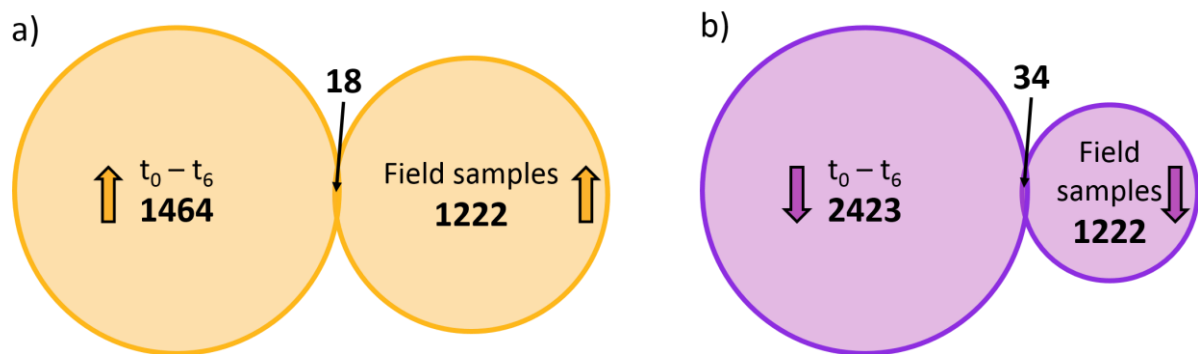
Figure 13: pH exposure experiment vs. field samples
The Venn diagrams show the relationship between the differentially expressed genes (DEGs) (adjusted $p > 0.01$) of the pH exposure experiment (t_0–t_6) and the field samples compared to their control as follows: **a)** upregulated genes. **b)** downregulated genes. Left circle t_0–t_6: number of all DEGs of the pH exposure experiment. Right circle: number of all DEGs of the field samples. Overlap between the circles: number of mutually regulated genes between the pH exposure experiment and the field samples.

3.7 Annotation of the differentially expressed genes

The exposure to low-pH conditions resulted in several differentially expressed genes involved in cellular stress response, protein formation and stability and cellular structure. These gene groups were chosen to show overall developments of the samples at different sampling times. Therefore, they are only a proportion of the total amount of annotated genes. A table of all annotated differentially expressed genes can be found in the **Supplementary table 4**.

Comparing the gene expression of the Treatment group with the Control group at different sampling times of the pH exposure experiment, some overall patterns were observed (**Figure 14**). Heat shock protein-like genes were downregulated at the end of the low-pH conditions, as well as two weeks after the low-pH conditions. Histone-like genes, ribosomal factors and elongation factor-like genes were downregulated at the beginning of the low-pH conditions (t_1) and slightly upregulated after the low-pH conditions (t_5–t_6). The same pattern was observed for ubiquitin. Cytoskeletal components (actin and tubulin) were strongly downregulated during (t_1–t_4) the low-pH conditions. After the low-pH conditions, the expression of actin- and tubulin-like genes increased slightly compared to the previous sampling times. Ribosomal factors, ubiquitin and cytoskeletal components were found downregulated before the start of the low-pH conditions (t_0). Only single genes of the here considered groups were found regulated for t_2 and t_3. In total, less than 4 % of the detected regulations were annotated at these two sampling times (**Figure 12**).

Regarding the differential gene expression of the field samples, all considered gene groups were differentially expressed comparing the low-pH conditions (E_{deep}) with the control ($E_{shallow}$). Apart from metalloproteinase and zinc finger-like genes, all examined gene groups were downregulated in the E_{deep} samples compared to $E_{shallow}$.
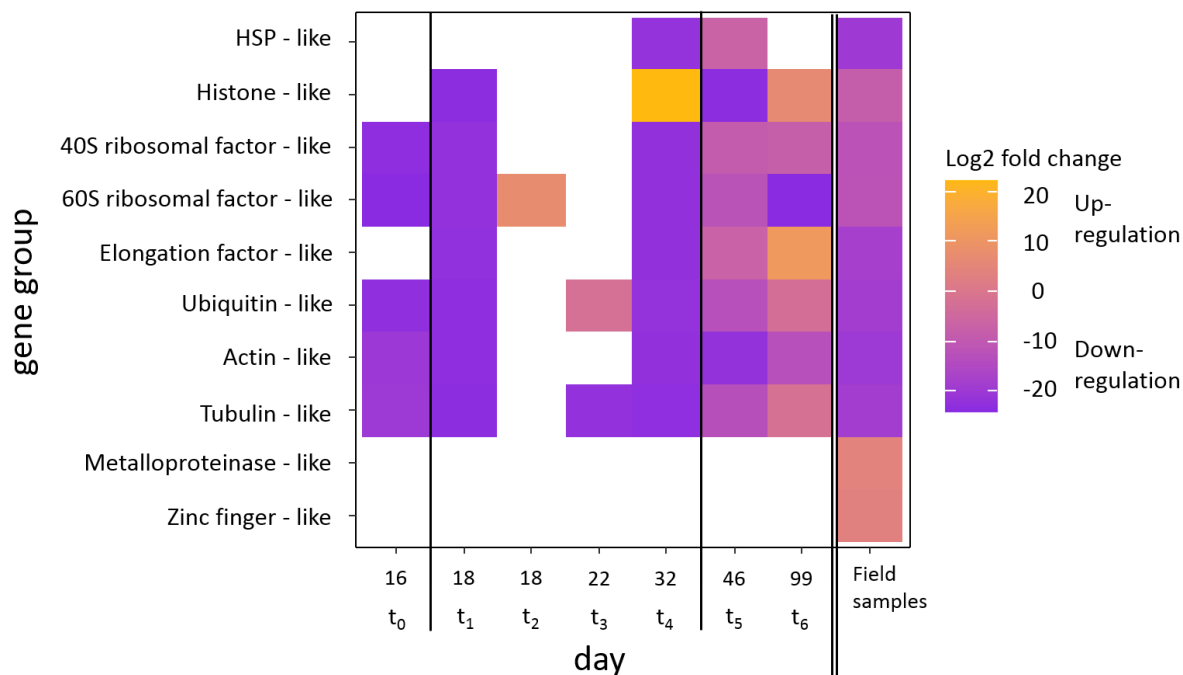
Figure 14: Differential expression of selected gene groups
Mean log2 fold change of selected gene groups of all sampling times of the pH exposure experiment (t_0–t_6) and the field samples whose expression level changed significantly (adjusted $p > 0.001$) compared to their control are indicated as follows: yellow: upregulated gene group; purple: downregulated gene group; white: gene group was not differentially expressed. Black vertical lines within pH exposure experiment: start and the end of the low-pH treatment (pH 7.4) of the Treatment group. Double black vertical line: separation of the pH exposure experiment from field samples.

Within the generated *de novo* assembly 29 carbonic anhydrase-like genes were annotated. Further, 586 genes were found, coding for bicarbonate ion transporters, and 729 genes were annotated coding for proton pumps. The expression level of none of these gene groups changed significantly.

4. Discussion

Scleractinian cold-water corals (CWCs) act as important foundation species in deep-sea ecosystems (Roberts et al. 2006). Currently, they are experiencing drastic changes in their habitat's environment. According to the RCP8.5 scenario, a decline of the seawater pH of 0.15 pH units on average in depths between 200 and 2,500 m is projected until the year 2100. This results in a decline of the aragonite saturation state (IPCC 2019) and a potential habitat loss for CWCs due to an increased energy demand for calcification that exceeds their tolerance range (McCulloch et al. 2012b). Several studies investigating the acclimation potential of CWCs to low-pH conditions, are reflecting the projected atmospheric carbon dioxide partial pressure range for the next century of $400\,\mu atm$–$1,000\,\mu atm$ (seawater ~pH 8.0–7.7), e.g. Form and Riebesell (2012), Maier et al. (2013), Carreiro-Silva et al. (2014), Gori et al. (2016) and Büscher et al. (2017). However, in the Chilean Comau fjord, the CWC *Desmophyllum dianthus* has been recorded to thrive at pH 7.4 and an aragonite saturation state of $\Omega_{arag} = 0.5$ (Fillinger and Richter 2013; Jantzen et al. 2013), which is why pH 7.4 was chosen as low-pH conditions in the conducted pH exposure experiment. Given the occurrence of natural fluctuation in seawater pH (Pelejero et al. 2010), this study can be considered a natural pH oscillation analogue.

The presented results contribute to the knowledge of regulatory processes enabling *D. dianthus* to thrive at natural low-pH conditions. An overall high tolerance of *D. dianthus* towards the experimental pH variations was detected, on a physiological and transcriptomic level. During the two week exposure to pH 7.4, a metabolic suppression as short-term reaction was observed. Further, the data suggest a high recovery potential of the corals on a physiological level. Detectable regulations became only evident on the transcriptomic level, showing an increased down-regulation of genes. After an increase of the available food during the recovery phase, a strong response of the physiology and the gene expression was observed, with significantly higher calcification and respiration rates. Regarding the number of differentially expressed genes after an increase in the food availability, a large difference was found between the Control and the Treatment group, indicating that the exposure to low-pH conditions influenced the reaction. The main findings of the conducted pH exposure experiment are summarised in the comprehensive **Figure 15**, illustrating the acclimation of *D. dianthus* towards the changes in pH in the course of the experiment. In the following, I will lead through these findings, based on the posed hypothesis (section 1.5) and provide an integrative discussion about the observed responses towards the experimental changes in seawater pH. Additionally, the gene expression patterns of the pH exposure experiment will be put in the context of the observed gene expression profiles of the field samples.
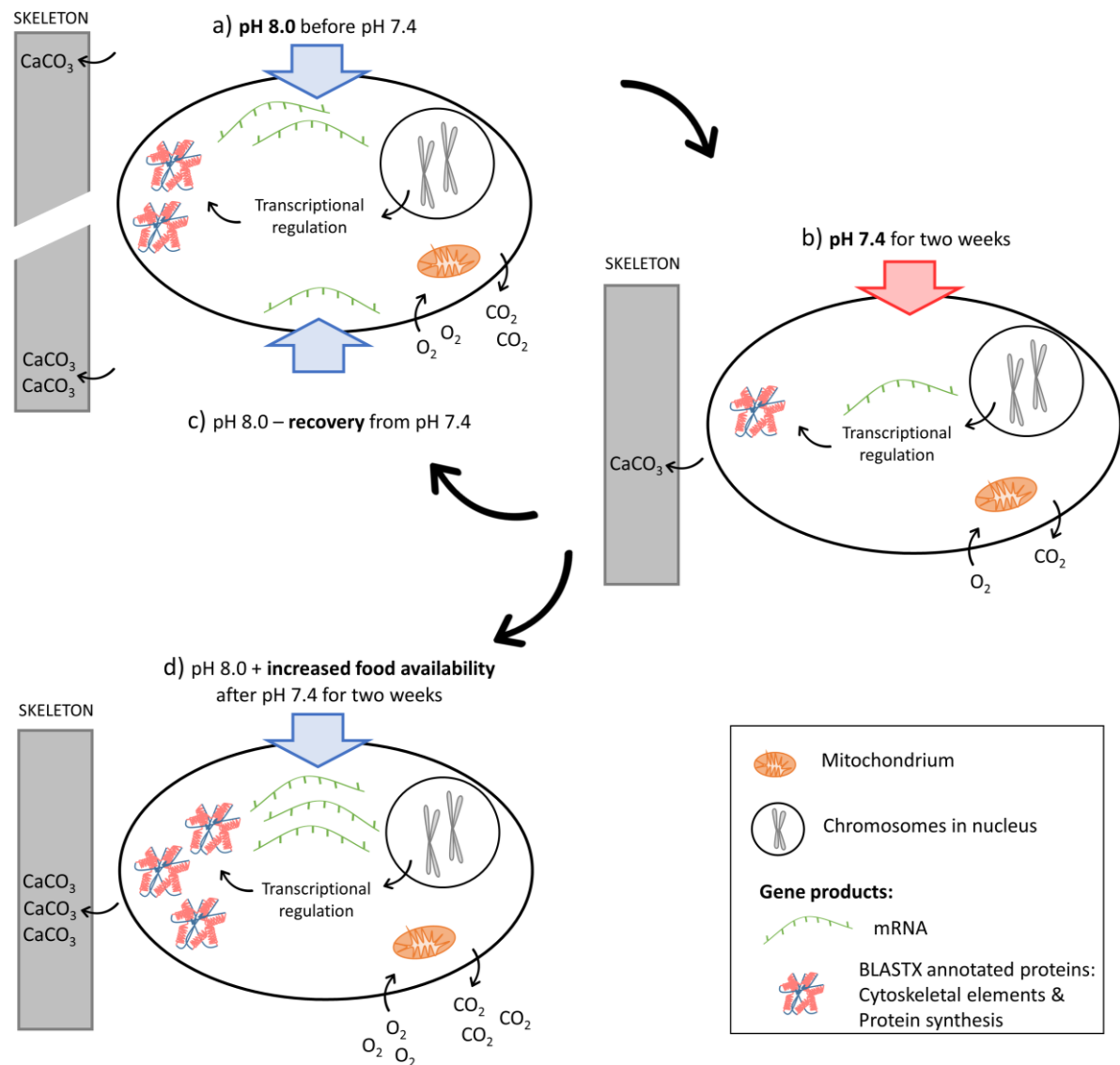
Figure 15: Schematic responses of *Desmophyllum dianthus* in the course of the pH exposure experiment

The regulations in the tissues of *D. dianthus* is illustrated during the pH exposure experiment (a–d), showing the impact on calcification ($CaCO_3$ deposition to the skeleton), respiration ($O_2 \Rightarrow CO_2$) and transcriptional regulation (chromosome $\Rightarrow$ BLASTX annotated proteins). **a)** Initial status of *D. dianthus* before the experimental pH reduction, being acclimated to pH 8.0. The calcification and respiration rate and number of differentially expressed genes are on a medium level. **b)** Compared to the initial status, the calcification rate remained unaffected during the exposure of corals to pH 7.4, while the respiration rate and transcriptional regulation are downregulated, indicating metabolic suppression. BLASTX annotated proteins coding for protein synthesis and cytoskeletal elements were downregulated. **c)** During the recovery phase at pH 8.0, the respiration rate was similar to the initial status and the calcification rate increased, indicating a high recovery potential. In the transcriptome more downregulated genes were observed compared to the initial status, suggesting that recovery from the exposure to pH 7.4 was not completed after two weeks of recovery. **d)** After the increase of the food availability during the recovery phase (pH 8.0), the calcification and respiration rate were significantly higher compared to the initial status. The overall increase of the calcification rate may be due to intrinsic controls. Further, the highest number of differentially expressed genes was found, indicating that the nutrition state has a high influence on the corals performance. Genes coding for protein synthesis and cytoskeletal elements were slightly upregulated.

4.1 Method development: RNA extraction from cold-water corals

The transcriptome is representing the linking step between cellular signalling pathways and physiological responses towards a stressor (Kültz 2005) and can be regulated within hours (acclimation) (Moya et al. 2015). Therefore, the sampling for transcriptomic analysis poses a critical step in the workflow, as it involves the risk to create artefacts in the gene expression patterns, reflecting a response to the sampling stress and not the tested environmental parameter. The best method to minimize these artefacts is by putting the samples in liquid nitrogen directly after sampling, as all chemical processes are immediately stopped by the very low temperatures (Mazur 1988). Therefore, the highest RNA quality was hypothesized after a sampling in liquid nitrogen (section 1.5; **Hypothesis I**), which was confirmed by this study.

However, during field expeditions, liquid nitrogen might not always be available. A further sampling possibility would be to put the samples directly in an RNA stabilising buffer (RSB). Evaluating the RNA quality after sampling in RSB, extracting a high-quality RNA seems to be possible. Sufficient RNA for a cDNA library preparation was extracted. Evaluating the spectrometric ratios, the 260 nm/230 nm indicated the presence of contaminants. However, this was probably due to a contamination with $CaCO_3$, as two of the four replicates were treated with ceramic beads (see next paragraph). Before applying this sampling method, the RNA integrity as well as the influence on the differential gene expression have to be evaluated, as biological processes might not be stopped immediately.

RNA was also extracted from biopsies of a coral's tentacle. Biopsies would enable to sample one individual throughout an experiment, excluding inter-individual differences as a confounding factor. Further, they would allow an experimental set-up with less individuals. However, the implementation of biopsies proved to be difficult, as a failed approach to take a biopsy led the corals to retract their tentacles for several hours. Furthermore, the extracted RNA yield was too little for a cDNA library preparation. Considering the high concentration of contaminants (low 260 nm/230 nm ratio), the RNA extraction might have been inhibited by coral mucus, clogging the extraction columns. The CWC-mucus is serving a variety of purposes, e.g. in feeding, reproduction or protection against pollutants and stressors (Brown and Bythell 2005). An extraction from coral tissue biopsies might require a previous washing step to reduce the mucus' carbohydrates in the samples.

CWCs consist of only four cell layers (Allemand et al. 2004) and therefore have a low tissue-to-skeleton ratio. As it is not possible to remove the tissue from frozen corals skeleton without thawing the tissue and risking RNA degradation, parts of the skeleton (and therefore $CaCO_3$) will always be present during RNA extractions from CWCs. Barton et al. (2006) found an inhibiting effect of $CaCO_3$ during DNA extraction from low-biomass carbonate rock. Following these results, the $CaCO_3$ concentrations were intended to be kept as small as possible for RNA extractions, expecting the RNA quality to be higher in samples with less dissolved $CaCO_3$ (section 1.5; **Hypothesis II**). The effect of different $CaCO_3$

concentrations in the samples was assessed by a different mechanical impact on the $CaCO_3$ skeleton during cellular disintegration. The concentration of $CaCO_3$ was assumed to be highest after a mechanical cellular disintegration using ceramic beads, and smallest after the incubation of coral pieces in proteinase K. Confirming this assumption, the RNA yield was three times higher after the proteinase K digestion than after a treatment with ceramic beads. Further, the spectrometric ratios indicated less contaminants. However, the RNA was strongly degraded after proteinase K digestion, probably due to long incubation times of the samples at high temperatures.

The best integrity and highest yield of RNA was obtained by grinding the corals under liquid nitrogen in a mortar to a fine powder and incubating them in Lysis Buffer. Bigger pieces of the skeleton were pelleted down and removed in the first step of the RNA protocol. No inhibiting impact of the remaining, dissolved $CaCO_3$ was detected. However, to be able to reject the second hypothesis completely, a linear regression analysis has to be conducted assessing the RNA quality as a function of the $CaCO_3$ concentrations.

4.2 Calcification and respiration rates

Regarding the physiological measurements of *D. dianthus* during the experiment, the calcification rate was expected to decrease and the respiration rate to increase under low-pH conditions (section 1.5, **Hypothesis III**).

No statistically significant difference in the calcification rate of the Control and the Treatment group was detected after two weeks of low-pH conditions (t_4). However, the calcification rate of the Treatment corals was close to zero or even negative, with the median being lower than in the Control corals. During a one week exposure to pH 7.7, Form and Riebesell (2012) found a decreasing trend in the calcification rate was also for the CWC *Lophelia pertusa*. After six months, the declining trend in calcification reversed, with the low-pH corals showing a higher calcification rate compared to their control. This indicates a multi-stage response of CWCs to low-pH conditions and that a decline of the seawater pH might have a less drastic long-term impacts on calcification than previously hypothesized. Contrary to these results were the findings by Maier et al. (2013), who also discriminated between the short- (immediately after lowering the pH) and long-term (9 months) responses of *L. pertusa* to low-pH conditions (pH 7.7). The different findings may be due to unknown intrinsic controls (e.g. season or age), having an impact on the CWCs performance.

Comparing the calcification rates before (t_0) and two weeks after the low-pH conditions (t_5), this study provides an insight into the recovery potential of *D. dianthus* after being exposed to low-pH conditions. Detecting no significant influences dependent on the previously experienced pH conditions and calcification rates that were higher on t_5 than on t_0, no negative effects of the low-pH exposure on the calcification rate was detected. Tough describing the recovery of zooxanthellate corals from several

months of low-pH stress, Fine and Tchernov (2007) and Movilla et al. (2012) also described a high recovery potential and acclimation capacities of corals to pH fluctuations.

An increase of the calcification rate during the entire experiment was detected that was independent of the experienced seawater pH. This was also observed by Maier et al. (2013) during a nine months experiment with *Lophelia pertusa*, indicating that either aquarium conditions other than pH or intrinsic controls have influenced the calcification rates. As the abiotic conditions of the aquarium systems remained stable throughout the here conducetd pH exposure experiment, the observed pattern of the calcification rate is thought unlikely to respond to abiotic factors. Considering intrinsic controls, Hamel et al. (2010) described a seasonal growth pattern for the CWC *Flabellum alabastrum*, with growth peaking at the end of summer. They further pointed out that the observed growth maximum for *F. alabastrum* correlated with the maximum detritus deposition, suggesting that greatest $CaCO_3$ precipitation depends on the food availability. Therefore, the significantly higher calcification at the end of the experiment rate may be due to the increased food availability.

The results on calcification presented in this study indicate that the short-term fluctuations in seawater pH might have a less drastic impact on the CWCs calcification than previously hypothesised. However, a decreased pH may have negative effects on the calcification of corals other than the ones tested in the present study. Hennige et al. (2015) and Büscher et al. (2017) demonstrated that although the CWC *L. pertusa* was found to be able to acclimate to a seawater pH 7.7 on a short- and long-term basis and showed no significant differences in the calcification rates, the crystal organisation of its aragonite skeleton changed under low-pH conditions. This led to less organisation of the aragonite crystals and a decreasing breaking strength of the coral skeleton.

Calcification is an energy-demanding process (Allemand et al. 2004) that depends on the carbonate chemistry of the seawater (Holcomb et al. 2014). Especially considering that the calcification rates were not significantly decreasing at low-pH conditions, the cellular costs were expected to increase, as the maintenance of performance at suboptimal conditions requires more energy (Kültz 2005) (section 1.5, **Hypothesis III**). The respiration rate was evaluated as proxy for a change in the cellular costs, since it is important to produce ATP and provide energy for metabolic processes. A high respiration rate would therefore indicate a high energy demand. However, this expectation was not confirmed. During the two weeks exposure to pH 7.4 (t_1–t_4), no significant increase of the Treatment group's respiration rate was detected. On the contrary, the median respiration rate was lower compared to the Control group. This might be an indicator for a decreased ATP requirement due to metabolic suppression (Findlay et al. 2011). Metabolic suppression as response to pH fluctuations has been demonstrated in several organisms (Pörtner 2008; Todgham and Hofmann 2009). A significant decrease of the respiration rates was also found by Hennige et al. (2014) for *L. pertusa* after exposure to pH 7.7 for two weeks. Regarding long-term exposure to low-pH conditions, Carreiro-Silva et al. (2014) found the highest respiration rates for *D. dianthus* after eight months being exposed to pH 7.7. These differences may be another indicator for

a multi-stage response of CWCs to low-pH conditions, with the reduction of energy-demanding pathways serving as short-term reaction rather than being a long-term solution, as it is likely to have fitness costs (Kaniewska et al. 2012).

Comparing the respiration rates of the Control and the Treatment group before (t_0) and two weeks after the low-pH conditions (t_5), no difference was observed, confirming the suggestion of a high recovery potential of *D. dianthus* from low-pH conditions.

On t_6, the respiration rates of the Control and the Treatment group was approx. twice as high as the respiration rates observed at all previous sampling times, indicating that the change of food availability had a higher impact on the metabolic rates than the low seawater pH within the experimental range. The negative impact of food exclusion on the respiration rate has previously been described by Naumann et al. (2011), who found a significant increase in the oxygen demand with increasing food availability.

Summarizing the physiological response to the short-term exposure of *D. dianthus* to pH 7.4, the hypothesis of a decrease in calcification and an increase in respiration was not confirmed. The calcification rate increased steadily, independently of the pH treatment, indicating an influence of intrinsic controls (**Figure 15**). Instead of an increased energy demand to mitigate negative impacts of the low-pH conditions, a general suppression of metabolism was found (**Figure 15b**). Considering the existence of large-scale natural fluctuations of the seawater pH (Pelejero et al. 2010), and the occurrence of *D. dianthus* in a wide range of seawater pH (Fillinger and Richter 2013; Jantzen et al. 2013), the observed physiological recovery potential might be the result of evolutionary adaption.

4.3 Differential gene expression analysis

The RNA quality of all 76 samples was high enough for the cDNA library preparation, due to the method development for RNA extraction from CWCs. After the cDNA preparation, two samples had a cDNA yield that was below 10 nM and could not be used for sequencing. Therefore, the *de novo* transcriptome was generated using 74 cDNA libraries (pH exposure experiment: 66; field samples: 8), including a wide range of organismal responses. This led to an almost complete *de novo* transcriptome, containing 99.4 % of conserved genes. The mean GC-content of the *de novo* transcriptome of 40.81 % is comparable to the reported GC-content of other azooxanthellate, deep-sea Hexacorallia (Yum et al. 2017).

The analysis of differential gene expression (DGE) profiles can be used to detect molecular mechanisms that are regulated to acclimate to a change of the abiotic conditions and maintain physiological performance (DeBiasse and Kelly 2016).

Analysing the gene expression patterns observed in this study, differences between the Control and the Treatment group were observed before the start of low-pH exposure (t_0). Considering that the

analysis was corrected for multiple testing and genes were only regarded as differentially expressed at a significance level of adjusted $p < 0.001$, only one of thousand significant results have to be regarded as statistically false positive. Given that the Control and the Treatment corals experienced the same handling and were exposed to identical controlled conditions before the reduction of the seawater pH, differences in the gene expression patterns on t_0 are attributed to inter-individual differences.

As response to the relatively sudden pH decrease of 0.6 pH units in the pH exposure experiment, a shock reaction was expected, becoming evident in a strong upregulation of genes (section 1.5; **Hypothesis IV**). However, directly after low-pH conditions were reached, the expression pattern did not show an upregulation but a general downregulation of genes. This immediate downregulation may be a further indicator for metabolic suppression that was observed on a physiological level. Vidal-Dupiol et al. (2013) detected a similar gene expression pattern for the tropical coral *Pocillopora damicornis*, showing more down- than upregulated genes after an exposure to pH 7.4 for three weeks. They found the level of downregulated genes increasing with lowering seawater pH (pH 8.0–7.2), hypothesising a trade-off mechanism, necessary for energy savings.

Within the following two weeks of low-pH conditions, the number of upregulated differentially expressed genes (DEGs) increased steadily, while the number of downregulated DEGs was decreasing within the first week (t_3) before it increased within the second week (t_4). The general dynamic gene expression is indicating an organismal acclimation processes to the pH fluctuations and exposure time.

Comparing the expression patterns directly before (t_0) and two weeks after (t_5) the low-pH treatment, it was hypothesised that the number of DEGs were similar, reflecting a high recovery potential (section 1.5, **Hypothesis IV**). That was confirmed for the number of upregulated genes. After the two weeks of low-pH treatment, more downregulated genes were found compared to the start of the experiment. This may be an indication for the influence of the low-pH conditions on the transcriptomic regulation lasting longer than two weeks of exposure to ambient pH conditions (pH 8.0).

The most explicit transcriptomic reaction of the Treatment corals, was found due to the change in food availability, showing the highest numbers of DEGs within the pH exposure experiment on t_6. The differential gene expression analysis performed in this study, only shows differences between the Control and the Treatment group at each sampling time. Considering that the abiotic conditions other than pH remained stable throughout the experimental time and assuming that the corals of the Control group did not experience stress, requiring transcriptomic regulation, the observed differences in gene regulation on t_6 are due to the two weeks of low-pH treatment in combination with the altered food availability. It might be that the metabolic suppression during the low-pH conditions had an influence on the metabolic reaction towards an increased food availability. Little is known about the nutrition of CWCs but the findings of Maier et al. (2016) and Martínez-Dios et al. (2020) show that the resistance of CWCs towards abiotic stressors, such as declining seawater pH is strongly dependent on the food availability. Büscher et al. (2017) further showed in a multi-stressor experiment that *Lophelia pertusa* was more susceptible to elevated temperatures and low-pH conditions after six months, if they had

experienced food limitation. To assess to which extend food availability influences the acclimation potential of *D. dianthus* towards low-pH conditions further multifactorial experiments have to be conducted, also analysing the impact of food limitation on the recovery potential.

In synopsis, the observed gene expression patterns displayed a high plasticity in regulation, showing a metabolic suppression at the beginning of the exposure of low-H conditions, which became evident in a general downregulation of genes (**Figure 15b**). Further it seemed, as if the recovery from low-pH conditions on a transcriptomic level had a high influence on the change in food availability five weeks after the start of the recovery phase (**Figure 15c-d**). As the detected regulations on a cellular level did not become evident on organismal level, the tested pH range is considered to be within the acclimation potential of *D. dianthus*, reflecting phenotypical buffering. The high acclimation potential of *D. dianthus* towards short- and long-term exposure to low-pH conditions was also shown by Vidal-Dupiol et al. (2013) and Carreiro-Silva et al. (2014).

4.4 Transcriptomic response due to experimental changes in pH

Although the analysis of differential gene expression patterns is a powerful method to resolve regulations on a cellular level, the gene ontology (GO) database (Ashburner et al. 2000) is still strongly biased towards highly conserved genes in model organisms (Moya et al. 2012). Interpreting the differential gene expression of non-model organisms is therefore difficult as only a small percentage of the differentially expressed genes are annotated. This became evident in less than 4 % of the DEGs being annotated at the sampling times t_2 and t_3. At these sampling times, within the first week of low-pH conditions, the regulation of many coral specific genes is expected, e.g. coding for modifications in the calcification metabolism or stress-responses. These pathways might be underestimated in the here shown results. In order to obtain as complete a picture as possible, all annotated genes were analysed, regardless of which taxon they were described for, assuming that the respective genes are orthologous.

As response to the low-pH conditions, the expression of genes that are involved in cellular stress were expected to be upregulated in those corals who experienced two weeks of exposure to pH 7.4 (section 1.5; **Hypothesis V**). However, the analysis of the differential expression of the cellular stress response (CSR) did not confirm this hypothesis.

The CSR is a mechanism that is activated in response to changes or fluctuations of environmental factors to prolong the survival of cells. Independently of the stressor, the CSR is activated to prevent macromolecular damage (Kültz 2003). Due to a core stress response appearing early in evolution, cell cycle controls, protein and DNA chaperoning and repair, and modifications of the metabolism are highly conserved across a wide range of species (Kültz 2003, 2005). Heat shock proteins (HSPs) of the gene families HSP70 and HSP90 are representing a part of the CSR that exist in all organisms. Although they

were first described as response to heat-stress, they were found to be induced by various other stressors (Lindquist and Craig 1988; Kaufmann 1990), e.g. Carreiro-Silva et al. (2014) found a significant increase in the expression of HSP70-genes of *D. dianthus* as response to low-pH conditions after an eight months exposure to pH 7.7. Despite HSPs being annotated in the generated *de novo* transcriptome, their differential expression was not prominently represented. Instead of the expected expression increase of HSPs in the Treatment group directly after the establishment of low-pH conditions, their expression did not differ between the Control and the Treatment corals. Interpreting this result, the cellular pool of HSPs has to be divided into constitutive and inducible HSPs (Chen et al. 2006). The cellular concentration of constitutive HSPs are determined by intrinsic controls, while the inducible HSPs are responding to variations of external factors. It has to be assumed, the constitutive HSP concentration would show no change in either of the coral groups, as both were treated the same except for the change in seawater pH. Therefore, the anticipated response in HSP was expected to be constraint to the inducible HSPs. However, as the inducible HSPs also showed no differential expression, the results of this study indicate either that i) *D. dianthus* has a low potential for the induced HSP response, and/or ii) the tested pH range did not trigger the induced HSP response due to a sufficient concentration of constitutive HSPs. After an exposure of *D. dianthus* to pH 7.7 for eight months, Carreiro-Silva et al. (2014) were able to demonstrate the differential expression of HSPs, showing that *D. dianthus* has the potential for an induced HSP response. Considering that the maintenance of high physiological performance and the observed suppression of metabolism, it is thought likely that the corals did not experience a stress level high enough to trigger the inducible HSP response.

After two weeks of low-pH conditions, HSP-like genes showed a significant downregulation, which was also found two weeks after pH 8.0 was re-established in the Treatment group. (Tomanek and Somero (1999) showed for marine intertidal snails that the induction and maximum HSP synthesis varied depending on the acclimation to different temperatures. Correspondingly, the downregulation of HSPs after two weeks of low-pH conditions (t_4) might be due to acclimation processes and the establishment of an alternative phenotype, requiring the differential expression of HSPs. Regarding the expression of HSPs during the recovery phase (t_5), only one gene belonging to the HSP-like proteins was downregulated in the Treatment corals compared to the Control. Therefore, the regulation of HSPs is not regarded as key process of the recovery phase and might be due to an involvement of the gene in some specific biological process.

Assessing the stress response, it further has to be considered that *D. dianthus* might have evolved stress proteins that specifically target stress inflicted by low-pH conditions. The differential expression of these genes may have been underestimated by the lack of annotation.

Regarding the transduction of the CSR, environmental changes first have to be recognized by intercellular signalling networks that influence the transcription of genes, which is followed by posttranslational modifications of proteins (Kültz 2005). The regulation of the CSR pathways due to the

change in seawater pH became evident in the differential regulation of the gene groups belonging to histone-, elongation factor- and ubiquitin-like genes.

Histones are important to form the chromatin structure, thereby directly influencing the transcription of genes (Li et al. 2007). Further, Feser et al. (2010) described histones to have a significant influence on the cellular life span. They found that a high concentration of histones led to significantly extended life spans in yeast. Therefore, the dynamic regulation of histones of the Treatment group in the course of the pH exposure experiment might modulate the transcription of certain genes and influence the cellular life span, depending on the actual stress level.

Regarding the process of protein synthesis, ribosomal factors as well as elongation factor-like gene groups are essential. While the ribosomal subunits are decoding the genetic message (40S) and facilitating the amino acid bonding (60S) (Gregory et al. 2019), elongation factors are catalysing the tRNA delivery step (eukaryotic elongation factor 1) and act as translocase (eukaryotic elongation factor 2) (Sasikumar et al. 2012). The downregulation of certain components of the protein synthesising apparatus may be an indication for metabolic suppression, necessary for energy re-allocation (Vidal-Dupiol et al. 2013). Two weeks after the end of the low-pH conditions, the expression of gene groups belonging to the protein synthesis increased slightly, indicating an upregulation of the metabolism and a recovery of the corals. The elongation factor-like genes were most strongly upregulated after the change in the feeding regime, suggesting a strong increase of protein synthesis, showing the high influence of food availability on the cellular level.

The ubiquitin system has been described for a selective degradation of proteins. It controls cell-cycle proteins and cellular growth, proliferation, development and apoptosis (Hershko and Ciechanover 1998). Monoubiquitination regulates, amongst others, DNA repair and gene silencing, while polyubiquitination regulates proteasome degradation and protein interactions (Malynn and Ma 2010). Both, monoubiquitination and polyubiquitination have been found to be differentially regulated. The downregulation of ubiquitin-like genes (and therefore protein degradation) at the beginning of the low-pH treatment may be a measure to maintain existing proteins despite the metabolic suppression.

Biogenic calcification requires calcium ions (Ca^{2+}) and dissolved inorganic carbon species (DIC). The calcification process occurs at the calcioblastic ectoderm of the aboral tissue and involves the transport of Ca^{2+} and DIC ions towards the calcification sites via ion transporters (Hennige et al. 2014). At a lower seawater pH and aragonite saturation state, the precipitation of solid $CaCO_3$ is thermodynamically less favoured (Atkinson and Cuet 2008). Therefore, it was expected that the transcription of different ion transporters would increase under low-pH conditions (section 1.5, **Hypothesis V**). However, the expectation was not fulfilled as response towards the here tested pH range. Even though several hundred genes were annotated, coding for bicarbonate and proton transporters, they were not differentially expressed. This finding was confirmed by Moya et al. (2012) for *Acropora millepora* larvae, reporting that the exposure to low-pH condition had no impact on ion transporters involved in calcification.

As response to the low-pH conditions, cytoskeletal actin and tubulin were differentially downregulated. After the two weeks of low-pH exposure, their expression increased slightly. The differential regulation of cytoskeletal components as response to low-pH conditions was also found by Kaniewska et al. (2012) for the tropical coral *Acropora millepora*. Actin plays an important role in a multitude of cellular processes, such as cell motility or intercellular transport. Tubulin is involved in vesicle transport (Alberts et al. 2005). Considering the change in the crystal structure of the $CaCO_3$ skeleton, Hennige et al. (2015) raises the question whether this might be due to less cellular resources being invested into the organisation of the cytoskeleton. However, this hypothesis requires further investigations on the role of cytoskeletal components in the calcification process.

Summarising the observed patterns of the differentially expressed genes, the original hypothesis of an upregulation of gene involved in the CSR and a downregulation of genes belonging to the biological process of biomineralisation was not confirmed in the present study. The differential regulation of inducible HSPs was not prominent, indicating a relatively low stress level. The downregulation of gene groups belonging to protein synthesis suggested a short-term downregulation of general metabolic processes during low-pH conditions that slowly reversed during recovery (**Figure 15b-d**). The transcription of ion transporters, necessary for calcification were also not affected by the exposure to the experimental pH fluctuations.

4.5 Comparison with field samples

Comparing the transcriptomic response of the pH exposure experiment with the gene expression pattern of the field samples, it was hypothesised that more differentially expressed genes were found in the field (section 1.5, **Hypothesis VI**). This could be confirmed by finding about 38 % of all transcripts in the field samples, indicating that the transcriptomic regulations of *D. dianthus* in the field is highly complex and variable, depending strongly on the sampling station.

Considering that less than 1 % of the DEGs were mutually expressed in the pH exposure experiment and the field samples, it has to be assumed that the conducted pH exposure experiment only reflects a small portion of the regulations necessary in the field at the sampling stations differing in the pH conditions.

In consistency with the pH exposure experiment, all previously discussed gene groups were differentially expressed in the field samples. They showed an overall downregulation of the samples that experienced low-pH conditions (E_{deep}). However, correlating the detected regulations directly to differences in the seawater pH has to be done with care, as the field samples were influenced by a multitude of varying environmental conditions. Considering the fluctuating salinity and temperature in the shallow water masses of the Comau fjord (Häussermann et al. 2009; Sánchez et al. 2011), the shallow-sampled *D. dianthus* might have shown a stress response, despite experiencing 'control-pH-

conditions' (pH 7.8). Apart from the abiotic factors, the field samples were exposed to biotic interactions, such as grazing or infections. Further, the shallow- and deep-sampled *D. dianthus* are likely to vary in their food availability, with the deeper samples being more food limited, depending on the vertical particle flux. It could be shown in this and other studies, e.g. Maier et al. (2016) and Martínez-Dios et al. (2020), that the food availability is an important factor, influencing the cellular and physiological response. The differential expression of metalloproteinase- and zinc-finger-like gene groups further showed that the transcriptomic response of the field samples is complex, showing additional stress responses and transcriptional regulations. Metalloproteinases are described for a multitude of functions, such as tissue remodelling or wound healing (Knapinska and Fields 2012). Zinc finger-like genes have mainly been described to participate in transcriptional or translation processes (Laity et al. 2001).

4.6 Ecological implications

The findings of this thesis suggest that *D. dianthus* has the potential for acclimation towards short-term pH variations within a natural range. However, assessing the consequences of low-pH conditions on the coral's physiology and future biogeographical distribution, the calcification rate might not be a sufficient proxy for acclimation, as it has to be considered that calcification does not occur in direct contact with the surround seawater but in a biologically controlled environment (Allemand et al. 2004; Anagnostou et al. 2012). Therefore, the capacity to maintain calcification in aragonite under saturated waters depends on the sensitivity of these regulatory mechanisms towards low-pH conditions. Pörtner (2008) suggests that the potential to regulate the internal acid-base homeostasis of body fluids thereby poses a key aspect in the performance of invertebrates experiencing a declining seawater pH. Amongst others, Pörtner et al. (1998) showed that the an internal acidosis of invertebrates was compensated by the internal accumulation of bicarbonate and the reduction of metabolism, becoming evident in a reduced respiration rate. This suppression of metabolic processes in response to a short-term exposure to low-pH conditions was also observed in this study. Considering that the projected future environmental changes will act as long-term stressors, the internal acidosis and low metabolic rates may have severe fitness consequences, eventually leading to habitat loss, despite positive calcification rates.

However, assessing the acclimation potential of CWCs to low-pH conditions on a short- and a long-term basis, the potential impacts on the corals life cycle has to be considered. Albright (2011) reviews the effect of low-pH conditions on scleractinian coral sexual reproduction, larvae metabolism, settlement, metamorphosis and physiology, finding that the negative effects on corals life history stages might cumulate drastically on the overall recruitment success.

Modelling the acclimation potential of CWCs to future conditions, it further has to be considered that the change in the ocean's carbonate chemistry is only one among other changing environmental factors, such as temperature, radiation, salinity, vertical particle fluxes, nutrients and pollution (Pandolfi et al.

2011). All of these factors have the potential to become stressors and influence the performance CWCs. Especially their interplay in future might lead to a different response than described for ocean acidification acting as single stressors, eventually exceeding the tolerance limits of CWCs (Büscher et al. 2017).

Regarding the development of CWC ecosystems in aragonite under saturated waters, not only the acclimation potential of the living polyps has to be determined. A large proportion of CWC reefs consist of bare $CaCO_3$ structures of dead corals. Lacking the protection of coral tissue, uncovered $CaCO_3$ structures are more susceptible to dissolution. Bioerosion of CWC reefs might therefore proceed faster in future (Büscher et al. 2017), which may have a major impact on associated species and the CWC reef biodiversity.

5. Conclusion and Outlook

The observed regulations enabling the scleractinian cold-water corals *Desmophyllum dianthus* to respond to a natural fluctuation in the seawater pH can be summarised as follows:

I. The calcification of *D. dianthus* was not affected by the pH range and exposure time tested in this study, showing no difference between the Control and the Treatment group. No pH-dependent difference in the calcification rate was observed after two weeks of exposure to pH 7.4. Further, the expression of genes coding for ion transporters, necessary for calcification, was not affected by the experimental changes in pH. The observed increase in calcification in the course of the experiment is suggested to be due to intrinsic controls.

II. As short-term response to low-pH conditions, *D. dianthus* showed a metabolic suppression. Though not being significant, this became evident in reduced respiration rates during the low-pH treatment, suggesting a lower energy demand. Further, a general downregulation of genes was observed, including genes belonging to the protein synthesis apparatus.

III. *D. dianthus* showed a high recovery potential after being exposed for two weeks to pH 7.4. No difference in physiological performance was seen, comparing the sampling times before and two weeks after the low-pH conditions. Regarding the number of differentially expressed genes, more regulations were found two weeks after the experimental pH increase to initial conditions, indicating that the re-acclimation to control conditions was not completed.

IV. A change in the food availability strongly influenced *D. dianthus* on both physiological and a transcriptomic level. The calcification and respiration rates were significantly higher compared to previous sampling times. Additionally, the transcriptome of the Control and the Treatment group showed large differences, indicating that the experienced low-pH conditions may influence the responses toward a change in food availability.

V. The pH exposure experiment reflected a small part of transcriptomic regulations necessary in field samples being exposed to low-pH conditions, as the proportion of mutually expressed genes was small. This shows that *D. dianthus* is exposed to a multitude of other factors in the field that require acclimation.

It was shown in this study that *D. dianthus* has a sufficient short-term acclimation potential towards pH fluctuations within a natural range. To further investigate the acclimation and adaptation potential of *D. dianthus* towards ocean acidification, the first aim should be to gather more information about intrinsic controls of CWCs and answer questions about the impact of season, age or reproduction cycle on the physiological performance and transcriptomic reactions. With this information, the response towards external stressors (e.g. low-pH) can be discussed more differentiated, considering that the environmental optimum and maximum performance may shift depending on intrinsic controls.

Regarding the impact of low-pH exposure, further research on the observed metabolic suppression is necessary, primarily focussing on how long the metabolic suppression lasts and when the corals re-establish their full metabolic capacities. The experimental set-up of this study should be extended by a further treatment with corals experiencing low-pH conditions throughout the whole experiment. Thereby, the status-quo (e.g. Control group), short-term exposure to low-pH conditions and recovery from pH fluctuations (e.g. Treatment group), and long-term responses to low-pH conditions (e.g. pH 7.4) could be investigated. Apart from the here considered physiological and transcriptomic responses, the internal acid-base parameter should additionally be determined at chosen sampling times. Further, it would be interesting to investigate the impact of the nutrition status on the metabolic suppression, i.e. in a multiple-stressor experiment.

Laboratory experiments cannot display all interactive effects having an impact on CWCs is the field. This study provided an insight into the status of *D. dianthus* individuals, being exposed to different pH conditions in the Chilean Comau fjord. Funding and workforce provided, a long-term monitoring of the abiotic conditions should be set-up in different water depths, e.g. in the Comau fjord. Data on seasonal oscillations of temperature, salinity, pH, currents, oxygen and food availability would provide information on the natural conditions maintaining thriving CWC reefs and environmental factors eventually exceeding the tolerance limits of CWCs. Based on the results of this study, showing that the transcriptome of the shallow and deep sampled *D. dianthus* individuals showed great variations, a population genetic analysis could be performed to assess whether the observed differences are due to acclimation or (beginning) ecotype formation. In addition, corals from different populations, experiencing different pH conditions, could be transplanted, analysing their performance over time. This would provide information of the potential of CWCs to acclimate and adapt towards environmental conditions and will help to model the future biogeographical distribution of CWCs.

6. Reference list

Alberts B, Bray D, Hopkin K, et al (2005) Lehrbuch der Molekularen Zellbiologie, 3. Edition. Wiley-VCH, Weinheim

Albright R (2011) Reviewing the effects of ocean acidification on sexual reproduction and early life history stages of reef-building corals. J Mar Biol 2011:1–14. https://doi.org/10.1155/2011/473615

Allemand D, Ferrier-Pagès C, Furla P, et al (2004) Biomineralisation in reef-building corals: from molecular mechanisms to environmental control. Comptes Rendus - Palevol 3:453–467. https://doi.org/10.1016/j.crpv.2004.07.011

Anagnostou E, Huang KF, You CF, et al (2012) Evaluation of boron isotope ratio as a pH proxy in the deep sea coral *Desmophyllum dianthus*: evidence of physiological pH adjustment. Earth Planet Sci Lett 349–350:251–260. https://doi.org/10.1016/j.epsl.2012.07.006

Andrew S (2010) A quality control tool for high troughput sequence data. http://www.bioinformatics.babraham.ac.uk/projects/fastqc

Aracena C, Lange CB, Luis Iriarte J, et al (2011) Latitudinal patterns of export production recorded in surface sediments of the Chilean Patagonian fjords (41-55°S) as a response to water column productivity. Cont Shelf Res 31:340–355. https://doi.org/10.1016/j.csr.2010.08.008

Ashburner M, Ball CA, Blake JA, et al (2000) Gene ontology: tool for the unification of biology. Nat Genet 25:25–29. https://doi.org/10.1038/75556

Atkinson MJ, Cuet P (2008) Possible effects of ocean acidification on coral reef biogeochemistry: topics for research. Mar Ecol Prog Ser 373:249–256. https://doi.org/10.3354/meps07867

Barton HA, Taylor NM, Lubbers BR, Pemberton AC (2006) DNA extraction from low-biomass carbonate rock: an improved method with reduced contamination and the low-biomass contaminant database. J Microbiol Methods 66:21–31. https://doi.org/10.1016/j.mimet.2005.10.005

Bauer JE, Cai WJ, Raymond PA, et al (2013) The changing carbon cycle of the coastal ocean. Nature 504:61–70. https://doi.org/10.1038/nature12857

Bolger AM, Lohse M, Usadel B (2014) Trimmomatic: a flexible trimmer for Illumina Sequence Data. Bioinformatics 15:2114–2120. https://doi.org/10.1093/bioinformatics/btu170

Brown BE, Bythell JC (2005) Perspectives on mucus secretion in reef corals. Mar Ecol Prog Ser 296:291–309. https://doi.org/10.3354/meps296291

Bryant DM, Johnson K, DiTommaso T, et al (2017) A tissue-mapped axolotl de novo transcriptome enables identification of limb regeneration factors. 3:762–776. https://doi.org/https://doi.org/10.1016/j.celrep.2016.12.063

Büscher J V., Form AU, Riebesell U (2017) Interactive effects of ocean acidification and warming on growth, fitness and survival of the cold-water coral *Lophelia pertusa* under different food availabilities. Front Mar Sci 4:1–14. https://doi.org/10.3389/fmars.2017.00101

Bushnell B (2014) BBMap: a fast, accurate, splice-aware aligner. Lawrence Berkeley Natl. Lab.

Caldeira K, Wickett ME (2003) Anthropogenic carbon and ocean pH. Nature 425:365. https://doi.org/10.1038/425365a

CarbonTracker (2021) Global monitoring Laboratory - trends in atmospheric carbon dioxide. https://gml.noaa.gov/ccgg/trends/global.html. Accessed 25 May 2021

Carreiro-Silva M, Cerqueira T, Godinho A, et al (2014) Molecular meachnisms underlying the physiological responses of the cold-water coral *Desmophyllum dianthus* to ocean acidification. Coral Reefs 33:465–476. https://doi.org/10.1007/s00338-014-1129-2

Chen B, Zhong D, Monteiro A (2006) Comparative genomics and evolution of the HSP90 family of genes across all kingdoms of organisms. BMC Genomics 19:1–19. https://doi.org/10.1186/1471-2164-7-156

Chevin L-M, Lande R, Mace GM (2010) Adaptation, plasticity, and extinction in a changing environment: towards a predictive theory. PLoS Biol 8:1–8. https://doi.org/10.1371/journal.pbio.1000357

Chisholm JRM, Gattuso J (1991) Validation of the alkalinity anomaly technique for investigating calcification of photosynthesis in coral reef communities. Limnol Oceanogr 36:1232–1239. https://doi.org/10.4319/lo.1991.36.6.1232

Darwin C (1859) On the origin of species by means of natural selection. London, UK

DeBiasse MB, Kelly MW (2016) Plastic and evolved responses to global change: what can we learn from comparative transcriptomics? J Hered 107:71–81. https://doi.org/10.1093/jhered/esv073

Deere JA, Chown SL (2006) Testing the beneficial acclimation hypothesis and its alternatives for locomotor

performance. Am Nat 168:630–644. https://doi.org/10.1086/508026

Dickson AG (1981) An exact definition of total alkalinity and a procedure for the estimation of alkalinity and total inorganic carbon from titration data. Deep Sea Res Part A, Oceanogr Res Pap 28:609–623. https://doi.org/10.1016/0198-0149(81)90121-7

Donelson JM, Sunday JM, Figueira WF, et al (2019) Understanding interactions between plasticity, adaptation and range shifts in response to marine environmental change. Philos Trans R Soc B Biol Sci 374:1–14. https://doi.org/10.1098/rstb.2018.0186

Doney SC, Fabry VJ, Feely RA, Kleypas JA (2009) Ocean acidification: the other CO_2 problem. Ann Rev Mar Sci 1:169–192. https://doi.org/10.1146/annurev.marine.010908.163834

Doney SC, Schimel DS (2007) Carbon and climate system coupling on timescales from the precambrian to the anthropocene. Annu Rev Environ Resour 32:31–66. https://doi.org/10.1146/annurev.energy.32.041706.124700

Earth G (2021) Google Earth. In: Version 9.132.0.6 - Web Assem. http://www.earth.google.com. Accessed 23 Mar 2021

Fabry VJ, Seibel BA, Feely RA, Orr JC (2008) Impacts of ocean acidification on marine fauna and ecosystem processes. Oxford Journals 65:185–195. https://doi.org/10.2307/j.ctv8jnzw1.25

Feely RA, Sabine CL, Byrne RH, et al (2012) Decadal changes in the aragonite and calcite saturation state of the Pacific Ocean. Global Biogeochem Cycles 26:1–15. https://doi.org/10.1029/2011GB004157

Feely RA, Sabine CL, Lee K, et al (2004) Impact of athropgenic CO_2 on the $CaCO_3$ system in the oceans. Science 305:362–366. https://doi.org/0.1126/science.1097329.

Feely RA, Sabine CL, Lee K, et al (2002) *In situ* calcium carbonate dissolution in the Pacific Ocean. Global Biogeochem Cycles 16:1–12. https://doi.org/10.1029/2002gb001866

Feser J, Truong D, Das C, et al (2010) Elevated histone expression promotes life span extension. Mol Cell 39:724–735. https://doi.org/10.1016/j.molcel.2010.08.015

Fillinger L, Richter C (2013) Vertical and horizontal distribution of *Desmophyllum dianthus* in Comau Fjord, Chile: a cold-water coral thriving at low pH. PeerJ 2013:1–22. https://doi.org/10.7717/peerj.194

Findlay HS, Wood HL, Kendall MA, et al (2011) Comparing the impact of high CO_2 on calcium carbonate structures in different marine organisms. Mar Biol Res 7:565–575. https://doi.org/10.1080/17451000.2010.547200

Fine M, Tchernov D (2007) Scleractinian coral species survive and recover from decalcification. Science 315:1811. https://doi.org/10.1126/science.1137094

Form AU, Riebesell U (2012) Acclimation to ocean acidification during long-term CO_2 exposure in the cold-water coral *Lophelia pertusa*. Glob Chang Biol 18:843–853. https://doi.org/10.1111/j.1365-2486.2011.02583.x

Försterra G, Beuck L, Häussermann V, Freiwald A (2005) Shallow-water Desmophyllum dianthus from Chile: characteristics of the biocoenoses, the bioeroding community, heterotrophiy interactions and (paleo)-bathymetric implications. In: Freiwald A, Roberts JM (eds) Cold-water corals and ecosystems. Berlin Heidelberg, pp 937–977

Försterra G, Häussermann V (2003) First report on large scleractinian (Cnidaria:Anthozoa) accumulations in cold-temperate shallow water of south Chilean fjords. Zool Verh Leiden 345:117–128

Fox RJ, Donelson JM, Schunter C, et al (2019) Beyond buying time: the role of plasticity in phenotypic adaptation to rapid environmental change. Philos Trans R Soc B Biol Sci 374:. https://doi.org/10.1098/rstb.2018.0174

Friedlingstein P, O'Sullivan M, Jones MW, et al (2019) Global carbon budget 2019. Earth Syst Sci Data 12:3269–3340. https://doi.org/10.5194/essd-12-3269-2020

Gopi S, Subramanian VK, Palanisamy K (2013) Aragonite-calcite-vaterite: a temperature influenced sequential polymorphic transformation of $CaCO_3$ in the presence of DTPA. Mater Res Bull 48:1906–1912. https://doi.org/10.1016/j.materresbull.2013.01.048

Gori A, Ferrier-Pagès C, Hennige SJ, et al (2016) Physiological response of the cold-water coral *Desmophyllum dianthus* to thermal stress and ocean acidification. PeerJ 4:e1606:1–16. https://doi.org/10.7717/peerj.1606

Gregory B, Rahman N, Bommakanti A, et al (2019) The small and large ribosomal subunits depend on each other for stability and accumulation. Life Sci Alliance 2:1–19. https://doi.org/10.26508/lsa.201800150

Guinotte JM, Orr J, Cairns S, et al (2006) Will human-induced changes in seawater chemistry alter the distribution of deep-sea scleractinian corals? Front Ecol Environ 4:141–146. https://doi.org/10.1890/1540-9295(2006)004[0141:WHCISC]2.0.CO;2

Haas BJ, Papanicolaou A, Yassour M, et al (2013) De novo transcript sequence reconstruction from RNA-seq using the Trinity platform for reference generation and analysis. 1494–1512. https://doi.org/https://doi.org/10.1038/nprot.2013.084

Hamel JF, Sun Z, Mercier A (2010) Influence of size and seasonal factors on the growth of the deep-sea coral *Flabellum alabastrum* in mesocosm. Coral Reefs 29:521–525. https://doi.org/10.1007/s00338-010-0590-9

Hauck J, Zeising M, Le Quéré C, et al (2020) Consistency and challenges in the ocean carbon sink estimate for the global carbon budget. Front Mar Sci 7:1–22. https://doi.org/10.3389/fmars.2020.571720

Häussermann V, Förterra G, Försterra G (2009) Marine benthic fauna of Chilean Patagonia, 1. Edition. Nature in Focus, Puerto Montt

Hennige SJ, Wicks LC, Kamenos NA, et al (2014) Short-term metabolic and growth responses of the cold-water coral *Lophelia pertusa* to ocean acidification. Deep Res Part II Top Stud Oceanogr 99:27–35. https://doi.org/10.1016/j.dsr2.2013.07.005

Hennige SJ, Wicks LC, Kamenos NA, et al (2015) Hidden impacts of ocean acidification to live and dead coral framework. Proc R Soc B Biol Sci 282:1–10. https://doi.org/10.1098/rspb.2015.0990

Hershko A, Ciechanover A (1998) The ubiquitin system. Annu Rev Biochem 67:425–479. https://doi.org/10.1038/458421a

Holcomb M, Venn AA, Tambutté E, et al (2014) Coral calcifying fluid pH dictates response to ocean acidification. Sci Rep 4:1–4. https://doi.org/10.1038/srep05207

IPCC (2019) Summary for Policymakers. In: Pörtner HO, Roberts DC, Masson-Delmotte V, et al. (eds) Special Report: The Ocean and Cryosphere in a Changing Climate

Iriarte JL, Pantoja S, Daneri G (2014) Oceanographic processes in Chilean fjords of Patagonia: from small to large-scale studies. Prog Oceanogr 129:1–7. https://doi.org/10.1016/j.pocean.2014.10.004

Iriarte JL, Pantoja S, González HE, et al (2013) Assessing the micro-phytoplankton response to nitrate in Comau Fjord (42°S) in Patagonia (Chile), using a microcosms approach. Environ Monit Assess 185:5055–5070. https://doi.org/10.1007/s10661-012-2925-1

Jantzen C, Häussermann V, Försterra G, et al (2013) Occurrence of a cold-water coral along natural pH gradients (Patagonia, Chile). Mar Biol 160:2597–2607. https://doi.org/10.1007/s00227-013-2254-0

Jiang JQ, Carter BR, Feely RA, et al (2019) Surface ocean pH and buffer capacity: past, present and future. Sci Rep 9:1–11. https://doi.org/10.1038/s41598-019-55039-4

Jury CP, Whitehead RF, Szmant AM (2010) Effects of variations in carbonate chemistry on the calcification rates of *Madracis auretenra* (= *Madracis mirabilis sensu* Wells, 1973): bicarbonate concentrations best predict calcification rates. Glob Chang Biol 16:1632–1644. https://doi.org/10.1111/j.1365-2486.2009.02057.x

Kaniewska P, Campbell PR, Kline DI, et al (2012) Major cellular and physiological impacts of ocean acidification on a reef building coral. PLoS One 7:1–12. https://doi.org/10.1371/journal.pone.0034659

Kaufmann SHE (1990) Heat shock proteins and the immune response. Immunol Today 11:129–136. https://doi.org/10.1016/0167-5699(90)90050-J

Kingsolver JG, Huey RB (2003) Introduction: the evolution of morphology, performance, and fitness. Integr Comp Biol 43:361–366. https://doi.org/10.1093/icb/43.3.361

Knapinska A, Fields GB (2012) Chemical biology for understanding matrix metalloproteinase function. ChemBioChem 13:2002–2020. https://doi.org/10.1002/cbic.201200298

Kültz D (2005) Molecular and evolutionary basis of the cellular stress response. Annu Rev Physiol 67:225–257. https://doi.org/10.1146/annurev.physiol.67.040403.103635

Kültz D (2003) Evolution of the cellular stress proteome: from monophyletic origin to ubiquitous function. J Exp Biol 206:3119–3124. https://doi.org/10.1242/jeb.00549

Laity JH, Lee BM, Wright PE (2001) Zinc finger proteins: new insights into structural and functional diversity. Curr Opin Struct Biol 11:39–46. https://doi.org/10.1016/S0959-440X(00)00167-6

Langmead B, Salzberg S (2012) Fast grapped-read alignment with Bowtie 2. Nat Methods 9:357–359. https://doi.org/https://doi.org/10.1038/nmeth.1923

Lauvset SK, Carter BR, Perez FF, et al (2020) Processes driving global interior ocean pH distribution. Global Biogeochem Cycles 34:1–17. https://doi.org/10.1029/2019GB006229

Lenth R V. (2021) Estimated Marginal Means, aka Least-Squares Means

Li B, Carey M, Workman JL (2007) The role of chromatin during transcription. Cell 128:707–719. https://doi.org/10.1016/j.cell.2007.01.015

Lindquist S, Craig EA (1988) The Heat-Shock Proteins. Annu Rev Genet 22:631–677. https://doi.org/10.1146/annurev.ge.22.120188.003215

Logan CA (2010) A review of ocean acidification and America's response. Bioscience 60:819–828. https://doi.org/10.1525/bio.2010.60.10.8

Love MI, Huber W, Anders S (2014) Moderate estimation of fold change and dispersion for RNA-seq data with DESeq2. Genome Biol 15:550. https://doi.org/https://doi.org/10.1186/s13059-014-0550-8

Mahner M, Kary M (1997) What exactly are genomes, genotypes and phenotypes? And what about phenomes? J Theor Biol 186:55–63. https://doi.org/10.1006/jtbi.1996.0335

Maier C, Popp P, Sollfrank N, et al (2016) Effects of elevated pCO_2 and feeding on net calcification and energy budget of the Mediterranean cold-water coral *Madrepora oculata*. J Exp Biol 219:3208–3217. https://doi.org/10.1242/jeb.127159

Maier C, Schubert A, Berzunza Sànchez MM, et al (2013) End of the century pCO_2 levels do not impact calcification in mediterranean cold-water corals. PLoS One 8:1–9. https://doi.org/10.1371/journal.pone.0062655

Maier C, Watremez P, Taviani M, et al (2012) Calcification rates and the effect of ocean acidification on Mediterranean cold-water corals. Proc R Soc B Biol Sci 279:1716–1723. https://doi.org/10.1098/rspb.2011.1763

Malynn BA, Ma A (2010) Ubiquitin makes its mark on immune regulation. Immunity 33:843–852. https://doi.org/10.1016/j.immuni.2010.12.007

Martínez-Dios A, Pelejero C, López-Sanz À, et al (2020) Effects of low pH and feeding on calcification rates of the cold-water coral *Desmophyllum dianthus*. PeerJ 2020:1–28. https://doi.org/10.7717/peerj.8236

Mazur P (1988) Stopping biological time: the freezing of living cells. Ann N Y Acad Sci 541:514–531. https://doi.org/10.1111/j.1749-6632.1988.tb22288.x

McCulloch M, Falter J, Trotter J, Montagna P (2012a) Coral resilience to ocean acidification and global warming through pH up-regulation. Nat Clim Chang 2:623–627. https://doi.org/10.1038/nclimate1473

McCulloch M, Trotter J, Montagna P, et al (2012b) Resilience of cold-water scleractinian corals to ocean acidification: boron isotopic systematics of pH and saturation state up-regulation. Geochim Cosmochim Acta 87:21–34. https://doi.org/10.1016/j.gca.2012.03.027

Morato T, González-Irusta JM, Dominguez-Carrió C, et al (2020) Climate-induced changes in the suitable habitat of cold-water corals and commercially important deep-sea fishes in the North Atlantic. Glob Chang Biol 26:2181–2202. https://doi.org/10.1111/gcb.14996

Movilla J, Calvo E, Pelejero C, et al (2012) Calcification reduction and recovery in native and non-native Mediterranean corals in response to ocean acidification. J Exp Mar Bio Ecol 438:144–153. https://doi.org/10.1016/j.jembe.2012.09.014

Moya A, Huisman L, Ball EE, et al (2012) Whole transcriptome analysis of the coral *Acropora millepora* reveals complex responses to CO_2-driven acidification during the initiation of calcification. Mol Ecol 21:2440–2454. https://doi.org/10.1111/j.1365-294X.2012.05554.x

Moya A, Huisman L, Forêt S, et al (2015) Rapid acclimation of juvenile corals to CO_2-mediated acidification by upregulation of heat-shock protein and Bcl-2 genes. Mol Ecol 24:438–452. https://doi.org/10.1111/mec.13021

Mueller O, Lightfoot S, Schroeder A (2016) RNA Integrity Number (RIN) – standardization of RNA quality control application. Agil Technol 1–8

Müller J (2019) The physiological short-term response of the cold-water coral *Desmophyllum dianthus* to an abrupt pH change in seawater - a manipulation experiment. Hochschule Bremerhaven

Naumann MS, Orejas C, Wild C, Ferrier-Pagès C (2011) First evidence for zooplankton feeding sustaining key physiological processes in a scleractinian cold-water coral. J Exp Biol 214:3570–3576. https://doi.org/10.1242/jeb.061390

Orejas C, Jiménez C (eds) (2019) Mediterranean cold-water corals: past, present and future understanding the deep-sea realms of coral. Springer International Publishing AG

Orr JC, Fabry VJ, Aumont O, et al (2005) Anthropogenic ocean acidification over the twenty-first century and its impact on calcifying organisms. Nature 437:681–686. https://doi.org/10.1038/nature04095

Pandolfi JM, Connolly SR, Marshall DJ, Cohen AL (2011) Projecting coral reef futures under global warming and ocean acidification. Science 333:418–422. https://doi.org/10.1126/science.1204794

Pantoja S, Luis Iriarte J, Daneri G (2011) Oceanography of the Chilean Patagonia. Cont Shelf Res 31:149–153. https://doi.org/10.1016/j.csr.2010.10.013

Patro R, Duggal G, Love MI, et al (2017) Salmon provides fast and bias-aware quantification of transcript expression. Nat Methods 14:417–419. https://doi.org/https://doi.org/10.1038/nmeth.4197

Pelejero C, Calvo E, Hoegh-Guldberg O (2010) Paleo-perspectives on ocean acidification. Trends Ecol Evol 25:332–344. https://doi.org/10.1016/j.tree.2010.02.002

Pinheiro J, Bates D, DebRoy S, et al (2020) Nlme: linear and nonlinear mixed effects models

Portier S, Rochelle C (2005) Modelling CO_2 solubility in pure water and NaCl-type waters from 0 to 300°C and from 1 to 300bar - application to the Utsira Formation at Sleipner. Chem Geol 217:187–199.

https://doi.org/10.1016/j.chemgeo.2004.12.007

Pörtner H., Lucassen M, Storch D (2005) Metabolic biochemistry: its role in thermal tolerance and in the capacities of physiological and ecological function. Fish Physiol 22:79–154. https://doi.org/10.1016/S1546-5098(04)22003-9

Pörtner HO (2008) Ecosystem effects of ocean acidification in times of ocean warming: A physiologist's view. Mar Ecol Prog Ser 373:203–217. https://doi.org/10.3354/meps07768

Pörtner HO, Reipschläger A, Heisler N (1998) Acid-base regulation, metabolism and energetics in *Sipunculus nudus* as a function of ambient carbon dioxide level. J Exp Biol 201:43–55. https://doi.org/https://doi.org/10.1242/jeb.201.1.43

Raven J, Caldeira K, Elderfield H, et al (2005) Ocean acidification due to increasing atmospheric carbon dioxide. Cardiff

Reusch TBH (2014) Climate change in the oceans: evolutionary versus phenotypically plastic responses of marine animals and plants. Evol Appl 7:104–122. https://doi.org/10.1111/eva.12109

Roberts JM, Wheeler AJ, Freiwald A (2006) Reefs of the deep: the biology and geology of cold-water coral ecosystems. Science 312:543–547. https://doi.org/10.1126/science.1119861

Sabine CL, Freely RA, Gruber N, et al (2004) The oceanic sink for anthropogenic CO_2. Science 305:5–12. https://doi.org/10.1126/science.aau5153

Sánchez N, González HE, Iriarte JL (2011) Trophic interactions of pelagic crustaceans in Comau Fjord (Chile): their role in the food web structure. J Plankton Res 33:1212–1229. https://doi.org/10.1093/plankt/fbr022

Sasikumar AN, Perez WB, Kinzy TG (2012) The many roles of the eukaryotic elongation factor 1 complex. Wiley Interdiscip Rev RNA 3:543–555. https://doi.org/10.1002/wrna.1118

Schneider U, Ziese M, Meyer-Christoffer A, et al (2016) The new portfolio of global precipitation data products of the Global Precipitation Climatology Centre suitable to assess and quantify the global water cycle and resources. Proc Int Assoc Hydrol Sci 374:29–34. https://doi.org/10.5194/piahs-374-29-2016

Seppy M, Manni M, Zdobnov EM (2019) BUSCO: assessing genome assembly and annotation completeness. In: Kollmar M (ed) Gene predicition. Methods in molecular Biology. Humana, New York

Sherwood OA, Jamieson RE, Edinger EN, Wareham VE (2008) Stable C and N isotopic composition of cold-water corals from the Newfoundland and Labrador continental slope: examination of trophic, depth and spatial effects. Deep Res Part I Oceanogr Res Pap 55:1392–1402. https://doi.org/10.1016/j.dsr.2008.05.013

Somero GN (2010) The physiology of climate change: how potentials for acclimatization and genetic adaptation will determine "winners" and "losers." J Exp Biol 213:912–920. https://doi.org/10.1242/jeb.037473

Spencer Davies P (1989) Short-term growth measurements of corals using an accurate buoyant weighing technique. Mar Biol 101:389–395. https://doi.org/10.1007/BF00428135

Stolarski J, Meibom A, Przeniosło R, Mazur M (2007) A cretaceous scleractinian coral with a calcitic skeleton. Science 318:92–94. https://doi.org/10.1126/science.1149237

Sunday JM, Calosi P, Dupont S, et al (2014) Evolution in an acidifying ocean. Trends Ecol Evol 29:117–125. https://doi.org/10.1016/j.tree.2013.11.001

Taucher J, Boxhammer T, Bach LT, et al (2021) Changing carbon-to-nitrogen ratios of organic-matter export under ocean acidification. Nat Clim Chang 11:52–57. https://doi.org/10.1038/s41558-020-00915-5

Thomas PD, Wood V, Mungall CJ, et al (2012) On the use of gene ontology annotations to assess functional similarity among orthologs and paralogs: a short report. PLoS Comput Biol 8:1–7. https://doi.org/10.1371/journal.pcbi.1002386

Todgham AE, Hofmann GE (2009) Transcriptomic response of sea urchin larvae Strongylocentrotus purpuratus to CO_2-driven seawater acidification. J Exp Biol 212:2579–2594. https://doi.org/10.1242/jeb.032540

Tomanek L, Somero GN (1999) Evolutionary and acclimation-induced variation in the heat-shock response of congeneric marine snails (genus Tegula) from different thermal habitats: implications for limits of thermotolerance and biogeography. J Exp Biol 2936:2925–2936. https://doi.org/https://doi.org/10.1242/jeb.202.21.2925

Townsend CR, Harper JL, Begon M, Harper JL (2008) Ökologie, 2. Edition. Springer Spektrum, Liverpool, England

Trotter J, Montagna P, McCulloch M, et al (2011) Quantifying the pH "vital effect" in the temperate zooxanthellate coral *Cladocora caespitosa*: validation of the boron seawater pH proxy. Earth Planet Sci Lett 303:163–173. https://doi.org/10.1016/j.epsl.2011.01.030

Vidal-Dupiol J, Zoccola D, Tambutté E, et al (2013) Genes related to ion-transport and energy production are upregulated in response to CO_2-driven pH decrease in corals: new insights from transcriptome analysis. PLoS One 8:. https://doi.org/10.1371/journal.pone.0058652

Wolf JBW (2013) Principles of transcriptome analysis and gene expression quantification: an RNA-seq tutorial. Mol Ecol Resour 13:559–572. https://doi.org/10.1111/1755-0998.12109

Yum LK, Baumgarten S, Röthig T, et al (2017) Transcriptomes and expression profiling of deep-sea corals from the Red Sea provide insight into the biology of azooxanthellate corals. Sci Rep 7:1–11. https://doi.org/10.1038/s41598-017-05572-x

Zeebe RE (2012) History of seawater carbonate chemistry, atmospheric CO_2, and ocean acidification. Annu Rev Earth Planet Sci 40:141–165. https://doi.org/10.1146/annurev-earth-042711-105521

Zeebe RE, Wolf-Gladrow D (2001) CO_2 in seawater: equilibrium, kinetics, isotops. Elsevier, Amsterdam

Zheng MD, Cao L (2014) Simulation of global ocean acidification and chemical habitats of shallow- and cold-water coral reefs. Adv Clim Chang Res 5:189–196. https://doi.org/10.1016/j.accre.2015.05.002

7. Supplementary material

7.1 Bioinformatic scripts

Fastqc – Quality Check

```
#!/bin/bash
#SBATCH --job-name=fastqc_test
#SBATCH --partition=smp
#SBATCH --time=02:00:00
#SBATCH --qos=normal
#SBATCH --cpus-per-task=12
module load bio/fastqc/0.11.9
INPUT=$(ls /work/ollie/saniedzw/210310_VH00246_3_AAACCKWHV_fq/*.fastq.gz)
OUTPUT="fastqc_out"
mkdir -p ${OUTPUT}
srun fastqc -q -o ${OUTPUT} -t ${SLURM_CPUS_PER_TASK} ${INPUT}
```

Trimmomatic – qualtity trimming of the rawdata

```
#!/bin/bash
#SBATCH --job-name=trim
#SBATCH --partition=smp
#SBATCH --time=01:30:00
#SBATCH --qos=normal
#SBATCH --array=1-74%6
#SBATCH --cpus-per-task=6
# set variables
#==========================
FQDIR="/work/ollie/saniedzw/210310_VH00246_3_AAACCKWHV_fq/"
#==========================
WORK=${PWD}
cd ${FQDIR}
FQ1=$(ls *_R1_001.fastq.gz | sed -n ${SLURM_ARRAY_TASK_ID}p)
FQ2=$(ls *_R2_001.fastq.gz | sed -n ${SLURM_ARRAY_TASK_ID}p)
cd ${WORK}
ID="${FQ1%_R1_001.fastq.gz}"
OUTDIR="out.trim"
LOGDIR="log.trim"
LOG="${LOGDIR}/${ID}_trim.log"
mkdir -p ${OUTDIR}
mkdir -p ${LOGDIR}
OUT1="${FQ1%_R1_001.fastq.gz}_trimmed.R1.fastq.gz"
OUT2="${FQ2%_R2_001.fastq.gz}_trimmed.R2.fastq.gz"
    OUT3="${FQ1%_R1_001.fastq.gz}_unpaired.R1.fastq.gz"
OUT4="${FQ2%_R2_001.fastq.gz}_unpaired.R2.fastq.gz"
module load bio/trimmomatic/0.39
srun trimmomatic PE -threads ${SLURM_CPUS_PER_TASK} -trimlog ${LOG} ${FQDIR}/${FQ1}
${FQDIR}/${FQ2} ${OUTDIR}/${OUT1} ${OUTDIR}/${OUT3} ${OUTDIR}/${OUT2}
${OUTDIR}/${OUT4} LEADING:3 TRAILING:3 SLIDINGWINDOW:4:15 MINLEN:36
```

BBmap – normalisation

```
#!/bin/bash
#SBATCH --job-name=norm
#SBATCH --partition=smp
#SBATCH --time=04:00:00
#SBATCH --qos=normal
#SBATCH --cpus-per-task=36
# set variables
#==========================
FORWARD="/work/ollie/saniedzw/reads.R1.fastq.gz"
REVERSE="/work/ollie/saniedzw/reads.R2.fastq.gz"
WORK="/work/ollie/saniedzw"
# prepare environment
#==========================
FILE1=${FORWARD##*/}
FILE2=${REVERSE##*/}
OUT1="${FILE1%.fastq.gz}.norm.fastq.gz"
OUT2="${FILE2%.fastq.gz}.norm.fastq.gz"
module load bio/bbmap/38.87
# execute process
#==========================
srun bbnorm.sh in=${FORWARD} in2=${REVERSE} out=${OUT1} out2=${OUT2} target=100 min=5
```

Trinity – *de novo* assembly

```
#!/bin/bash
#SBATCH --job-name=trinity
#SBATCH --partition=xfat
#SBATCH --time=96:00:00
#SBATCH --qos=large
#SBATCH --cpus-per-task=28
#SBATCH --mem=1400G
#SBATCH --mail-type=ALL
#SBATCH --mail-user=sarina.niedzwiedz@awi.de
# set variables [combine all samples – "e.g. cat *_R1.fastq.gz > reads.R1.fastq.gz"]
#==========================
FORWARD="/work/ollie/saniedzw/reads.R1.norm.fastq.gz"
REVERSE="/work/ollie/saniedzw/reads.R2.norm.fastq.gz"
WORK="/work/ollie/saniedzw"
#==========================
OUTPUT="/tmp/tmp_${SLURM_JOB_ID}/out.trinity"
module load bio/trinity/2.11.0
srun Trinity --seqType fq --max_memory 1400G --left ${FORWARD} --right ${REVERSE} --CPU ${SLURM_CPUS_PER_TASK} --SS_lib_type RF --no_normalize_reads --output ${OUTPUT}
cp -u ${OUTPUT}/Trinity.fasta ${WORK}
```

Assembly statistics and Alignment

```
#!/bin/bash
#BATCH --job-name=postTran
#SBATCH --partition=mini
#SBATCH --time=04:00:00
#SBATCH --qos=normal
#SBATCH --cpus-per-task=12
#SBATCH --mail-type=END
#SBATCH --mail-user=sarina.niedzwiedz@awi.de
ASSEMBLY="output/Trinity_ml300.fasta"
FORWARD="forward.R1.fastq.gz"
REVERSE="reverse.R2.fastq.gz"
DB="db.busco/metazoa_odb10"
DB2="db.busco/eukaryota_odb10"
TMP="tmp.out"
```

```
module load bio/trinity/2.11.0
srun bowtie2-build ${ASSEMBLY} ${ASSEMBLY}
srun bowtie2 -p 12 -q -x ${ASSEMBLY} -1 ${FORWARD} -2 ${REVERSE} -S
${ASSEMBLY}_read_representation_bowtie2.sam > ${ASSEMBLY}_assembly_read_representation.stat
2>&1
srun samtools view -@ 6 -u ${ASSEMBLY}_read_representation_bowtie2.sam | samtools sort -@ 6 - >
${ASSEMBLY}_read_representation_bowtie2_sorted.bam
rm ${ASSEMBLY}_read_representation_bowtie2.sam
srun TrinityStats.pl ${ASSEMBLY} > ${ASSEMBLY}.Trinity_assembly_Nx.stat 2>&1
module unload bio/trinity/2.11.0
```

Trinotate preparation

```
#!/bin/bash
#==========================
# Slurm batch script to prepare the trinotate pipeline
# Version 1.0 (21-03-25)
# by Lars Harms
# contact: lars.harms@awi.de
#==========================
#SBATCH --job-name=trinoprep
#SBATCH -p smp
#SBATCH --qos=short
#SBATCH --time=00:30:00
#SBATCH --cpus-per-task=2
#SBATCH --error="slurm_trinoPrep_%A_%a.err"
#SBATCH --output="slurm_trinoPrep_%A_%a.out"
#SBATCH --mail-type=ALL
#SBATCH --mail-user=lars.harms@awi.de
# given variables
#==========================
WORK=${PWD}
DBDIR="db.trino"
TRINOTATE="trinotate/3.2.1"
DIAMOND="diamond/2.0.6"
# preparing the working environment
#==========================
mkdir -p ${DBDIR}
cd ${DBDIR}
module load bio/${TRINOTATE}
srun Build_Trinotate_Boilerplate_SQLite_db.pl Trinotate
srun makeblastdb -in uniprot_sprot.pep -dbtype prot
rm Pfam-A.hmm.gz
module unload bio/${TRINOTATE}
module load bio/${DIAMOND}
srun diamond makedb --in uniprot_sprot.pep -d uniprot_sprot
module unload bio/${DIAMOND}
cd ${WORK}
```

Trinotate

```
#!/bin/bash
#===========================
# slurm batch script to run the trinotate pipeline
# on several sample using arrays
# by Lars Harms
# contact: lars.harms@awi.de
# slurm options and variables under >set variables<
# have to be modified by the user
#===========================
#SBATCH --job-name=trino
#SBATCH -p smp
#SBATCH --qos=normal
#SBATCH --time=06:00:00
#SBATCH --array=1-15%5
#SBATCH --cpus-per-task=12
#SBATCH --error="slurm_trino_%A_%a.err"
#SBATCH --output="slurm_trino_%A_%a.out"
#SBATCH --mail-type=END
#SBATCH --mail-user=sarina.niedzwiedz@awi.de
# set variables
#===========================
INDIR="/work/ollie/lharms/tmp/sarina/data"
OUTPUT="out.trino"
#set aligner to diamond or blast
ALIGN="diamond"
#set used assembly to trinity or other
ASSEMBLY="trinity"
# given variables
#===========================
WORK=${PWD}
TMP="tmp.trino"
CPU=${SLURM_CPUS_PER_TASK}
DBDIR="db.trino"
SCRIPT="src/trinotate_exec.sh"
INPUT=$(ls ${INDIR}/*.fasta | sed -n ${SLURM_ARRAY_TASK_ID}p)
FASTA=${INPUT##*/}
# set modules
#===========================
TRINOTATE="trinotate/3.2.1"
TRINITY="trinity/2.11.0"
DIAMOND="diamond/2.0.6"
TRANSDECODER="transdecoder/5.5.0"
SIGNALP="signalp/4.1"
TMHMM="tmhmm/2.0c"
RNAMMER="rnammer/1.2"
PERL="perl/5.26.2"
# preparing the working environment
#===========================
mkdir -p ${OUTPUT}
mkdir -p ${TMP}
#cd ${WORK}
# tasks to be performed
#===========================
srun ${SCRIPT} ${DBDIR} ${INDIR} ${FASTA} ${CPU} ${OUTPUT} ${TMP} ${TRINOTATE}
${TRINITY} ${TRANSDECODER} ${SIGNALP} ${TMHMM} ${DIAMOND} ${ALIGN}
${RNAMMER} ${PERL} ${ASSEMBLY}
# cleanup
#===========================
cp ${TMP}/${FASTA}.transdecoder.pep ${OUTPUT}/
```

Differential gene expression analysis

```
#!/bin/sh
#SBATCH --job-name=DEA_T6
#SBATCH --partition=mini
#SBATCH --time=03:00:00
#SBATCH --qos=normal
#SBATCH --cpus-per-task=12
#SBATCH --mail-type=END
#SBATCH --mail-user=sarina.niedzwiedz@awi.de
ASSEMBLY="/work/ollie/lharms/tmp/sarina/output/Trinity_ml300.fasta"
SAMPLE="/work/ollie/lharms/tmp/sarina/sample_files/SamplesT6.txt"
OUTALIGN="out.align"
PATTERN="rep"
EST="salmon"
METHOD="DESeq2"
WORK=${PWD}
#=========================
## prepare environment
module load bio/trinity/2.11.0
module load bio/R/4.0.0
TMP=${SAMPLE##*/}
COMPARISON=${TMP%.txt}
mkdir -p ${COMPARISON}
cd ${COMPARISON}
## prep the reference and run the alignment/estimation
#srun align_and_estimate_abundance.pl --transcripts ${ASSEMBLY} --est_method ${EST} --thread_count
${SLURM_CPUS_PER_TASK} --trinity_mode --prep_reference
```

7.2 Spectrometric ratios

Supplementary table 1: Spectrometric ratios
The table shows the mean ± SD ratios of the spectrometric absorbance at 260 nm/280 nm and 260 nm/230 nm of the method development, pH exposure experiment samples and field samples
.

Sample	*n*	260 nm/280 nm	260 nm/230 nm
Method development			
M1	2	2.2±0,07	0.51±0.12
M2	2	1.94±0.16	1.58±0.38
M3	2	2.3±0.04	0.87±0.15
M4	2	1.7±0.15	0.97±0.15
M5	2	2.25±0.01	1.73±0.14
M6	2	2.01±0.01	1.73±0.13
M7	2	2.21±0.03	0.6±0.55
M8	2	2.0±0.04	1.61±0.03
M9	2	1.68±0.2	0.6±0.01
M10	4	2.24±0.03	2.2±0.11
M11	2	2.6±0.01	2.32±0.02
M12	2	2.25±0.014	2.29±0.04
M13	2	2.21±0.04	2.12±0.23
M14	6	2.21±0.03	1.94±0.31
M15	6	2.07±0.02	2.22±0.08
pH exposure experiment samples			
Control t_0	4	2.08±0.09	2.03±0.17
Treatment t_0	4	2.12±0.10	2.20±0.05
Control t_1	5	2.12±0.07	1.99±0.13
Treatment t_1	5	2.06±0.09	1.88±0.58
Control t_2	5	2.13±0.12	2.18±0.09
Treatment t_2	5	2.14±0.10	1.99±0.35
Control t_3	5	2.14±0.12	2.03±0.13
Treatment t_3	5	2.14±0.11	2.17±0.05
Control t_4	5	2.15±0.09	1.98±0.26
Treatment t_4	5	2.14±0.05	2.16±0.05
Control t_5	5	2.16±0.12	2.21±0.11
Treatment t_5	5	2.14±0.11	2.14±0.23
Control t_6	5	2.19±0.11	2.25±0.13
Treatment t_6	5	2.13±0.10	2.21±0.05
Field samples			
$E_{shallow}$	4	2.17±0.02	1.67±0.17
E_{deep}	4	2.11±0.03	1.64±0.41

7.3 FastQC output

Supplementary table 2: FastQC output
The table shows the FastQC output of the raw- and quality trimmed reads of the pH exposure experiment and the field samples, with the mean total sequences ±SD and mean % GC (Guanine-Cytosine) content ± SD (n=4-5).

Sample	n	Raw-reads		Quality trimmed reads	
		Total sequences	**% GC**	**Total sequences**	**% GC**
pH exposure experiment					
Control t_0	4	15,336,008±2,788,344	44±2.1	14,709,721±2,756,179	43.9±2.0
Treatment t_0	4	13,512,758±6,440,756	43.4±1.8	12,859,995±6,156,221	43.2±1.6
Control t_1	5	115,643,547±2,496,152	43.9±2.0	14,948,079±2,517,432	43.5±1.7
Treatment t_1	5	17,330,233±2,370,264	43.4±1.9	16,520,419±2,354,310	43.1±1.8
Control t_2	5	15,777,057±4,311,845	43.7±2.0	15,002,561±4,302,860	43.4±1.6
Treatment t_2	5	12,679,550±3,068,038	42.5±2.4	12,007,476±3,052,906	42.2±2.0
Control t_3	5	15,353,572±3,284,720	43.8±1.9	14,653495±3,302,675	42.7±2.2
Treatment t_3	5	13,411,637±2,425,870	43.9±2.3	12,635,192±2,352,773	43.7±2.1
Control t_4	5	16,100,273±1,803,085	42.9±2.2	5,337,748±1,794,884	42.7±2.1
Treatment t_4	5	15,912,725±1,734,481	43.1±1.6	15,157,369±1,719,826	43.4±1.8
Control t_5	5	14,904,631±3,444,168	43.6±2.0	14,096,233±3,358,678	43.3±2.1
Treatment t_5	5	14,179,339±1,849,186	43.8±2.1	13,453,773±1,806,795	43.4±1.7
Control t_6	5	17,242,830±3,919,038	43.3±2.0	16,416,802±3,890,100	42.8±1.6
Treatment t_6	5	11,326,835±1,465,311	43.4±2.8	10,649,802±1,838,268	43.1±2.4
Field samples					
$E_{shallow}$	4	16,030,315±586,767	43.4±1.4	15,388318±635,499	43.3±1.2
E_{deep}	4	16,258,982±1,705,188	44.1±1.8	15,404,302±1,673,373	43.8±1.5
Mean		**15,062,518±1,682,659**	**43.5±0.4**	**14,327,580±1,643,244**	**43.3±0.4**
Sum		**2,197,254,100**		**2,196,074,100**	

7.4 Assembly and alignment statistics

Supplementary table 3: Assembly and alignment statistics
The table shows the statistics of the assembly and alignment obtained by the analysis with Busco v4.1.4 (Seppy et al. 2019).

Description	Statistics
Number of raw-reads after quality trimming	2,196,074,100
Assembly statistics with transcripts < 300 bp	
GC %	40.81 %
Number of contigs	1,429,568
Total assembled bases	1,122,974,128
Average length	785 bp
N10	3551
N20	2358
N30	1714
N40	1276
N50	958
Assembly annotation	
Complete BUSCOs	99.1 % [S: 9.1 %, D: 90.0 %]
Fragmented BUSCOs	0.3 %
Missing BUSCOs	0.6 %
Number of annotated genes	252,905
Alignment statistics	
Overall alignment rate	95.08 %

7.5 Differential gene expression analysis

Supplementary table 4: Differential gene expression
The table shows the differentially expressed genes of all sampling times of the pH exposure experiment (t0–t6) and the field samples (Tt). The log2 fold change ± SE describes how much the expression of the respective gene changed between the compared groups (pH exposure experiment: Control vs. Treatment; field samples: $E_{shallow}$ vs. E_{deep}). Negative log2 fold change: upregulation; positive log2 fold change: downregulation (due to bioinformatic scripts). Mean Control±SD Control and mean low-pH±SD low-pH describe the normalised expression of the transcripts coding for the respective genes.

Sampling time	Regulation low-pH group	Gene name	log2 fold change	SE	Mean Control	SD Control	Mean low-pH	SD low-pH
pH exposure experiment: 24 hours before pH reduction of the treatment group to pH 7.4								
T0	up	ubiquitin-protein ligase SRFP1	-7.37	1.52	0.00	0.00	2.48	2.08
T0	down	40S ribosomal protein	22.78	2.69	3.80	6.33	0.00	0.00
T0	down	40S ribosomal protein	24.13	3.19	9.84	13.70	0.00	0.00
T0	down	40S ribosomal protein	23.40	3.19	5.74	7.90	0.00	0.00
T0	down	60S ribosomal protein	23.88	3.19	8.18	11.05	0.00	0.00
T0	down	60S ribosomal protein	23.82	3.19	8.06	13.15	0.00	0.00
T0	down	60S ribosomal protein	24.79	3.19	16.03	22.55	0.00	0.00
T0	down	Tubulin alpha chain	22.59	1.96	3.26	3.74	0.00	0.00
T0	down	Tubulin alpha-3 chain	22.72	2.66	3.35	4.27	0.00	0.00
T0	down	Tubulin beta chain	22.69	2.65	3.28	4.03	0.00	0.00
T0	down	Tubulin alpha-2 chain	22.25	2.65	3.55	4.44	0.00	0.00
T0	down	Tubulin beta chain	23.85	3.08	7.76	9.68	0.00	0.00
T0	down	Tubulin alpha-1 chain	2.10	0.29	275.14	106.46	64.57	17.83
T0	down	Tubulin beta chain	23.05	3.20	4.25	5.54	0.00	0.00
T0	down	Tubulin beta-2 chain;	23.30	3.19	5.13	7.58	0.00	0.00
T0	down	Actin	23.12	3.20	4.39	7.57	0.00	0.00
T0	down	Actin-1/2	23.11	3.20	4.59	5.70	0.00	0.00
T0	down	Actin	22.56	2.66	3.02	3.56	0.00	0.00
T0	down	Actin	22.26	2.63	3.93	4.98	0.00	0.00
T0	down	Actin	22.67	2.71	3.20	5.26	0.00	0.00
T0	down	Actin-10	23.05	3.20	4.25	5.85	0.00	0.00
T0	down	Actin	6.28	1.32	3.05	3.36	0.03	0.06
T0	down	Polyubiquitin	22.32	1.99	3.26	3.99	0.00	0.00
T0	down	Polyubiquitin	21.57	2.00	5.28	6.55	0.00	0.00
T0	down	Polyubiquitin	24.20	3.19	16.18	20.57	0.00	0.00
T0	down	Polyubiquitin	23.40	3.09	5.47	7.56	0.00	0.00
T0	down	Ubiquitin-60S ribosomal protein	24.16	3.19	10.27	17.05	0.00	0.00
T0	down	Ubiquitin	23.03	3.20	4.57	6.08	0.00	0.00
T0	down	Polyubiquitin;	22.57	2.26	3.14	4.63	0.00	0.00
T0	down	Polyubiquitin 11	22.77	2.59	3.76	5.25	0.00	0.00
T0	down	Hemicentin-1	23.08	1.90	4.93	4.99	0.00	0.00
T0	down	Oryzain alpha chain	22.69	2.20	3.25	4.92	0.00	0.00
T0	down	Elongation factor	22.88	2.24	3.99	5.78	0.02	0.02
T0	down	Chloride transport protein 6	22.93	2.57	4.15	4.86	0.00	0.00
T0	down	NAD-dependent protein deacylase sirtuin-5	22.81	2.60	3.74	4.74	0.00	0.00
T0	down	Cytochrome b	22.58	2.67	2.98	4.56	0.00	0.00
T0	down	Probable RNA-directed DNA polymerase from transposon BS	3.34	0.70	4.14	2.25	0.36	0.23
T0	down	L-rhamnose-binding lectin SML	2.46	0.52	62.80	44.73	11.96	4.81
pH exposure experiment: 2 hours after the Treatment group reached pH 7.4								
T1	up	Contactin-associated protein-like	-22.02	2.88	0.00	0.00	3.21	4.26
T1	up	Dynein heavy chain, cytoplasmic	-22.15	2.92	0.00	0.00	3.48	4.03
T1	up	Techylectin-5B	-4.89	0.65	3.37	0.90	53.04	18.03
T1	up	Diencephalon/mesencephalon homeoboxprotein	-4.15	0.69	0.24	0.22	3.60	1.82
T1	up	Chitotriosidase-1	-2.97	0.51	16.40	7.31	104.46	71.69
T1	up	Chymotrypsin-C	-2.81	0.49	4.04	1.72	20.44	5.40
T1	up	Chitinase	-3.01	0.54	8.64	2.96	50.66	34.74
T1	up	Hemicentin-1	-2.00	0.39	3.03	1.17	9.52	3.20
T1	up	Chitinase-3-like protein	-3.04	0.62	2.72	1.65	21.18	18.97
T1	up	Myocilin	-4.08	0.83	8.87	1.19	75.39	60.90
T1	up	Chymotrypsinogen	-2.99	0.61	24.71	15.91	142.40	63.50
T1	up	Fibrinogen C domain-containing protein	-2.58	0.53	7.29	3.97	32.65	16.30
T1	up	Trypsin-3	-3.04	0.63	1.88	0.96	14.46	12.52
T1	up	Collagen alpha-1(XX) chain	-3.45	0.72	8.76	4.57	85.51	101.67

Supplementary table 4: Differential gene expression – continued

Sampling time	Regulation low-pH group	Gene name	log2 fold change	SE	Mean Control	SD Control	Mean low-pH	SD low-pH
T1	up	Olfactomedin-like protein 2B	-3.63	0.77	6.26	4.37	52.58	25.96
T1	up	Pituitary homeobox	-4.19	0.89	0.06	0.04	0.99	0.63
T1	up	Stromelysin-1	-2.93	0.62	3.55	2.16	19.67	6.87
T1	down	40S ribosomal protein	22.35	2.72	2.62	3.93	0.00	0.00
T1	down	40S ribosomal protein S29	22.51	3.23	2.93	5.24	0.00	0.00
T1	down	40S ribosomal protein S13	22.41	2.69	2.80	3.71	0.00	0.00
T1	down	60S ribosomal protein	22.67	2.78	3.22	4.74	0.00	0.00
T1	down	60S ribosomal protein	22.50	2.77	2.88	4.05	0.00	0.00
T1	down	60S ribosomal protein L34	22.40	2.72	4.32	6.04	0.00	0.00
T1	down	60S ribosomal protein L13-1	22.51	2.67	2.87	3.96	0.00	0.00
T1	down	60S ribosomal protein L27	21.16	2.13	2.66	3.53	0.00	0.00
T1	down	60S ribosomal protein L18-2	23.02	2.72	4.16	5.89	0.00	0.00
T1	down	60S ribosomal protein L35-4	23.00	2.23	4.17	5.52	0.00	0.00
T1	down	Tubulin alpha chain	23.00	2.23	4.16	5.53	0.00	0.00
T1	down	Tubulin alpha-1 chain	25.06	3.23	43.37	77.16	0.00	0.00
T1	down	Tubulin alpha chain	23.39	2.82	5.90	7.97	0.00	0.00
T1	down	Actin-1	23.20	2.77	4.65	8.02	0.00	0.00
T1	down	Actin-1	24.48	3.23	11.90	20.66	0.00	0.00
T1	down	Actin-1	23.70	3.23	6.72	12.48	0.00	0.00
T1	down	Actin-85C	23.67	3.23	6.54	11.92	0.00	0.00
T1	down	Actin-85C	23.36	3.23	5.22	9.92	0.00	0.00
T1	down	Actin-85C	22.85	3.23	3.58	6.71	0.00	0.00
T1	down	Ubiquitin	23.07	3.23	4.23	8.45	0.00	0.00
T1	down	Polyubiquitin-B	22.45	2.83	2.69	5.14	0.00	0.00
T1	down	Polyubiquitin-B	25.08	3.23	18.91	37.58	0.00	0.00
T1	down	Histone H4	23.76	2.82	7.27	10.13	0.00	0.00
T1	down	Cytochrome c oxidase subunit 2	22.62	3.23	3.05	6.09	0.00	0.00
T1	down	Gamma-glutamyl hydrolase	22.40	2.65	2.80	4.08	0.00	0.00
T1	down	Actophorin	22.59	2.75	2.97	5.06	0.00	0.00
T1	down	Stress-associated endoplasmic reticulum protein 2	23.24	3.23	5.01	8.31	0.00	0.00
T1	down	Prefoldin subunit 2	22.96	3.23	4.13	6.60	0.00	0.00
T1	down	Elongation factor 1	22.91	3.23	3.75	6.13	0.00	0.00
T1	down	H/ACA ribonucleoprotein complex subunit 3	22.84	3.23	3.58	7.15	0.00	0.00
T1	down	Ras-related protein Rab-7a	22.46	3.23	2.76	4.58	0.00	0.00
T1	down	Small nuclear ribonucleoprotein E	22.36	3.23	2.76	3.79	0.00	0.00
T1	down	Muscle LIM protein 1	2.36	0.48	108.19	44.08	17.54	12.41
T1	down	Homeobox protein otx5-B	2.33	0.49	13.75	6.83	2.34	1.08
T1	down	Sushi, von Willebrand factor type A, EGF and pentraxin domain-containing protein	23.29	1.33	5.22	4.06	0.00	0.00
T1	down	Fibrinogen-like protein 1	23.33	2.75	5.28	9.29	0.00	0.00
pH exposure experiment: 24 hours after the Treatment group reached pH 7.4								
T2	up	60S ribosomal protein L7	-6.86	1.49	2.62	2.96	278.24	261.95
T2	up	Ficolin-2	-21.79	1.55	0.00	0.00	2.68	2.00
T2	up	Pancreatic secretory granule membrane major glycoprotein GP2	-22.35	3.03	0.00	0.00	4.14	6.02
T2	down	Hemicentin-1	21.95	1.32	2.89	2.57	0.00	0.00
T2	down	Spectrin beta chain, non-erythrocytic 1	22.75	1.57	4.54	4.56	0.00	0.00
T2	down	Tenascin-R	22.25	1.76	3.37	4.73	0.00	0.00
T2	down	Tripartite motif-containing protein 2	22.05	1.89	2.71	4.79	0.00	0.00
T2	down	TNF receptor-associated factor 1	23.49	3.03	7.88	11.12	0.00	0.00
T2	down	Phospholipid-transporting ATPase ABCA3	22.60	3.03	4.06	5.89	0.00	0.00
T2	down	Chloride transport protein 6	22.58	3.03	3.90	6.12	0.00	0.00
T2	down	Polyunsaturated fatty acid 5-lipoxygenase	2.02	0.36	19.54	8.28	4.58	1.22
T2	down	Retinal dehydrogenase 1	2.52	0.51	28.41	19.33	4.65	0.57
T2	down	116 kDa U5 small nuclear ribonucleoprotein component	6.36	1.33	1.53	1.19	0.00	0.00
T2	down	Tetratricopeptide repeat protein 39C	6.16	1.34	1.34	0.95	0.00	0.00
T2	down	TNF receptor-associated factor 1	5.53	1.20	2.36	1.73	0.04	0.09
pH exposure experiment: 5 days after the Treatment group reached pH 7.4								
T3	up	60S ribosomal protein L3	-6.88	1.22	0.21	0.11	23.95	42.28
T3	up	Cytochrome c oxidase subunit 1	-21.89	2.22	0.00	0.00	2.88	3.66
T3	up	Cytochrome b	-22.14	3.03	0.00	0.00	3.50	4.81
T3	up	Peptidyl-prolyl cis-trans isomerase	-21.88	2.36	0.00	0.00	2.94	4.63

Supplementary table 4: Differential gene expression – continued

Sampling time	Regulation low-pH group	Gene name	log2 fold change	SE	Mean Control	SD Control	Mean low-pH	SD low-pH
T3	up	TBC domain-containing protein kinase-like protein	-21.64	2.76	0.00	0.00	2.44	3.67
T3	up	Vitellogenin-6	-22.32	3.03	0.01	0.01	3.72	6.85
T3	up	SPRY domain-containing protein 3	-3.48	0.73	0.34	0.24	3.54	2.43
T3	down	Tubulin beta chain	22.31	2.79	3.14	5.76	0.00	0.00
T3	down	Tubulin alpha chain	22.61	3.03	3.81	5.22	0.00	0.00
T3	down	Polyubiquitin	2.23	0.44	2.65	0.53	0.51	0.27
pH exposure experiment: 2 weeks after the Treatment group reached pH 7.4								
T4	up	Tubulin alpha-1 chain	-22.49	2.62	0.00	0.00	5.74	6.79
T4	up	Tubulin beta chain	-22.44	2.63	0.00	0.00	5.19	6.26
T4	up	Tubulin beta chain	-22.42	2.63	0.00	0.00	5.12	5.92
T4	up	Tubulin beta chain	-22.01	2.70	0.00	0.00	3.88	5.79
T4	up	Tubulin beta chain	-21.90	2.70	0.00	0.00	3.60	5.35
T4	up	Tubulin beta-1 chain	-21.81	2.70	0.00	0.00	3.34	4.53
T4	up	Tubulin beta chain	-21.84	2.70	0.00	0.00	3.39	4.82
T4	up	Tubulin beta chain	-21.20	2.65	0.00	0.00	4.49	5.65
T4	up	Tubulin beta chain	-21.60	2.71	0.00	0.00	2.83	3.35
T4	up	Tubulin beta chain	-21.04	2.63	0.00	0.00	4.99	5.79
T4	up	Tubulin beta-4B chain	-21.84	2.74	0.00	0.00	3.40	5.68
T4	up	Tubulin beta chain	-21.73	2.72	0.00	0.00	3.14	4.77
T4	up	Tubulin beta chain	-21.41	2.72	0.00	0.00	2.49	2.89
T4	up	Tubulin beta chain	-21.42	2.73	0.00	0.00	2.47	3.07
T4	up	Tubulin alpha-2 chai	-23.07	3.19	0.00	0.00	8.18	9.51
T4	up	Tubulin beta chain	-22.96	3.19	0.00	0.00	11.47	13.78
T4	up	Tubulin beta-1 chain	-22.94	3.19	0.00	0.00	7.42	8.97
T4	up	Tubulin alpha-3 chain;	-22.65	3.19	0.00	0.00	6.54	7.60
T4	up	Tubulin beta chain	-21.94	3.19	0.00	0.00	8.67	10.02
T4	up	Tubulin alpha chain	-21.05	3.19	0.00	0.00	7.18	9.10
T4	up	Tubulin alpha-4 chain	-22.11	2.67	0.00	0.00	4.09	5.35
T4	up	Tubulin alpha chain	-22.07	2.69	0.00	0.00	3.96	4.60
T4	up	Tubulin beta-1 chain	-21.52	2.77	0.00	0.00	2.68	4.44
T4	up	Tubulin alpha-2 chain	-21.80	2.69	0.00	0.00	3.31	3.97
T4	up	Actin-85C	-21.61	2.08	0.00	0.00	2.87	3.32
T4	up	Actin, non-muscle 6 2	-21.90	2.68	0.00	0.00	3.52	4.07
T4	up	Actin	-21.84	2.68	0.00	0.00	3.39	3.96
T4	up	Actin, alpha skeletal muscle	-21.58	2.71	0.00	0.00	2.81	3.59
T4	up	Actin, muscle	-23.13	3.19	0.00	0.00	8.55	10.21
T4	up	Polyubiquitin	-21.77	2.08	0.00	0.00	3.20	3.73
T4	up	Polyubiquitin	-21.59	2.71	0.00	0.00	2.83	3.49
T4	up	Polyubiquitin	-21.47	2.75	0.00	0.00	2.57	4.39
T4	up	Histone H3 1	-22.12	2.66	0.00	0.00	4.13	4.86
T4	up	Histone H2A 1	-21.97	2.75	0.00	0.00	3.64	6.46
T4	up	Arginine kinase	-21.79	2.69	0.00	0.00	3.24	3.74
T4	up	Proliferating cellular nuclear antige	-21.54	2.71	0.00	0.00	2.72	3.15
T4	up	Cold shock protein 1	-20.70	2.63	0.00	0.00	5.48	6.78
T4	up	Phospholipase B-like 1	-21.39	2.75	0.00	0.00	2.41	3.75
T4	up	C-type lectin BpLec	-7.28	1.40	0.01	0.03	2.48	1.91
T4	up	U5 small nuclear ribonucleoprotein 200 kDa helicase	-3.35	0.68	0.33	0.28	3.64	1.28
T4	up	P-selectin	-3.31	0.73	1.86	1.51	19.26	14.82
T4	down	40S ribosomal protein S8	22.18	2.02	2.35	2.51	0.00	0.00
T4	down	40S ribosomal protein S23	22.94	2.29	4.09	4.18	0.00	0.00
T4	down	40S ribosomal protein S7	22.81	2.29	3.75	3.83	0.00	0.00
T4	down	40S ribosomal protein S17	22.89	2.30	3.98	4.38	0.00	0.00
T4	down	40S ribosomal protein S5	22.84	2.30	3.82	4.18	0.00	0.00
T4	down	40S ribosomal protein S2	22.66	2.30	3.37	3.47	0.00	0.00
T4	down	40S ribosomal protein S11	22.50	2.31	3.00	3.29	0.00	0.00
T4	down	40S ribosomal protein S26	22.63	2.32	3.30	3.78	0.00	0.00
T4	down	40S ribosomal protein S18	22.61	2.32	3.17	3.71	0.00	0.00
T4	down	40S ribosomal protein SA	22.43	2.31	2.86	2.98	0.00	0.00
T4	down	40S ribosomal protein S3a	22.45	2.31	2.89	3.09	0.00	0.00
T4	down	40S ribosomal protein S21	22.69	2.34	3.35	4.33	0.00	0.00
T4	down	40S ribosomal protein S27-like	22.48	2.32	2.98	3.41	0.00	0.00
T4	down	40S ribosomal protein S9	22.34	2.31	2.66	2.83	0.00	0.00
T4	down	40S ribosomal protein S2	22.22	2.30	3.18	3.29	0.00	0.00
T4	down	40S ribosomal protein S19S	22.34	2.32	2.69	3.05	0.00	0.00

Supplementary table 4: Differential gene expression – continued

Sampling time	Regulation low-pH group	Gene name	log2 fold change	SE	Mean Control	SD Control	Mean low-pH	SD low-pH
T4	down	40S ribosomal protein S4	22.31	2.32	2.63	3.01	0.00	0.00
T4	down	40S ribosomal protein S16	22.26	2.32	2.50	2.71	0.00	0.00
T4	down	40S ribosomal protein S14	22.32	2.32	2.63	2.99	0.00	0.00
T4	down	40S ribosomal protein S15	22.35	2.35	2.68	3.21	0.00	0.00
T4	down	40S ribosomal protein S3	20.34	2.33	2.98	3.49	0.00	0.00
T4	down	40S ribosomal protein S28	24.02	3.23	9.08	10.52	0.00	0.00
T4	down	40S ribosomal protein S30	23.57	3.23	6.92	7.30	0.00	0.00
T4	down	40S ribosomal protein S15Aa	23.99	3.23	8.71	11.01	0.00	0.00
T4	down	40S ribosomal protein S24	23.24	3.23	5.15	5.30	0.00	0.00
T4	down	40S ribosomal protein S10b;	23.00	3.23	4.29	4.59	0.00	0.00
T4	down	40S ribosomal protein S12	23.00	3.23	4.30	4.42	0.00	0.00
T4	down	60S ribosomal protein L28-1	22.01	1.96	2.38	3.43	0.00	0.00
T4	down	60S ribosomal protein L6	22.18	2.02	2.37	2.56	0.00	0.00
T4	down	60S ribosomal protein L34	22.96	2.29	4.19	4.30	0.00	0.00
T4	down	60S ribosomal protein L23	22.85	2.29	3.86	3.98	0.00	0.00
T4	down	60S ribosomal protein L21	22.84	2.30	3.84	4.12	0.00	0.00
T4	down	60S ribosomal protein L32	22.81	2.30	3.82	4.24	0.00	0.00
T4	down	60S ribosomal protein L11-2	22.82	2.31	3.79	4.20	0.00	0.00
T4	down	60S ribosomal protein L12	22.78	2.30	3.66	3.92	0.00	0.00
T4	down	60S ribosomal protein L38	22.79	2.31	3.60	4.04	0.00	0.00
T4	down	60S ribosomal protein L7a	22.78	2.31	3.62	3.96	0.00	0.00
T4	down	60S ribosomal protein L31	22.73	2.31	3.57	3.89	0.00	0.00
T4	down	60S ribosomal protein L13	22.63	2.30	3.29	3.43	0.00	0.00
T4	down	60S ribosomal protein L36	22.73	2.32	3.54	4.05	0.00	0.00
T4	down	60S acidic ribosomal protein P1	22.59	2.31	3.21	3.43	0.00	0.00
T4	down	60S ribosomal protein L44	22.57	2.31	3.14	3.36	0.00	0.00
T4	down	60S ribosomal protein L8	22.61	2.32	3.28	3.69	0.00	0.00
T4	down	60S ribosomal protein L26	22.53	2.31	3.07	3.30	0.00	0.00
T4	down	60S ribosomal protein L15	22.64	2.33	3.25	3.95	0.00	0.00
T4	down	60S ribosomal protein L13a	22.52	2.32	3.06	3.48	0.00	0.00
T4	down	60S ribosomal protein L44	22.32	2.30	2.55	2.50	0.00	0.00
T4	down	60S ribosomal protein L14	22.61	2.33	3.31	4.18	0.00	0.00
T4	down	60S ribosomal protein L27	22.44	2.32	2.89	3.26	0.00	0.00
T4	down	60S ribosomal protein L27a	22.40	2.32	3.36	3.82	0.00	0.00
T4	down	60S ribosomal protein L9	22.32	2.31	2.61	2.76	0.00	0.00
T4	down	60S ribosomal protein L17	22.23	2.30	2.42	2.40	0.00	0.00
T4	down	60S ribosomal protein L35	22.34	2.32	2.69	2.98	0.00	0.00
T4	down	60S ribosomal protein L19	22.26	2.32	2.53	2.76	0.00	0.00
T4	down	60S ribosomal protein L3	22.21	2.33	2.42	2.71	0.00	0.00
T4	down	60S ribosomal protein L7	22.13	2.33	2.29	2.57	0.00	0.00
T4	down	60S ribosomal protein L38	22.50	2.40	2.84	4.82	0.00	0.00
T4	down	60S acidic ribosomal protein P1	23.10	3.23	4.59	5.24	0.00	0.00
T4	down	60S ribosomal protein L18a	23.42	3.23	5.84	6.35	0.00	0.00
T4	down	60S ribosomal protein L30	23.18	3.23	4.90	5.42	0.00	0.00
T4	down	60S ribosomal protein L37a	23.05	3.23	4.50	5.42	0.00	0.00
T4	down	60S ribosomal protein L24	23.02	3.23	4.37	4.64	0.00	0.00
T4	down	60S ribosomal protein L35a	23.01	3.23	4.30	4.39	0.00	0.00
T4	down	Probable 60S ribosomal protein L37-A	22.33	2.32	2.64	2.91	0.00	0.00
T4	down	Tubulin beta chain	23.54	1.93	6.25	9.16	0.00	0.00
T4	down	Tubulin beta chain	22.96	2.40	4.53	8.32	0.00	0.00
T4	down	Tubulin alpha-1 chain	22.31	2.43	2.84	4.87	0.00	0.00
T4	down	Tubulin alpha-2 chain	22.96	2.98	3.93	7.63	0.00	0.00
T4	down	Tubulin beta chain	24.59	2.82	14.42	22.04	0.00	0.00
T4	down	Actin	22.15	1.89	2.55	3.38	0.00	0.00
T4	down	Actin	22.75	2.37	3.48	5.23	0.00	0.00
T4	down	Actin	22.43	2.44	2.84	4.59	0.00	0.00
T4	down	Actin-10	24.26	3.23	10.31	17.07	0.00	0.00
T4	down	Actin, cytoplasmic	24.25	3.23	11.21	15.32	0.00	0.00
T4	down	Actin-5C	23.92	3.23	8.64	10.57	0.00	0.00
T4	down	Actin, muscle	23.81	3.23	7.94	9.97	0.00	0.00
T4	down	Microtubule-actin cross-linking factor 1	21.46	2.32	2.63	2.96	0.00	0.00
T4	down	Actin-1	21.37	2.98	2.58	4.03	0.00	0.00
T4	down	Actin, cytoplasmic	20.31	2.98	2.45	3.63	0.00	0.00
T4	down	Ubiquitin-60S ribosomal protein L40	22.32	2.33	2.65	3.03	0.00	0.00
T4	down	Ubiquitin-40S ribosomal protein S27a	21.47	2.31	3.10	3.39	0.00	0.00
T4	down	Polyubiquitin	19.74	2.32	2.49	2.76	0.00	0.00

Supplementary table 4: Differential gene expression – continued

Sampling time	Regulation low-pH group	Gene name	log2 fold change	SE	Mean Control	SD Control	Mean low-pH	SD low-pH
T4	down	Polyubiquitin	22.84	2.99	3.59	6.98	0.00	0.00
T4	down	Actin, acrosomal process isoform	23.78	3.23	7.84	9.89	0.00	0.00
T4	down	Polyubiquitin-B	23.05	3.23	11.94	14.62	0.00	0.00
T4	down	Polyubiquitin-B	23.05	3.23	11.94	14.62	0.00	0.00
T4	down	Heat shock protein hsp-1	23.13	3.23	4.77	5.24	0.00	0.00
T4	down	Heat shock protein 83	21.15	2.04	3.43	3.88	0.00	0.00
T4	down	Heat shock 70 kDa protein 5	22.61	1.89	3.23	3.26	0.00	0.00
T4	down	Heat shock protein 90	22.68	2.32	3.46	3.92	0.00	0.00
T4	down	10 kDa heat shock protein	22.32	2.34	2.65	3.13	0.00	0.00
T4	down	Heat shock 70 kDa protein 1-like	22.23	2.41	2.42	3.39	0.00	0.00
T4	down	Elongation factor 1-alpha	24.00	3.23	9.04	10.05	0.00	0.00
T4	down	Elongation factor 1-alpha	21.96	2.97	2.58	3.59	0.00	0.00
T4	down	Elongation factor 1-alpha	22.45	2.32	2.72	2.81	0.00	0.00
T4	down	Elongation factor 1-alpha	22.36	2.99	2.51	4.13	0.00	0.00
T4	down	Elongation factor 1-alpha 3	22.33	2.49	2.55	4.86	0.01	0.02
T4	down	Elongation factor 1-beta	22.88	2.31	3.97	4.54	0.00	0.00
T4	down	Elongation factor 2	22.26	2.35	2.53	3.03	0.00	0.00
T4	down	Serine protease inhibitor swm-1	22.86	2.29	3.84	3.85	0.00	0.00
T4	down	Serine/arginine-rich splicing factor 3	22.87	2.30	3.88	4.15	0.00	0.00
T4	down	Serine/arginine-rich splicing factor 3	22.80	2.31	3.77	4.41	0.00	0.00
T4	down	Dynein light chain 1	22.83	2.31	3.79	4.21	0.00	0.00
T4	down	Myosin, essential light chain	22.68	2.30	3.31	3.26	0.00	0.00
T4	down	ADP/ATP translocase 1	22.52	2.32	3.01	3.30	0.00	0.00
T4	down	ATP-dependent RNA helicase eIF4A	21.80	2.31	3.21	3.53	0.00	0.00
T4	down	ADP-ribosylation factor 1-like 2	23.12	3.23	4.64	4.98	0.00	0.00
T4	down	Cytochrome c oxidase subunit 1	24.91	3.23	16.97	17.62	0.00	0.00
T4	down	Superoxide dismutase [Cu-Zn]	23.14	3.23	4.82	5.24	0.00	0.00
T4	down	Catalase	22.22	2.34	2.50	3.03	0.00	0.00
T4	down	High mobility group protein 1 2	23.78	3.23	7.78	12.00	0.00	0.00
T4	down	Lactadherin	23.28	1.89	5.41	5.17	0.00	0.00
T4	down	Pancreatic secretory granule membrane major glycoprotein GP2	21.67	1.89	3.67	3.81	0.00	0.00
T4	down	Neurobeachin-like protein 2	22.14	2.07	2.09	2.79	0.00	0.00
T4	down	Nucleoside diphosphate kinase	22.81	2.30	3.72	4.02	0.00	0.00
T4	down	Guanine nucleotide-binding protein subunit beta-2-like 1	22.73	2.31	3.59	4.01	0.00	0.00
T4	down	Equistatin	22.59	2.30	3.57	3.67	0.00	0.00
T4	down	Eukaryotic translation initiation factor 5A-2	22.84	2.32	3.90	4.64	0.00	0.00
T4	down	Peptidyl-prolyl cis-trans isomerase D	22.74	2.32	3.59	4.06	0.00	0.00
T4	down	Fructose-bisphosphate aldolase 1	22.55	2.30	3.10	3.20	0.00	0.00
T4	down	Legumain	22.97	2.36	4.35	5.85	0.00	0.00
T4	down	S-phase kinase-associated protein 1 homolog	22.93	2.36	4.11	5.24	0.00	0.00
T4	down	NPC intracellular cholesterol transporter 2	22.52	2.33	3.44	4.35	0.00	0.00
T4	down	Transthyretin-like protein	22.65	2.35	3.33	4.15	0.00	0.00
T4	down	Probable S-adenosylmethionine synthase 3	22.45	2.34	2.92	3.49	0.00	0.00
T4	down	Translationally-controlled tumor protein homolog	22.38	2.33	2.74	3.18	0.00	0.00
T4	down	Selenoprotein F	22.15	2.32	2.27	2.48	0.00	0.00
T4	down	Protein disulfide-isomerase 2	22.35	2.34	2.75	3.43	0.00	0.00
T4	down	Protein LLP homolog	22.42	2.35	2.88	3.69	0.00	0.00
T4	down	Retinol dehydrogenase 12	22.74	2.39	3.71	5.05	0.00	0.00
T4	down	Probable glutathione S-transferase 8	22.33	2.37	2.71	3.58	0.00	0.00
T4	down	Sepiapterin reductase	22.07	2.35	2.45	3.19	0.00	0.00
T4	down	Galectin-4	21.49	2.35	4.04	5.21	0.00	0.00
T4	down	Putative aminopeptidase W07G4 4	21.60	2.37	2.48	3.09	0.00	0.00
T4	down	Ficolin-2	22.34	2.52	2.55	4.93	0.00	0.00
T4	down	Dual adapter for phosphotyrosine and 3-phosphotyrosine and 3-phosphoinositide	22.46	2.59	2.75	5.43	0.00	0.00
T4	down	Vitellogenin-6	26.57	3.23	62.02	88.69	0.00	0.00
T4	down	Ragulator complex protein LAMTOR2-B	22.71	3.00	3.32	6.58	0.00	0.00
T4	down	Peptidyl-prolyl cis-trans isomerase 7	24.24	3.23	10.70	12.96	0.00	0.00
T4	down	NADH-ubiquinone oxidoreductase chain	24.18	3.23	9.94	10.91	0.00	0.00
T4	down	Peptidyl-prolyl cis-trans isomerase;	24.13	3.23	9.76	10.60	0.00	0.00
T4	down	Intermediate filament protein A	24.06	3.23	9.68	12.06	0.00	0.00
T4	down	Procathepsin L	22.54	3.03	2.91	5.83	0.00	0.00
T4	down	Kielin/chordin-like protein	22.13	3.01	2.06	3.87	0.00	0.00
T4	down	Aspartic protease 4	23.58	3.23	6.81	8.37	0.00	0.00

Supplementary table 4: Differential gene expression – continued

Sampling time	Regulation low-pH group	Gene name	log2 fold change	SE	Mean Control	SD Control	Mean low-pH	SD low-pH
T4	down	Mitochondrial import inner membrane translocase subunit TIM14	22.13	3.03	2.17	4.24	0.00	0.00
T4	down	Cathepsin L	23.50	3.23	6.38	8.36	0.00	0.00
T4	down	Lipid droplet localized protein	23.46	3.23	6.27	8.37	0.00	0.00
T4	down	Glyceraldehyde-3-phosphate dehydrogenase;	23.19	3.23	4.95	5.28	0.00	0.00
T4	down	Fatty acid-binding protein, adipocyte	23.16	3.23	5.17	8.31	0.00	0.00
T4	down	3-oxoacyl-[acyl-carrier-protein] reductase FabG	23.12	3.23	4.76	5.45	0.00	0.00
T4	down	FK506-binding protein 2	21.61	3.02	2.73	5.45	0.00	0.00
T4	down	Protein transport protein Sec61 subunit gamma	23.06	3.23	4.42	4.47	0.00	0.00
T4	down	Retinal dehydrogenase 1	23.00	3.23	4.45	5.69	0.00	0.00
T4	down	Anionic trypsin-2;	7.06	1.34	110.42	145.49	0.82	0.80
T4	down	Phosphoserine aminotransferase	4.89	1.02	1.37	0.49	0.06	0.11
pH exposure experiment: 2 weeks after the Treatment group re-reached pH 8.0								
T5	up	E3 ubiquitin-protein ligase hecd-1	-21.58	2.01	0.00	0.00	2.92	3.25
T5	up	Mitogen-activated protein kinase kinase kinase 2	-22.56	1.37	0.00	0.00	5.88	5.89
T5	up	Spectrin alpha chain, non-erythrocytic 1	-6.77	1.31	0.06	0.13	7.28	6.05
T5	up	Molybdenum cofactor biosynthesis protein 1	-6.19	1.28	0.05	0.06	2.72	2.62
T5	down	40S ribosomal protein S24	22.27	1.46	2.75	2.51	0.00	0.00
T5	down	40S ribosomal protein S10-1	22.55	1.53	3.39	4.27	0.00	0.00
T5	down	40S ribosomal protein S17	7.54	1.41	2.35	1.91	0.00	0.00
T5	down	40S ribosomal protein S18	7.55	1.41	2.36	1.97	0.00	0.00
T5	down	40S ribosomal protein S21	7.60	1.44	2.40	2.22	0.00	0.00
T5	down	40S ribosomal protein S6	7.47	1.42	2.23	2.17	0.00	0.00
T5	down	40S ribosomal protein S11	7.44	1.41	2.16	2.15	0.00	0.00
T5	down	40S ribosomal protein S3a	7.01	1.37	1.61	1.14	0.00	0.00
T5	down	40S ribosomal protein S15	7.46	1.42	2.21	1.89	0.00	0.00
T5	down	40S ribosomal protein S13	7.18	1.41	1.83	1.41	0.00	0.00
T5	down	40S ribosomal protein S5-2	7.28	1.45	1.95	1.71	0.00	0.00
T5	down	40S ribosomal protein S20	7.12	1.42	1.73	1.35	0.00	0.00
T5	down	40S ribosomal protein S14	7.05	1.43	1.70	1.40	0.00	0.00
T5	down	40S ribosomal protein S7	6.90	1.49	1.51	1.13	0.00	0.00
T5	down	40S ribosomal protein S8	6.96	1.52	1.53	1.66	0.00	0.00
T5	down	60S ribosomal protein L23	22.17	1.39	2.66	2.39	0.00	0.00
T5	down	60S ribosomal protein L24	22.39	1.54	3.43	4.59	0.00	0.00
T5	down	60S ribosomal protein L36a	22.47	1.50	3.13	3.38	0.00	0.00
T5	down	60S ribosomal protein L26	21.19	1.51	2.50	2.38	0.00	0.00
T5	down	60S ribosomal protein L22	22.34	1.83	2.83	3.99	0.00	0.00
T5	down	60S ribosomal protein L8	7.43	1.37	2.20	1.67	0.00	0.00
T5	down	60S ribosomal protein L13	7.52	1.42	2.30	2.21	0.00	0.00
T5	down	60S ribosomal protein L11	7.40	1.43	2.12	1.90	0.00	0.00
T5	down	60S ribosomal protein L35a	7.38	1.36	2.09	1.64	0.00	0.00
T5	down	60S ribosomal protein L5	7.41	1.37	2.16	1.46	0.00	0.00
T5	down	60S ribosomal protein L7 2	7.26	1.43	1.93	1.70	0.00	0.00
T5	down	60S ribosomal protein L27a	6.71	1.34	1.36	0.91	0.00	0.00
T5	down	60S ribosomal protein L18	7.34	1.46	2.02	1.92	0.00	0.00
T5	down	60S acidic ribosomal protein P0	6.84	1.42	1.46	1.15	0.00	0.00
T5	down	Ribosomal protein L3	7.27	1.36	1.98	1.56	0.00	0.00
T5	down	Tubulin alpha chain	25.26	1.29	26.11	21.37	0.00	0.00
T5	down	Tubulin alpha-1 chain	21.73	1.50	4.25	3.90	0.00	0.00
T5	down	Tubulin beta chain	22.23	2.82	3.12	6.08	0.00	0.00
T5	down	Tubulin alpha chain	7.11	0.95	12.06	7.04	0.10	0.13
T5	down	Tubulin alpha-1C chain	22.61	3.23	4.13	8.06	0.00	0.00
T5	down	Tubulin beta chain	6.17	0.96	10.74	7.18	0.17	0.20
T5	down	Tubulin beta chain	5.10	0.86	26.74	14.84	0.89	0.92
T5	down	Tubulin beta chain	4.53	0.88	15.30	8.44	0.71	0.87
T5	down	Tubulin alpha chain	4.80	1.03	6.66	4.72	0.26	0.34
T5	down	Actin, cytoplasmic	22.32	2.81	3.33	6.54	0.00	0.00
T5	down	Actin, macronuclear	22.44	1.40	3.75	3.03	0.00	0.00
T5	down	Polyubiquitin-B	22.85	1.28	4.36	2.50	0.00	0.00
T5	down	Ubiquinol-cytochrome c reductase iron-sulfur subunit	7.05	1.44	1.67	1.32	0.00	0.00
T5	down	Ubiquinol-cytochrome c reductase iron-sulfur subunit	7.05	1.44	1.67	1.32	0.00	0.00
T5	down	Ubiquitin-conjugating enzyme variant MMS2	6.92	1.45	1.54	1.26	0.00	0.00
T5	down	Polyubiquitin-C	21.98	1.32	3.18	1.82	0.00	0.00

Supplementary table 4: Differential gene expression – continued

Sampling time	Regulation low-pH group	Gene name	log2 fold change	SE	Mean Control	SD Control	Mean low-pH	SD low-pH
T5	down	Heat shock protein 90-2	7.03	1.43	1.68	1.28	0.00	0.00
T5	down	Elongation factor 1-alpha	7.03	1.21	1.72	0.55	0.00	0.00
T5	down	Elongation factor 1-alpha	7.23	1.44	1.89	1.40	0.00	0.00
T5	down	Elongation factor 1-alpha 2	7.62	1.53	2.45	2.67	0.00	0.00
T5	down	Histone H2A Z	24.13	1.37	12.35	14.07	0.00	0.00
T5	down	Histone H3	23.10	1.36	5.23	3.81	0.00	0.00
T5	down	ATP synthase subunit beta	22.92	1.41	4.43	4.67	0.00	0.00
T5	down	ADP-ribosylation factor 1	22.59	1.35	3.50	2.81	0.00	0.00
T5	down	ATP synthase subunit alpha, mitochondrial	6.96	1.40	1.57	1.41	0.00	0.00
T5	down	ATP synthase subunit alpha, mitochondrial	7.46	1.50	2.21	1.80	0.00	0.00
T5	down	ADP,ATP carrier protein 1, mitochondrial	6.76	1.44	1.39	1.00	0.00	0.00
T5	down	ATP synthase subunit 5, mitochondrial	6.92	1.48	1.55	1.20	0.00	0.00
T5	down	ATP synthase subunit alpha	6.43	1.40	1.09	0.71	0.00	0.00
T5	down	Superoxide dismutase	19.87	1.37	5.56	4.12	0.00	0.00
T5	down	Superoxide dismutase [Fe	7.32	1.50	2.00	2.19	0.00	0.00
T5	down	Peroxisomal catalase	6.55	1.35	1.21	0.58	0.00	0.00
T5	down	Putative glutathione peroxidase 7, chloroplastic	7.34	1.52	2.01	2.11	0.00	0.00
T5	down	Cathepsin L 2	23.57	1.30	7.84	5.90	0.00	0.00
T5	down	Caltractin ICL1e	23.33	1.21	7.60	4.23	0.00	0.00
T5	down	Cathepsin L 2	23.31	1.23	9.32	5.15	0.00	0.00
T5	down	Putative cathepsin L 3	22.62	1.38	3.57	3.02	0.00	0.00
T5	down	Cathepsin L 2	10.70	1.23	28.79	19.45	0.02	0.03
T5	down	Cathepsin D	5.20	0.89	6.33	3.73	0.20	0.23
T5	down	Cathepsin Z	7.47	1.30	2.27	1.38	0.00	0.00
T5	down	Cathepsin L	22.42	3.23	3.59	7.25	0.00	0.00
T5	down	Cathepsin L 2	6.96	1.32	1.58	0.88	0.00	0.00
T5	down	Cathepsin L 2	7.00	1.33	1.66	0.96	0.00	0.00
T5	down	Cathepsin L 2	5.41	1.02	100.48	71.99	2.75	2.94
T5	down	Cathepsin B	4.98	1.00	10.76	6.20	0.39	0.53
T5	down	Cathepsin B	4.98	1.00	10.76	6.20	0.39	0.53
T5	down	Acyl-CoA-binding protein	23.48	1.45	7.04	7.62	0.00	0.00
T5	down	Succinate--CoA ligase [GDP-forming] subunit beta, mitochondrial	6.88	1.42	1.51	1.33	0.00	0.00
T5	down	Succinate--CoA ligase [ADP-forming] subunit alpha	6.67	1.47	1.27	1.15	0.00	0.00
T5	down	Calcium-binding protein CML19	5.71	1.52	0.75	1.13	-0.01	0.01
T5	down	Cytochrome c1, heme protein, mitochondrial	7.24	1.34	1.91	1.29	0.00	0.00
T5	down	Calcium-binding protein CML19	22.56	1.37	3.51	2.67	0.00	0.00
T5	down	Probable calcium-binding protein CML13	5.79	0.95	10.37	6.08	0.20	0.32
T5	down	Calcium-binding protein CML19	22.34	1.45	3.13	2.34	0.00	0.00
T5	down	Calcium-transporting ATPase 8, plasma membrane-type	6.23	1.36	0.99	0.50	0.00	0.00
T5	down	Carboxypeptidase Q	6.99	1.36	1.64	0.97	0.00	0.00
T5	down	Carboxypeptidase Q;	7.31	1.35	2.03	1.19	0.00	0.00
T5	down	Probable cysteine protease RDL2	24.78	1.26	20.96	12.85	0.00	0.00
T5	down	Legumain	23.66	1.25	7.78	4.72	0.00	0.00
T5	down	Oryzain alpha chain	23.91	1.27	9.27	6.49	0.00	0.00
T5	down	Cysteine protease XCP1	22.98	1.28	4.75	2.82	0.00	0.00
T5	down	Oryzain alpha chain	22.58	1.32	3.53	2.37	0.00	0.00
T5	down	Caltractin ICL1e	22.95	1.35	5.11	4.63	0.00	0.00
T5	down	Thioredoxin H-type	23.49	1.38	6.66	6.30	0.00	0.00
T5	down	Peptidyl-prolyl cis-trans isomerase	22.43	1.40	3.10	2.57	0.00	0.00
T5	down	V-type proton ATPase 16 kDa proteolipid subunit	22.44	1.47	3.11	2.87	0.00	0.00
T5	down	Sterol carrier protein 2	22.42	1.49	3.06	3.20	0.00	0.00
T5	down	FK506-binding protein 1	23.04	1.56	4.71	5.93	0.00	0.00
T5	down	Caltractin ICL1e	22.25	1.52	2.76	2.80	0.00	0.00
T5	down	Small cysteine-rich protein 8	28.02	3.19	226.91	363.23	0.00	0.00
T5	down	Coagulation factor V	21.84	3.23	8.86	13.26	0.00	0.00
T5	down	Luminal-binding protein 5	7.33	1.31	2.09	1.07	0.00	0.00
T5	down	Cell division cycle protein 48 homolog	7.40	1.35	2.16	1.41	0.00	0.00
T5	down	Retinoid-inducible serine carboxypeptidase	7.08	1.29	1.75	0.91	0.00	0.00
T5	down	Exoglucanase	7.45	1.39	2.22	1.71	0.00	0.00
T5	down	Protein disulfide-isomerase	7.37	1.38	2.12	1.51	0.00	0.00
T5	down	Cystathionine gamma-lyase	7.31	1.37	2.06	1.23	0.00	0.00
T5	down	Glucoamylase	6.72	1.28	1.38	0.56	0.00	0.00
T5	down	Ras-related protein RIC1	7.21	1.38	1.92	1.06	0.00	0.00

Supplementary table 4: Differential gene expression – continued

Sampling time	Regulation low-pH group	Gene name	log2 fold change	SE	Mean Control	SD Control	Mean low-pH	SD low-pH
T5	down	Casein kinase 1-like protein 2	7.22	1.39	1.92	1.42	0.00	0.00
T5	down	Peptidyl-prolyl cis-trans isomerase B	7.07	1.40	1.71	1.22	0.00	0.00
T5	down	Beta-1,3-glucan-binding protein	6.77	1.35	1.43	0.81	0.00	0.00
T5	down	Profilin	7.25	1.45	1.90	1.93	0.00	0.00
T5	down	Ras-related protein Rab-7b	6.57	1.32	1.25	0.76	0.00	0.00
T5	down	Eukaryotic translation initiation factor 5A	7.17	1.44	1.91	1.31	0.00	0.00
T5	down	Caltractin ICL1e	7.35	1.49	2.05	1.74	0.00	0.00
T5	down	Putative voltage-gated potassium channel subunit beta	7.17	1.47	1.85	1.38	0.00	0.00
T5	down	Nascent polypeptide-associated complex subunit alpha-like protein 1	6.96	1.44	1.60	1.32	0.00	0.00
T5	down	Calmodulin	7.28	1.53	1.96	2.01	0.00	0.00
T5	down	Nucleoside diphosphate kinase	7.04	1.48	1.65	1.67	0.00	0.00
T5	down	Glutathione S-transferase Mu 1	7.36	1.55	2.06	1.77	0.00	0.00
T5	down	Putative voltage-gated potassium channel subunit beta	7.01	1.48	1.63	1.42	0.00	0.00
T5	down	Probable dual specificity protein phosphatase DDB_G0269404	7.00	1.48	1.67	1.25	0.00	0.00
T5	down	Lysosomal protective protein	6.63	1.40	1.26	0.80	0.00	0.00
T5	down	Dynein heavy chain 17, axonemal	6.97	1.48	1.58	1.36	0.00	0.00
T5	down	DNA repair and recombination protein RAD54B	4.48	0.95	99.57	140.05	4.90	2.16
T5	down	Metal tolerance protein B	6.60	1.41	1.25	0.86	0.00	0.00
T5	down	Temperature-induced lipocalin-	6.85	1.47	1.47	1.18	0.00	0.00
T5	down	Serine carboxypeptidase ctsa-4 1	6.61	1.43	1.26	0.90	0.00	0.00
T5	down	V-type proton ATPase subunit B	6.49	1.41	1.13	0.85	0.00	0.00
T5	down	Putative K(+)-stimulated pyrophosphate-energized sodium pump	6.55	1.42	1.28	0.99	0.00	0.00
T5	down	N-acylethanolamine-hydrolyzing acid amidase	6.71	1.47	1.32	1.01	0.00	0.00
T5	down	Isocitrate dehydrogenase [NADP] cytoplasmic	7.06	1.56	1.64	1.71	0.00	0.00
T5	down	Small COPII coat GTPase SAR1	6.76	1.50	1.39	1.29	0.00	0.00
T5	down	Probable cysteine protease RDL2	1.81	1.41	3.93	4.30	0.20	0.08
pH exposure experiment: 2 months after the Treatment group re-reached pH 8.0								
T6	up	40S ribosomal protein S3a	-7.39	1.37	0.00	0.00	1.75	1.54
T6	up	40S ribosomal protein S14	-7.55	1.48	0.00	0.00	1.93	2.18
T6	up	40S ribosomal protein S10	-7.08	1.40	0.00	0.00	1.40	0.94
T6	up	40S ribosomal protein S5-2	-6.93	1.47	0.00	0.00	1.30	0.89
T6	up	40S ribosomal protein S12;	-6.82	1.48	0.00	0.00	1.24	0.88
T6	up	40S ribosomal protein S19-1	-6.62	1.50	0.00	0.00	1.05	0.81
T6	up	40S ribosomal protein S24-1	-6.47	1.47	0.00	0.00	0.95	0.66
T6	up	40S ribosomal protein S15Aa	-6.99	1.59	0.00	0.00	1.33	1.43
T6	up	40S ribosomal protein S26-3;	-7.32	1.37	0.00	0.00	1.68	1.01
T6	up	60S acidic ribosomal protein P2	-22.30	2.04	0.00	0.00	3.37	5.21
T6	up	60S ribosomal protein L31	-5.69	0.92	0.59	0.42	27.71	39.58
T6	up	60S ribosomal protein L23	-7.07	1.19	0.00	0.00	1.42	0.52
T6	up	60S ribosomal protein L39-2	-7.03	1.26	0.00	0.00	1.43	0.73
T6	up	60S ribosomal protein L21	-7.24	1.26	0.00	0.00	1.59	0.98
T6	up	60S ribosomal protein L27a	-6.95	1.31	0.00	0.00	1.29	0.73
T6	up	60S ribosomal protein L24	-7.36	1.42	0.00	0.00	1.73	1.54
T6	up	60S ribosomal protein L12-A	-6.94	1.25	0.00	0.00	1.31	0.58
T6	up	60S ribosomal protein L11-2	-7.04	1.28	0.00	0.00	1.42	0.72
T6	up	60S ribosomal protein L35	-7.40	1.43	0.00	0.00	1.78	1.83
T6	up	60S ribosomal protein L35a-3	-7.44	1.45	0.00	0.00	1.82	1.68
T6	up	60S ribosomal protein L10a	-6.70	1.33	0.00	0.00	1.11	0.64
T6	up	60S ribosomal protein L8	-7.00	1.37	0.00	0.00	1.33	0.86
T6	up	60S ribosomal protein L3	-7.05	1.41	0.00	0.00	1.40	1.14
T6	up	60S ribosomal protein L31	-6.92	1.39	0.00	0.00	1.26	0.90
T6	up	60S ribosomal protein L10-A	-6.19	1.31	0.01	0.03	1.14	0.62
T6	up	60S ribosomal protein L27	-6.59	1.41	0.00	0.00	1.01	0.73
T6	up	60S ribosomal protein L6	-6.68	1.49	0.00	0.00	1.10	0.73
T6	up	60S ribosomal protein L14-2	-7.02	1.62	0.00	0.00	1.34	1.53
T6	up	Tubulin alpha chain	-22.03	1.60	0.00	0.00	2.80	2.95
T6	up	Tubulin alpha chain	-21.11	1.68	0.00	0.00	3.57	5.55
T6	up	Tubulin beta-2 chain	-7.16	1.53	0.00	0.00	1.51	1.57
T6	up	Actin-1	-23.86	1.20	0.00	0.00	10.74	8.95
T6	up	Actin-10	-6.51	0.96	0.07	0.10	6.57	5.20

Supplementary table 4: Differential gene expression – continued

Sampling time	Regulation low-pH group	Gene name	log2 fold change	SE	Mean Control	SD Control	Mean low-pH	SD low-pH
T6	up	Actin-1	-7.01	1.15	0.13	0.18	16.57	20.03
T6	up	Actin, muscle	-6.01	1.07	0.14	0.20	8.75	8.43
T6	up	Actin-1;	-7.94	1.47	0.00	0.00	2.57	3.06
T6	up	Actin, cytoplasmic	-6.05	1.17	0.10	0.14	6.24	4.60
T6	up	Actin, cytoplasmic 1	-7.28	1.50	0.00	0.00	1.60	1.80
T6	up	Actin, plasmodial isoform	-4.44	0.92	0.53	0.49	10.72	9.09
T6	up	Actin, plasmodial isoform	-6.75	1.31	0.00	0.00	1.16	0.57
T6	up	Polyubiquitin-D	-6.31	1.37	0.02	0.04	1.89	1.69
T6	up	E3 ubiquitin-protein ligase ZNRF3	-2.74	0.64	6.10	1.32	36.88	41.33
T6	up	Ubiquitin-40S ribosomal protein S27a	-7.42	1.26	0.00	0.00	1.80	1.23
T6	up	Ubiquitin-60S ribosomal protein L4	-6.85	1.35	0.00	0.00	1.22	0.70
T6	up	Elongation factor 1-alpha	-22.24	1.60	0.00	0.00	3.08	4.23
T6	up	Elongation factor 1-alpha	-7.94	1.47	0.00	0.00	2.62	2.59
T6	up	Elongation factor 1-alpha	-6.12	1.16	0.06	0.08	4.21	3.68
T6	up	Elongation factor 1-alpha	-8.67	1.25	0.01	0.03	4.47	4.20
T6	up	Histone H2A	-6.28	0.80	0.18	0.09	14.40	12.93
T6	up	Histone H3	-5.94	1.27	0.11	0.16	7.33	7.54
T6	up	Cytochrome c oxidase subunit 1	-7.35	1.31	0.08	0.08	11.41	18.64
T6	up	Cytochrome c oxidase subunit 3	-4.20	0.95	12.02	7.92	203.82	220.56
T6	up	Uncharacterized skeletal organic matrix protein 5	-6.81	1.36	0.23	0.31	22.90	21.94
T6	up	Scavenger receptor cysteine-rich type 1 protein M160	-6.36	1.48	0.13	0.13	8.81	11.74
T6	up	Profilin-A	-22.51	1.28	0.00	0.00	4.92	4.25
T6	up	Atrial natriuretic peptide receptor 1	-23.47	3.19	0.01	0.01	7.74	10.29
T6	up	Phosphoethanolamine N-methyltransferase 1	-5.69	0.85	2.06	1.58	100.17	83.16
T6	up	Uncharacterized protein ORF91	-5.99	0.90	0.14	0.10	8.41	9.97
T6	up	NADH-ubiquinone oxidoreductase chain 3	-6.09	0.95	0.18	0.11	10.56	13.55
T6	up	Blastula protease 10	-5.01	0.80	1.37	1.16	39.84	35.95
T6	up	Uncharacterized protein ORF91	-5.56	0.90	0.19	0.17	7.78	5.53
T6	up	Neurexin-4	-4.72	0.77	0.53	0.33	13.40	14.36
T6	up	14-3-3-like protein	-7.95	1.36	0.00	0.00	2.63	2.12
T6	up	Translationally-controlled tumor protein homolog	-7.45	1.28	0.00	0.00	1.83	1.18
T6	up	Uncharacterized protein ORF91	-6.59	1.18	0.06	0.08	4.29	4.45
T6	up	Adenylyl cyclase-associated protein	-7.75	1.40	0.00	0.00	2.24	2.32
T6	up	Cysteine proteinase 5	-7.07	1.30	0.01	0.02	2.85	2.99
T6	up	Ethanolamine-phosphate cytidylyltransferase	-6.72	1.25	0.00	0.00	1.11	0.40
T6	up	Severin	-6.08	1.14	0.02	0.02	2.22	1.90
T6	up	Probable glutathione S-transferase 8	-6.16	1.17	0.07	0.08	4.23	3.87
T6	up	Beta-parvin	-2.25	0.43	22.46	6.96	99.46	58.13
T6	up	Poly [ADP-ribose] polymerase 2-A	-4.83	0.93	0.25	0.14	6.11	6.94
T6	up	Probable serine/threonine-protein kinase SIS8	-6.98	1.35	0.00	0.00	1.31	1.02
T6	up	NADH-ubiquinone oxidoreductase chain 4	-4.01	0.78	1.99	0.90	29.17	33.36
T6	up	14-3-3 protein epsilon	-6.38	1.24	0.02	0.04	1.92	1.11
T6	up	Homeobox protein MOX-1	-2.74	0.54	0.77	0.33	4.77	2.36
T6	up	tRNA-splicing endonuclease subunit Sen2	-2.21	0.44	11.11	2.88	47.39	22.56
T6	up	LINE-1 retrotransposable element ORF2 protein	-4.99	1.00	0.25	0.11	6.91	10.45
T6	up	Ribonuclease P protein subunit p40	-2.80	0.56	20.83	5.35	133.60	106.39
T6	up	Peptidyl-prolyl cis-trans isomerase	-7.27	1.49	0.00	0.00	1.63	1.57
T6	up	NADH-ubiquinone oxidoreductase chain 5	-3.60	0.75	2.39	0.86	26.50	26.07
T6	up	Cofilin	-6.30	1.32	0.02	0.05	1.85	1.43
T6	up	Cysteine protease XCP2	-6.11	1.31	0.04	0.08	2.75	2.02
T6	up	Putative uncharacterized protein ART2	-5.04	1.11	7.60	6.48	228.46	259.19
T6	up	Xanthine dehydrogenase/oxidase;	-4.57	1.00	2.95	1.53	63.06	93.55
T6	up	Transcription initiation factor TFIID subunit 2	-7.05	1.60	0.00	0.00	1.36	1.28
T6	up	Replicase polyprotein	-5.76	1.31	0.51	0.66	25.12	37.08
T6	up	ollagen triple helix repeat-containing protein 1	-2.85	0.66	1.18	0.66	7.82	5.98
T6	up	Uncharacterized protein ORF91	-4.43	1.03	0.88	0.72	17.50	19.98
T6	down	40S ribosomal protein SA	8.23	1.14	96.70	70.67	0.32	0.48
T6	down	60S ribosomal protein L5	24.26	3.23	21.70	29.28	0.00	0.00
T6	down	Tau-tubulin kinase 2	2.12	0.50	2.34	0.39	0.48	0.28
T6	down	Microtubule-actin cross-linking factor 1	22.94	3.23	8.10	12.23	0.00	0.00
T6	down	Contactin-associated protein like 5-3	3.35	0.67	7.12	3.87	0.65	0.47
T6	down	E3 ubiquitin-protein ligase MARCHF8	2.99	0.57	4.74	2.33	0.54	0.25
T6	down	Phospholipid-transporting ATPase ABCA3	2.87	0.67	2.79	1.37	0.36	0.24
T6	down	ATP-binding cassette sub-family C member 4	3.23	0.70	1.98	0.48	0.19	0.14

Supplementary table 4: Differential gene expression – continued

Sampling time	Regulation low-pH group	Gene name	log2 fold change	SE	Mean Control	SD Control	Mean low-pH	SD low-pH
T6	down	Protein mono-ADP-ribosyltransferase TIPARP	22.68	3.23	6.75	9.32	0.00	0.00
T6	down	Protein lifeguard 2	2.41	0.43	13.46	7.20	2.39	0.55
T6	down	Cathepsin L 2	21.69	1.93	3.25	4.97	0.00	0.00
T6	down	RNA-binding protein 10	21.45	2.27	2.71	2.80	0.00	0.00
T6	down	Alpha-L-fucosidase	21.41	2.97	2.63	4.04	0.00	0.00
T6	down	Mitogen-activated protein kinase kinase kinase 2	4.91	0.73	6.41	2.28	0.18	0.21
T6	down	Fucolectin	2.30	0.36	6.12	0.92	1.15	0.56
T6	down	Protein FAM91A1	3.09	0.50	4.44	1.31	0.53	0.20
T6	down	Dimethylaniline monooxygenase [N-oxide-forming] 4	3.74	0.64	22.17	11.08	1.58	1.30
T6	down	Protein phosphatase 1 regulatory subunit 12A	2.04	0.36	12.92	4.98	2.97	0.73
T6	down	SPRY domain-containing protein 7	2.40	0.43	6.20	1.90	1.08	0.42
T6	down	Secretory carrier-associated membrane protein 3	2.93	0.53	2.99	0.68	0.37	0.18
T6	down	Protein kinase C delta type	2.14	0.39	4.27	0.73	0.89	0.37
T6	down	BCL-6 corepressor	2.09	0.38	5.21	1.06	1.13	0.52
T6	down	Sialin	6.17	1.14	1.65	0.45	0.00	0.00
T6	down	Progranulin	2.42	0.45	60.14	34.05	10.57	4.89
T6	down	Transcriptional regulator ATRX	2.41	0.45	5.09	1.87	0.91	0.30
T6	down	Epithelial discoidin domain-containing receptor 1	3.12	0.61	7.45	4.90	0.78	0.50
T6	down	Sortilin-related receptor	2.48	0.49	15.71	8.41	2.66	1.22
T6	down	Endoplasmic reticulum resident protein 44	2.09	0.42	6.56	2.82	1.48	0.25
T6	down	Beta-mannosidas	2.14	0.43	3.06	0.46	0.60	0.29
T6	down	Nuclear pore complex protein Nup155	6.22	1.25	1.69	0.91	0.00	0.00
T6	down	Grainyhead-like protein 2 homolog	2.30	0.47	10.17	5.46	1.94	0.54
T6	down	Peptidyl-prolyl cis-trans isomerase G	4.09	0.84	6.41	6.48	0.37	0.27
T6	down	Lipid droplet-regulating VLDL assembly factor AUP1	2.48	0.51	2.81	0.54	0.44	0.30
T6	down	Coagulation factor VIII	3.32	0.69	10.08	8.87	0.94	0.54
T6	down	High affinity copper uptake protein 1	2.73	0.57	19.85	13.87	2.81	1.18
T6	down	TBC1 domain family member 4;	2.48	0.52	11.19	6.70	1.87	0.56
T6	down	Proprotein convertase subtilisin/kexin type 6	3.02	0.63	11.96	10.08	1.38	0.77
T6	down	Low-density lipoprotein receptor-related protein 6	3.53	0.73	5.02	3.14	0.40	0.38
T6	down	F-box only protein 9	2.56	0.54	7.21	3.85	1.15	0.35
T6	down	Amyloid-beta precursor-like protein	2.03	0.43	21.11	9.35	4.87	2.01
T6	down	Endoplasmin homolog	2.42	0.51	9.84	4.32	1.73	1.19
T6	down	Ryncolin-1	6.09	1.29	1.56	1.04	0.00	0.00
T6	down	UDP-N-acetylglucosamine--peptide N-acetylglucosaminyltransferase 110 kDa subunit	2.29	0.49	52.96	16.07	10.35	9.08
T6	down	Synaptotagmin-12	2.63	0.56	2.82	0.89	0.43	0.22
T6	down	RNA-binding protein Musashi homolog 2	2.28	0.49	2.56	0.38	0.52	0.33
T6	down	Protocadherin-like wing polarity protein stan	2.10	0.45	10.10	4.77	2.23	0.53
T6	down	Splicing factor U2AF 65 kDa subunit	2.33	0.50	12.85	6.38	2.42	1.47
T6	down	Cytoplasmic dynein 1 heavy chain 1	6.29	1.36	1.80	1.21	0.00	0.00
T6	down	E3 ubiquitin-protein ligase RNF13	2.22	0.48	13.69	7.30	2.74	1.18
T6	down	Scaffold attachment factor B1	2.07	0.45	9.45	2.23	2.09	1.58
T6	down	Importin-13	3.69	0.81	2.80	1.07	0.22	0.26
T6	down	RNA polymerase-associated protein RTF1 homolog	2.02	0.44	4.00	1.40	0.91	0.16
T6	down	5'-AMP-activated protein kinase catalytic subunit alpha-1	2.60	0.57	8.48	5.34	1.31	0.70
T6	down	Store-operated calcium entry-associated regulatory factor	3.60	0.80	3.74	1.65	0.32	0.36
T6	down	Peroxidasin homolog pxn-2	2.60	0.58	10.83	6.83	1.68	0.72
T6	down	Supervilli	2.50	0.56	6.85	3.63	1.13	0.64
T6	down	Cytochrome P450 27C1	2.33	0.52	5.92	3.56	1.09	0.27
T6	down	Probable iron/ascorbate oxidoreductase DDB_G0283291	5.69	1.27	1.18	0.59	0.00	0.00
T6	down	Transmembrane channel-like protein 7	2.25	0.51	4.31	1.99	0.87	0.25
T6	down	Prominin-1-A	2.25	0.51	6.36	2.65	1.27	0.82
T6	down	63 kDa sperm flagellar membrane protein	2.32	0.52	31.56	18.77	5.97	3.61
T6	down	Adenylate kinase isoenzyme 5	2.04	0.46	3.34	0.97	0.73	0.35
T6	down	Alpha-1,6-mannosyl-glycoprotein 2-beta-N-acetylglucosaminyltransferase	2.33	0.53	5.97	3.43	1.08	0.37
T6	down	Chloride channel protein 1	2.42	0.55	9.74	5.12	1.65	1.00

Supplementary table 4: Differential gene expression – continued

Sampling time	Regulation low-pH group	Gene name	log2 fold change	SE	Mean Control	SD Control	Mean low-pH	SD low-pH
T6	down	PAN2-PAN3 deadenylation complex subunit pan3	2.11	0.49	3.30	0.73	0.70	0.52
T6	down	Solute carrier family 22 member 5	2.36	0.55	9.16	3.16	1.66	1.24
T6	down	Mitochondrial uncoupling protein 2	2.36	0.55	4.91	2.52	0.88	0.33
T6	down	Calcium-activated potassium channel subunit alpha-1	3.06	0.71	1.79	0.41	0.21	0.18
T6	down	Glycosaminoglycan xylosylkinase	3.10	0.72	1.57	0.23	0.19	0.13
T6	down	Receptor-type tyrosine-protein phosphatase N2	2.78	0.65	3.52	2.24	0.47	0.24
T6	down	Exosome complex exonuclease RRP44	5.72	1.34	1.24	0.74	0.00	0.00
T6	down	Dorsal-ventral patterning tolloid-like protein 1	2.68	0.63	4.82	2.11	0.71	0.58
T6	down	Protein sidekick-1	2.31	0.54	7.40	2.64	1.39	1.13
T6	down	Solute carrier family 15 member 2	2.11	0.50	6.07	2.68	1.28	0.64
T6	down	Synaptophysin-like protein 2	2.32	0.54	6.56	4.19	1.23	0.44
T6	down	Tetratricopeptide repeat protein 28	2.35	0.55	5.02	2.20	0.91	0.60
T6	down	Neurotrypsin	3.62	0.85	2.17	1.24	0.17	0.10
T6	down	Fibronectin type III domain-containing protein	2.45	0.58	8.18	4.58	1.42	0.69
T6	down	Diphosphoinositol polyphosphate phosphohydrolase 1	2.61	0.61	3.37	1.59	0.55	0.23
Field samples: E deep: pH 7.5								
Tt	up	E3 ubiquitin-protein ligase TRIM71	-3.26	0.59	0.57	0.35	5.76	1.61
Tt	up	E3 ubiquitin-protein ligase RNF19A	-2.30	0.44	3.34	1.17	16.70	7.91
Tt	up	Polyubiquitin-B	-2.24	0.35	87.16	39.66	417.94	75.98
Tt	up	Polyubiquitin-B	-2.27	0.31	52.78	21.23	258.50	36.62
Tt	up	Polyubiquitin	-2.59	0.28	16.54	4.84	100.92	21.62
Tt	up	Polyubiquitin-B	-3.37	0.44	15.73	6.06	165.48	82.35
Tt	up	Probable ATP-dependent RNA helicase DDX43	-6.86	1.48	0.00	0.00	1.59	1.21
Tt	up	ATP-binding cassette sub-family F member 2	-2.82	0.31	6.16	2.32	43.90	7.51
Tt	up	ADP-ribosylation factor 1;	-6.13	1.44	0.02	0.03	1.59	1.66
Tt	up	ADP-ribosylation factor	-2.85	0.65	1.23	0.64	8.98	6.50
Tt	up	ADP-ribosylation factor GTPase-activating protein 1	-2.37	0.55	2.04	0.34	10.80	8.07
Tt	up	Adenosine receptor A2a	-6.61	1.26	0.01	0.02	1.35	0.43
Tt	up	Adenosine receptor A3;	-2.15	0.50	0.42	0.07	1.90	0.41
Tt	up	Adenosine receptor A1	-3.96	0.78	0.14	0.09	2.34	1.28
Tt	up	GTP-binding protein Rho1	-2.43	0.52	1.37	0.92	7.53	2.50
Tt	up	Serine--pyruvate aminotransferase, mitochondrial	-2.97	0.50	2.36	0.91	18.54	11.28
Tt	up	Serine--pyruvate aminotransferase	-2.41	0.40	28.14	7.62	151.20	78.03
Tt	up	Serine/threonine-protein kinase SIK2	-3.96	0.45	8.73	0.43	137.71	79.96
Tt	up	Serine/threonine-protein kinase Nek6	-24.01	3.38	0.00	0.00	18.36	30.44
Tt	up	Serine/threonine-protein kinase Nek10	-2.37	0.45	3.94	1.01	20.59	10.78
Tt	up	Testis-specific serine/threonine-protein kinase 1	-6.53	1.36	0.16	0.13	14.29	22.86
Tt	up	Serine--pyruvate aminotransferase, mitochondrial	-2.40	0.52	4.04	2.57	21.69	8.85
Tt	up	Serine/threonine-protein kinase SIK2	-3.95	0.86	0.08	0.05	1.45	0.50
Tt	up	Phosphatidylserine decarboxylase proenzyme, mitochondrial	-2.53	0.58	1.81	1.03	10.51	4.61
Tt	up	Serine/threonine-protein kinase NLK	-3.09	0.72	1.56	0.53	13.49	14.92
Tt	up	Heat shock protein Hsp-16 48/Hsp-16 49	-6.68	1.02	0.44	0.36	44.48	41.25
Tt	up	Heat shock 70 kDa protein II	-5.12	0.91	0.15	0.18	5.05	2.53
Tt	up	Heat shock protein HSP 90-beta	-2.25	0.40	20.21	3.12	98.02	56.32
Tt	up	Heat shock 70 kDa protein 13x	-2.60	0.55	1.09	0.58	6.72	3.27
Tt	up	Heat shock 70 kDa protein 12B	-3.39	0.73	1.26	0.62	13.27	11.48
Tt	up	Heat shock 70 kDa protein II	-2.30	0.53	1.24	0.47	6.16	3.13
Tt	up	Heat shock cognate 71 kDa protein	-2.40	0.32	20.71	4.06	110.95	43.96
Tt	up	Zinc finger CW-type PWWP domain protein 2	-3.43	0.29	1.95	0.09	21.20	5.46
Tt	up	Zinc finger protein 106	-2.64	0.27	6.84	1.73	43.45	8.65
Tt	up	Juxtaposed with another zinc finger protein 1	-2.68	0.35	7.61	1.80	49.45	17.91
Tt	up	Ras-related protein Rab-30	-5.51	0.46	2.27	0.96	103.87	46.87
Tt	up	Ras-related protein Rab-1A	-4.11	0.37	6.18	2.06	108.28	37.49
Tt	up	Ras guanine nucleotide exchange factor A	-2.63	0.37	5.67	1.39	35.75	14.71
Tt	up	Ras-related and estrogen-regulated growth inhibitor	-2.22	0.43	1.24	0.28	5.88	2.13
Tt	up	Ras-related and estrogen-regulated growth inhibitor	-3.30	0.76	1.18	0.51	11.69	13.19
Tt	up	Matrix metalloproteinase-16	-5.64	0.47	2.96	1.29	149.46	63.24

Supplementary table 4: Differential gene expression – continued

Sampling time	Regulation low-pH group	Gene name	log2 fold change	SE	Mean Control	SD Control	Mean low-pH	SD low-pH
Tt	up	Metalloproteinase inhibitor 1	-3.70	0.36	1.99	0.43	25.75	8.81
Tt	up	Matrix metalloproteinase-25	-4.11	0.42	4.76	1.38	83.69	45.67
Tt	up	Matrix metalloproteinase-25	-4.58	0.60	1.69	0.72	41.16	37.17
Tt	up	Matrix metalloproteinase-25	-4.38	0.62	17.33	9.52	367.87	264.89
Tt	up	Matrix metalloproteinase-14	-3.54	0.51	2.18	0.42	25.55	16.78
Tt	up	A disintegrin and metalloproteinase with thrombospondin motifs 2	-2.26	0.35	4.47	0.22	21.84	9.13
Tt	up	Metalloproteinase inhibitor 3	-2.34	0.47	2.13	0.82	10.89	5.64
Tt	up	Metalloproteinase inhibitor 2	-3.42	0.70	2.15	1.58	23.12	14.91
Tt	up	Phosphoenolpyruvate carboxykinase, cytosolic [GTP]	-4.42	0.48	1.68	0.60	36.51	20.64
Tt	up	Phosphoenolpyruvate carboxykinase [GTP], mitochondrial	-3.44	0.43	5.21	0.96	57.53	34.95
Tt	up	Phosphoenolpyruvate carboxykinase [GTP], mitochondrial;	-2.47	0.35	22.72	6.42	127.99	43.66
Tt	up	Phosphoenolpyruvate carboxykinase [GTP]	-2.51	0.50	34.39	22.99	198.08	60.18
Tt	up	Basement membrane-specific heparan sulfate proteoglycan core protein	-3.32	0.73	1.70	0.35	17.20	19.46
Tt	up	Basement membrane-specific heparan sulfate proteoglycan core protein	-3.32	0.73	1.70	0.35	17.20	19.46
Tt	up	SPRY domain-containing SOCS box protein 3	-3.13	0.39	30.04	17.05	267.40	50.02
Tt	up	SPRY domain-containing SOCS box protein 3	-3.30	0.43	32.55	20.24	324.72	51.87
Tt	up	TNF receptor-associated factor 3	-4.74	0.40	27.83	4.65	753.87	343.78
Tt	up	TNF receptor-associated factor 4	-3.71	0.79	5.65	6.01	74.54	70.45
Tt	up	Tauropine dehydrogenase	-2.07	0.36	137.59	56.06	585.42	159.68
Tt	up	Tauropine dehydrogenase	-2.02	0.38	203.97	67.69	838.68	367.33
Tt	up	Tauropine dehydrogenase	-2.29	0.45	36.11	22.91	178.32	8.09
Tt	up	50 kDa hatching enzyme	-7.00	0.79	0.77	0.34	101.03	109.71
Tt	up	50 kDa hatching enzyme	-5.57	0.67	5.63	0.66	272.64	255.58
Tt	up	Homeobox protein OTX1 B	-2.95	0.42	4.45	1.98	35.06	10.56
Tt	up	Homeobox protein Nkx-2 5	-2.42	0.56	2.45	0.71	13.27	10.93
Tt	up	Homeobox protein otx5-B	-3.46	0.60	1.48	0.91	16.74	10.97
Tt	up	Aristaless-related homeobox protein	-2.96	0.58	1.09	0.41	8.53	6.23
Tt	up	Transcription factor AP-1	-4.00	0.58	12.12	8.39	196.87	127.69
Tt	up	Doublesex and mab-3 related transcription factor 3, truncated	-5.04	0.53	1.10	0.35	36.58	24.14
Tt	up	Transcription factor ETV6	-2.28	0.34	70.93	21.43	350.75	112.77
Tt	up	Thyroid transcription factor 1	-2.32	0.36	1.32	0.45	6.66	1.08
Tt	up	Runt-related transcription factor 2	-2.74	0.47	10.76	4.52	73.29	37.20
Tt	up	Transcription factor HES-1	-2.47	0.52	6.38	1.32	35.97	23.55
Tt	up	Histone-lysine N-methyltransferase, H3 lysine-79 specific	-2.28	0.39	7.03	2.05	34.73	15.58
Tt	up	Cytochrome P450 1A2	-2.66	0.58	0.76	0.40	4.92	2.19
Tt	up	Forkhead box protein O	-5.42	0.35	0.64	0.33	28.00	1.58
Tt	up	DnaJ homolog subfamily C member 21	-2.65	0.23	4.77	0.99	30.23	4.28
Tt	up	p55-v-Fos-transforming protein	-4.93	0.44	20.01	5.50	617.42	332.03
Tt	up	Thyrotropin-releasing hormone receptor;	-4.34	0.39	5.13	1.05	105.51	47.34
Tt	up	Segmentation protein paired	-5.92	0.57	1.58	0.94	96.75	44.33
Tt	up	Tissue factor pathway inhibitor 2	-6.11	0.62	0.72	0.53	48.72	34.30
Tt	up	Delta-like protein B	-4.77	0.51	7.05	2.62	196.35	101.67
Tt	up	Cytosolic phospholipase A2	-4.90	0.53	1.76	0.86	53.91	31.90
Tt	up	SH3 and PX domain-containing protein 2A	-3.25	0.36	3.26	0.79	31.57	10.51
Tt	up	Paired box protein Pax-1	-6.01	0.70	5.65	4.62	369.66	300.99
Tt	up	Protein C-ets-2	-3.33	0.40	0.58	0.13	5.98	1.08
Tt	up	Kelch-like protein 1	-2.44	0.29	2.06	0.23	11.27	2.43
Tt	up	Isocitrate lyase	-4.03	0.49	2.78	0.41	46.07	34.03
Tt	up	1-acylglycerol-3-phosphate O-acyltransferase ABHD5	-2.61	0.32	6.07	0.59	37.49	12.09
Tt	up	ETS domain-containing protein Elk-1	-3.25	0.40	1.30	0.39	12.70	4.54
Tt	up	Protein BTG1	-4.98	0.62	12.91	9.01	414.62	268.62
Tt	up	Protein phosphatase 1 regulatory subunit 3D	-3.62	0.47	12.66	7.67	157.13	40.36
Tt	up	Probable G-protein coupled receptor tkr-1	-3.81	0.51	3.47	1.06	49.22	34.06
Tt	up	Myocilin	-22.77	3.04	0.00	0.00	8.73	10.40
Tt	up	Nuclear factor erythroid 2-related factor 3	-2.41	0.32	19.03	2.90	102.47	38.66
Tt	up	Transmembrane protein 205	-6.10	0.83	2.10	2.25	145.62	130.63
Tt	up	QRFP-like peptide receptor	-3.46	0.48	1.10	0.54	12.25	4.98
Tt	up	Lon protease homolog 2, peroxisomal	-2.18	0.30	24.53	5.95	112.45	32.10

Supplementary table 4: Differential gene expression – continued

Sampling time	Regulation low-pH group	Gene name	log2 fold change	SE	Mean Control	SD Control	Mean low-pH	SD low-pH
Tt	up	Prickle planar cell polarity protein 3	-2.64	0.37	7.39	0.72	46.62	22.71
Tt	up	Heart- and neural crest derivatives-expressed protein 2	-3.03	0.42	1.82	0.25	14.90	7.84
Tt	up	Pleckstrin homology-like domain family B member 1	-2.27	0.31	4.46	1.60	21.72	4.41
Tt	up	Serotransferrin	-2.91	0.41	14.75	4.93	111.90	39.60
Tt	up	Protein gustavus	-3.60	0.51	7.81	3.25	95.66	61.89
Tt	up	mRNA decay activator protein ZFP36L1	-2.66	0.38	34.93	4.12	224.19	106.91
Tt	up	Interstitial collagenase	-7.03	1.01	0.54	0.42	70.98	81.99
Tt	up	Escargot/snail protein homolog	-3.17	0.46	0.55	0.21	5.03	1.35
Tt	up	Mucin-4	-3.65	0.54	5.09	1.01	65.09	48.20
Tt	up	Protein ABHD8	-2.15	0.32	2.58	0.57	11.61	3.06
Tt	up	Protein sprouty homolog 2	-2.34	0.35	3.85	1.41	20.02	4.72
Tt	up	Protein FEV	-3.02	0.46	54.70	14.14	453.17	260.57
Tt	up	Toll-like receptor 13	-3.44	0.52	1.07	0.63	11.70	5.24
Tt	up	Fibrinogen-like protein A	-22.16	3.38	0.00	0.00	4.83	6.73
Tt	up	Tenascin-R	-22.00	3.38	0.00	0.00	4.34	7.58
Tt	up	Protein SpAN	-6.82	1.05	0.13	0.05	14.56	17.03
Tt	up	Capsule biosynthesis protein CapD proenzyme	-3.24	0.51	12.07	7.46	115.67	41.28
Tt	up	Dual specificity protein phosphatase 2	-2.37	0.37	11.15	1.73	58.46	23.06
Tt	up	Octopine dehydrogenase	-2.54	0.40	27.67	13.21	162.96	40.33
Tt	up	Fibroblast growth factor receptor 1	-3.78	0.60	4.52	1.22	62.79	59.21
Tt	up	MICAL-like protein 2	-2.47	0.40	2.06	1.01	11.38	2.00
Tt	up	La-related protein 6	-3.67	0.59	11.48	8.56	147.39	79.70
Tt	up	Hypoxia-inducible factor 1-alpha	-2.72	0.44	18.55	7.10	123.28	65.19
Tt	up	StAR-related lipid transfer protein 13	-2.18	0.36	6.40	1.13	29.50	13.21
Tt	up	Calcium/calmodulin-dependent protein kinase type II subunit delta	-3.65	0.61	1.17	0.81	14.89	7.85
Tt	up	Steroid 17-alpha-hydroxylase/17,20 lyase;	-2.53	0.42	16.00	8.00	93.68	16.22
Tt	up	Protein FAM166C	-20.11	3.38	0.00	0.00	3.90	6.86
Tt	up	Angiopoietin-2	-3.84	0.65	1.42	0.85	20.42	12.37
Tt	up	Metabotropic glutamate receptor 3	-2.05	0.35	3.08	1.39	12.96	1.65
Tt	up	Collagen triple helix repeat-containing protein 1	-4.57	0.78	2.12	0.95	51.17	60.39
Tt	up	Glycine betaine transporter 1	-4.13	0.71	3.26	2.64	57.55	47.57
Tt	up	Lysophospholipid acyltransferase 2	-2.04	0.35	1.41	0.21	5.92	1.61
Tt	up	Lipase member K;	-2.10	0.37	20.08	5.66	87.35	37.05
Tt	up	HSPB1-associated protein 1	-2.23	0.39	8.79	2.70	42.16	18.41
Tt	up	N-sulphoglucosamine sulphohydrolase	-4.67	0.83	3.63	1.84	94.27	80.39
Tt	up	Sodium-coupled monocarboxylate transporter 2	-2.73	0.49	2.01	0.72	13.29	6.37
Tt	up	FERM domain-containing protein 8	-2.31	0.42	17.81	8.22	89.87	35.23
Tt	up	PRELI domain containing protein 3B	-2.28	0.42	7.32	1.62	36.25	19.96
Tt	up	1-acylglycerol-3-phosphate O-acyltransferase ABHD5	-2.94	0.54	1.80	0.89	13.96	6.31
Tt	up	Colorectal mutant cancer protein	-2.51	0.46	1.67	0.25	9.54	4.90
Tt	up	Influenza virus NS1A-binding protein homolog B	-2.16	0.40	12.54	6.15	56.87	16.17
Tt	up	Glutamine synthetase	-2.24	0.41	5.76	1.35	27.59	14.11
Tt	up	Papilin	-4.11	0.76	0.68	0.20	11.99	13.12
Tt	up	Formin	-2.42	0.45	5.23	2.16	28.22	14.83
Tt	up	Cholinesterase	-2.63	0.49	1.02	0.35	6.49	2.81
Tt	up	ETS domain-containing protein Elk-1	-6.34	1.20	0.04	0.04	3.00	1.59
Tt	up	Cholecystokinin receptor	-2.88	0.55	0.58	0.35	4.34	1.28
Tt	up	Fibrocystin-L	-2.65	0.51	4.68	2.66	29.81	12.43
Tt	up	Rhophilin-2	-2.07	0.40	2.45	0.61	10.45	3.73
Tt	up	Extracellular calcium-sensing receptor;	-2.74	0.54	0.81	0.23	5.37	2.69
Tt	up	Adhesion G protein-coupled receptor L2	-2.37	0.47	177.46	110.25	930.38	306.88
Tt	up	Sphingosine-1-phosphate phosphatase 2	-2.01	0.40	2.50	0.80	10.19	3.83
Tt	up	Pappalysin-1	-3.74	0.75	1.33	0.89	17.87	17.21
Tt	up	Zyxin	-2.52	0.50	2.73	1.01	15.76	10.71
Tt	up	Mitochondrial basic amino acids transporter	-2.19	0.44	2.43	0.61	11.10	6.02
Tt	up	Creatine kinase M-type	-2.65	0.53	4.42	2.14	28.37	16.30
Tt	up	Solute carrier family 22 member 1	-2.34	0.47	1.58	0.79	8.00	2.94
Tt	up	Laminin subunit alpha-3	-2.51	0.51	0.51	0.12	2.77	0.97
Tt	up	Smoothelin-like protein 1	-2.45	0.50	3.37	2.02	18.74	6.51
Tt	up	Ovotransferrin	-2.87	0.59	1.08	0.60	7.90	3.45
Tt	up	START domain-containing protein 10	-2.36	0.48	3.08	0.90	15.95	9.87
Tt	up	Tax1-binding protein 1 homolog B	-2.94	0.61	1.71	0.64	13.25	10.25

Supplementary table 4: Differential gene expression – continued

Sampling time	Regulation low-pH group	Gene name	log2 fold change	SE	Mean Control	SD Control	Mean low-pH	SD low-pH
Tt	up	Protein muscleblind	-2.95	0.61	3.80	1.77	29.88	26.51
Tt	up	Mothers against decapentaplegic homolog 4	-3.11	0.65	0.66	0.44	5.80	3.13
Tt	up	Bifunctional 3'-phosphoadenosine 5'-phosphosulfate synthase	-2.53	0.53	45.94	12.48	269.82	173.48
Tt	up	Radial spoke head protein 4 homolog A	-2.65	0.56	2.03	0.90	13.02	8.25
Tt	up	Histamine H2 receptor	-3.82	0.81	0.23	0.16	3.39	2.53
Tt	up	Plastin-3	-7.06	1.49	0.12	0.09	14.76	24.16
Tt	up	Cdc42 homolog	-2.22	0.47	13.70	3.33	64.84	44.70
Tt	up	Tyrosine-protein kinase transmembrane receptor Ror	-2.99	0.64	0.93	0.39	7.63	5.89
Tt	up	Blastula protease 10	-3.22	0.69	0.49	0.08	4.67	4.16
Tt	up	Adrenocorticotropic hormone receptor	-3.50	0.77	0.17	0.12	1.87	0.77
Tt	up	PI-actitoxin-Aeq3b	-2.91	0.64	5.49	2.27	41.74	33.35
Tt	up	Tolloid-like protein 1	-4.12	0.92	0.16	0.06	2.88	2.96
Tt	up	Inositol-3-phosphate synthase 1-A;	-2.48	0.56	1.42	0.43	7.93	4.86
Tt	up	Adhesion G protein-coupled receptor L2	-2.78	0.62	1.91	0.90	13.20	9.81
Tt	up	CUB and peptidase domain-containing protein 1	-3.30	0.74	1.63	1.17	16.38	12.08
Tt	up	S-adenosyl-L-methionine:benzoic acid/salicylic acid carboxyl methyltransferase 3	-2.93	0.66	21.49	4.88	166.89	173.60
Tt	up	Malate synthase	-3.64	0.82	0.87	0.60	10.89	6.36
Tt	up	Probable RNA-directed DNA polymerase from transposon X-element	-5.05	1.14	0.16	0.24	5.18	4.88
Tt	up	Sodium-dependent phosphate transport protein 2B	-2.15	0.49	6.54	2.54	29.44	18.54
Tt	up	5'-3' exoribonuclease 2	-6.22	1.42	0.00	0.00	1.03	0.45
Tt	up	Endoribonuclease ZC3H12A	-2.21	0.51	0.98	0.61	4.66	1.27
Tt	up	Protein BTG1	-2.03	0.47	45.86	27.14	189.41	66.09
Tt	up	Metastasis-associated protein MTA2	-2.09	0.48	2.57	0.53	11.09	7.19
Tt	up	Galanin receptor 2a	-4.22	0.98	0.13	0.10	2.46	1.89
Tt	up	BTB/POZ domain-containing protein KCTD6	-2.34	0.54	3.90	1.15	20.06	15.45
Tt	up	Creatine kinase, testis isozyme	-9.17	2.13	0.14	0.17	90.48	131.60
Tt	up	Thioredoxin reductase 3	-2.00	0.47	8.29	0.93	33.68	22.85
Tt	up	BMP-binding endothelial regulator protein	-2.66	0.62	2.39	1.48	15.28	8.77
Tt	up	Neuropeptide SIFamide receptor	-2.90	0.68	0.28	0.07	2.07	1.24
Tt	up	Protection of telomeres protein 1	-4.97	1.17	1.65	0.36	52.85	88.02
Tt	up	Microfibril-associated glycoprotein 4	-6.48	1.54	0.08	0.09	6.80	10.55
Tt	up	Collagen triple helix repeat-containing protein 1	-2.48	0.59	9.33	2.28	52.65	40.00
Tt	up	Interferon regulatory factor 2-binding protein-like A;	-2.25	0.54	4.37	1.55	21.01	16.13
Tt	up	Cubilin	-4.54	1.09	0.43	0.30	9.61	13.32
Tt	up	Rhamnose-binding lectin	-4.23	1.01	3.02	3.20	57.19	51.76
Tt	up	Transient receptor potential cation channel subfamily A member 1	-2.48	0.60	0.65	0.26	3.66	1.71
Tt	down	40S ribosomal protein S23	22.08	1.17	2.41	0.72	0.00	0.00
Tt	down	40S ribosomal protein S27	22.44	1.85	3.17	2.26	0.00	0.00
Tt	down	40S ribosomal protein S25	21.93	1.83	5.74	4.12	0.00	0.00
Tt	down	40S ribosomal protein S20	22.11	2.01	2.55	2.68	0.00	0.00
Tt	down	40S ribosomal protein S1	22.16	2.62	2.71	3.19	0.00	0.00
Tt	down	40S ribosomal protein S20	22.19	2.62	2.58	2.98	0.00	0.00
Tt	down	40S ribosomal protein S14	22.04	2.65	2.31	3.06	0.00	0.00
Tt	down	40S ribosomal protein S15a	22.12	2.67	2.48	3.70	0.00	0.00
Tt	down	40S ribosomal protein S25	21.98	2.71	2.26	3.75	0.00	0.00
Tt	down	40S ribosomal protein S30	23.56	3.16	7.30	12.08	0.00	0.00
Tt	down	40S ribosomal protein S27-like	23.49	3.38	6.87	11.38	0.00	0.00
Tt	down	40S ribosomal protein S15	22.56	3.39	3.38	4.21	0.00	0.00
Tt	down	40S ribosomal protein S7	22.40	3.39	3.28	4.06	0.00	0.00
Tt	down	40S ribosomal protein S26-3	7.45	1.17	2.20	0.67	0.00	0.00
Tt	down	40S ribosomal protein S15	6.75	1.23	1.36	0.34	0.00	0.00
Tt	down	40S ribosomal protein S12	6.80	1.25	1.42	0.46	0.00	0.00
Tt	down	40S ribosomal protein S18	6.58	1.23	1.21	0.12	0.00	0.00
Tt	down	40S ribosomal protein S20	6.74	1.27	1.35	0.45	0.00	0.00
Tt	down	40S ribosomal protein S27-2	6.49	1.26	1.14	0.15	0.00	0.00
Tt	down	40S ribosomal protein S1	6.48	1.27	1.12	0.22	0.00	0.00
Tt	down	40S ribosomal protein S21	7.00	1.43	1.61	1.13	0.00	0.00
Tt	down	40S ribosomal protein S2	6.98	1.43	1.62	0.97	0.00	0.00
Tt	down	40S ribosomal protein S16;	6.47	1.38	1.13	0.53	0.00	0.00

Supplementary table 4: Differential gene expression – continued

Sampling time	Regulation low-pH group	Gene name	log2 fold change	SE	Mean Control	SD Control	Mean low-pH	SD low-pH
Tt	down	40S ribosomal protein S11	6.43	1.37	1.08	0.49	0.00	0.00
Tt	down	40S ribosomal protein S4	5.74	1.25	1.10	0.32	0.02	0.04
Tt	down	40S ribosomal protein S28-A	6.70	1.45	1.29	0.76	0.00	0.00
Tt	down	40S ribosomal protein S10	6.42	1.39	1.10	0.56	0.00	0.00
Tt	down	40S ribosomal protein S6	6.30	1.35	1.01	0.31	0.00	0.00
Tt	down	40S ribosomal protein S24-1	6.32	1.41	1.00	0.41	0.00	0.00
Tt	down	40S ribosomal protein S28	6.64	1.50	1.27	0.96	0.00	0.00
Tt	down	40S ribosomal protein S15-A	7.06	1.60	1.69	1.95	0.00	0.00
Tt	down	40S ribosomal protein S14b	6.16	1.44	0.90	0.38	0.00	0.00
Tt	down	40S ribosomal protein S19-3	6.63	1.55	1.23	0.78	0.00	0.00
Tt	down	40S ribosomal protein S5	6.27	1.47	0.96	0.57	0.00	0.00
Tt	down	40S ribosomal protein S8	6.30	1.48	0.99	0.63	0.00	0.00
Tt	down	60S ribosomal protein L31	7.24	1.23	1.93	0.85	0.00	0.00
Tt	down	60S ribosomal protein L37a	7.39	1.26	2.13	1.18	0.00	0.00
Tt	down	60S ribosomal protein L27a	7.11	1.22	1.74	0.57	0.00	0.00
Tt	down	60S ribosomal protein L30	6.88	1.19	1.46	0.21	0.00	0.00
Tt	down	60S ribosomal protein L39	22.42	1.54	3.50	3.68	0.00	0.00
Tt	down	60S ribosomal protein L27a	22.85	1.85	4.22	3.28	0.00	0.00
Tt	down	60S acidic ribosomal protein P0	22.12	1.86	2.63	1.92	0.00	0.00
Tt	down	60S ribosomal protein L23	22.28	1.96	2.77	3.05	0.00	0.00
Tt	down	60S acidic ribosomal protein P2	22.13	2.05	2.50	3.47	0.00	0.00
Tt	down	60S ribosomal protein L10;	22.01	2.15	2.30	2.87	0.00	0.00
Tt	down	60S ribosomal protein L22	22.24	2.63	2.69	3.60	0.00	0.00
Tt	down	60S ribosomal protein L7	22.12	2.63	2.45	2.83	0.00	0.00
Tt	down	60S ribosomal protein L36	22.18	2.64	2.57	3.43	0.00	0.00
Tt	down	60S ribosomal protein L36a	22.24	2.65	2.75	4.16	0.00	0.00
Tt	down	60S ribosomal protein L14	21.98	2.64	2.21	2.58	0.00	0.00
Tt	down	60S ribosomal protein L37a	22.05	2.67	2.36	3.47	0.00	0.00
Tt	down	60S ribosomal protein L34	21.98	2.66	2.23	3.03	0.00	0.00
Tt	down	60S ribosomal protein L31	25.32	3.25	26.31	40.84	0.00	0.00
Tt	down	Probable 60S ribosomal protein L37-A	22.63	3.38	3.55	4.25	0.00	0.00
Tt	down	60S acidic ribosomal protein P2	22.61	3.38	3.55	6.03	0.00	0.00
Tt	down	60S acidic ribosomal protein P2	22.48	3.39	3.19	3.70	0.00	0.00
Tt	down	60S ribosomal protein L32	7.37	1.16	2.09	0.50	0.00	0.00
Tt	down	60S ribosomal protein L11	7.01	1.17	1.62	0.09	0.00	0.00
Tt	down	60S ribosomal protein L8	6.88	1.22	1.49	0.35	0.00	0.00
Tt	down	60S acidic ribosomal protein P1	7.14	1.27	1.76	0.97	0.00	0.00
Tt	down	60S ribosomal protein L13	6.86	1.26	1.45	0.51	0.00	0.00
Tt	down	60S ribosomal protein L19-3	6.79	1.24	1.38	0.39	0.00	0.00
Tt	down	60S ribosomal protein L35;	6.87	1.28	1.49	0.57	0.00	0.00
Tt	down	60S ribosomal protein L10	6.24	1.16	1.57	0.19	0.02	0.05
Tt	down	60S ribosomal protein L22	7.06	1.33	1.68	0.95	0.00	0.00
Tt	down	60S acidic ribosomal protein P0	6.76	1.30	1.37	0.66	0.00	0.00
Tt	down	60S ribosomal protein L12-A	6.66	1.31	1.28	0.53	0.00	0.00
Tt	down	60S ribosomal protein L14-B	6.63	1.31	1.27	0.48	0.00	0.00
Tt	down	60S ribosomal protein L37a	6.93	1.42	1.53	1.24	0.00	0.00
Tt	down	60S ribosomal protein L34-B	6.53	1.34	1.18	0.52	0.00	0.00
Tt	down	60S ribosomal protein L8	6.52	1.36	1.15	0.51	0.00	0.00
Tt	down	60S ribosomal protein L7-2	6.43	1.34	1.09	0.42	0.00	0.00
Tt	down	60S ribosomal protein L13	6.81	1.45	1.41	1.05	0.00	0.00
Tt	down	60S ribosomal protein L24	6.46	1.40	1.12	0.62	0.00	0.00
Tt	down	60S ribosomal protein L44;	6.41	1.41	1.07	0.51	0.00	0.00
Tt	down	60S ribosomal protein L21-1	6.23	1.38	0.95	0.32	0.00	0.00
Tt	down	60S ribosomal protein L9	6.21	1.41	0.94	0.35	0.00	0.00
Tt	down	60S ribosomal protein L27	7.31	1.64	2.02	2.33	0.00	0.00
Tt	down	60S ribosomal protein L35	6.48	1.50	1.12	0.60	0.00	0.00
Tt	down	60S ribosomal protein L26-1	6.10	1.42	0.87	0.32	0.00	0.00
Tt	down	60S ribosomal protein L27	6.54	1.53	1.18	0.78	0.00	0.00
Tt	down	60S ribosomal protein L34	6.87	1.61	1.48	1.55	0.00	0.00
Tt	down	60S ribosomal protein L23a;	6.68	1.58	1.29	1.20	0.00	0.00
Tt	down	60S ribosomal protein L23	6.68	1.60	1.29	1.33	0.00	0.00
Tt	down	60S ribosomal protein L37	6.07	1.45	0.82	0.28	0.00	0.00
Tt	down	Tubulin beta-3 chain	6.90	1.47	1.50	1.16	0.00	0.00
Tt	down	Tubulin beta chain	3.75	0.77	3.03	2.08	0.22	0.12
Tt	down	Tubulin alpha chain	7.42	1.55	2.16	1.74	0.00	0.00
Tt	down	Tubulin beta chain	6.42	1.36	1.08	0.46	0.00	0.00

Supplementary table 4: Differential gene expression – continued

Sampling time	Regulation low-pH group	Gene name	log2 fold change	SE	Mean Control	SD Control	Mean low-pH	SD low-pH
Tt	down	Tubulin alpha chain	6.61	1.34	1.22	0.60	0.00	0.00
Tt	down	Tubulin alpha chain, nucleomorph	6.93	1.42	9.04	10.12	0.07	0.15
Tt	down	Tubulin beta-4 chain	7.26	1.44	1.96	1.65	0.00	0.00
Tt	down	Tubulin beta chain	5.17	1.03	5.10	3.43	0.16	0.18
Tt	down	Tubulin alpha chain	5.94	1.15	3.17	2.66	0.05	0.06
Tt	down	Tubulin beta chain	6.71	1.30	9.73	9.74	0.10	0.11
Tt	down	Tubulin beta chain	6.71	1.30	9.73	9.74	0.10	0.11
Tt	down	Tubulin alpha chain	5.77	1.10	10.80	13.20	0.19	0.20
Tt	down	Tubulin alpha-1 chain	5.77	1.10	10.80	13.20	0.19	0.20
Tt	down	Tubulin beta chain	7.66	1.43	7.31	9.62	0.04	0.08
Tt	down	Tubulin alpha chain	7.69	1.24	11.15	11.45	0.06	0.11
Tt	down	Tubulin beta chain	23.43	3.38	6.61	10.26	0.00	0.00
Tt	down	Tubulin alpha-1 chain	22.46	3.24	7.58	11.85	0.00	0.00
Tt	down	Tubulin beta-1 chain	23.43	3.38	6.58	11.73	0.00	0.00
Tt	down	Tubulin beta chain	23.41	3.38	6.46	10.75	0.00	0.00
Tt	down	Tubulin beta chain	23.24	3.38	5.71	8.65	0.00	0.00
Tt	down	Tubulin alpha-2 chain	23.18	3.38	5.46	7.79	0.00	0.00
Tt	down	Tubulin beta-5 chain	24.30	3.38	12.53	22.38	0.00	0.00
Tt	down	Tubulin beta chain	24.19	3.38	11.53	19.54	0.00	0.00
Tt	down	Tubulin alpha-1 chain	22.01	2.67	2.39	3.61	0.00	0.00
Tt	down	Tubulin alpha chain	22.43	2.62	3.14	4.39	0.00	0.00
Tt	down	Tubulin beta-4B chain	22.05	2.18	3.72	5.61	0.00	0.00
Tt	down	Tubulin alpha-2 chain	22.74	2.12	3.97	5.20	0.00	0.00
Tt	down	Tubulin alpha-1 chain	22.64	2.08	3.71	5.96	0.00	0.00
Tt	down	Tubulin beta chain	22.71	2.05	3.87	4.96	0.00	0.00
Tt	down	Tubulin beta-3 chain	22.33	2.02	3.46	4.55	0.00	0.00
Tt	down	Tubulin beta-2 chain	20.82	1.87	2.44	3.02	0.00	0.00
Tt	down	Tubulin beta chain	22.55	2.02	3.44	4.76	0.00	0.00
Tt	down	Tubulin beta chain	22.92	1.95	4.49	5.01	0.00	0.00
Tt	down	Tubulin alpha chain	22.90	1.96	4.43	4.81	0.00	0.00
Tt	down	Tubulin beta chain	25.44	2.19	28.77	39.89	0.00	0.00
Tt	down	Tubulin beta chain	25.71	2.22	34.90	49.88	0.00	0.00
Tt	down	Tubulin beta-2 chain	22.01	1.90	2.29	1.96	0.00	0.00
Tt	down	Tubulin alpha chain	22.47	1.94	3.40	3.37	0.00	0.00
Tt	down	Tubulin alpha-3 chain;	22.32	1.94	2.95	3.09	0.00	0.00
Tt	down	Tubulin alpha-2 chain	22.27	1.94	2.77	2.89	0.00	0.00
Tt	down	Tubulin beta-1 chain	22.76	1.99	4.03	4.50	0.00	0.00
Tt	down	Tubulin alpha chain	24.26	1.80	12.11	19.97	0.00	0.00
Tt	down	Tubulin beta chain	23.22	1.72	5.62	8.04	0.00	0.00
Tt	down	Tubulin alpha chain	22.08	1.64	2.54	3.24	0.00	0.00
Tt	down	Tubulin alpha-3 chain	22.54	1.68	5.96	8.10	0.00	0.00
Tt	down	Tubulin alpha-2 chain	22.39	1.26	2.99	1.58	0.00	0.00
Tt	down	Tubulin beta chain;	21.25	1.29	2.63	1.78	0.00	0.00
Tt	down	Tubulin beta-4 chain	22.54	1.44	4.21	4.13	0.00	0.00
Tt	down	Tubulin alpha-2 chain	22.60	1.45	3.57	3.97	0.00	0.00
Tt	down	Tubulin beta chain	24.21	1.63	19.76	27.01	0.00	0.00
Tt	down	Tubulin beta-3 chain	21.52	1.45	3.18	3.65	0.00	0.00
Tt	down	Tubulin beta chain	24.21	1.65	14.54	22.04	0.00	0.00
Tt	down	Tubulin beta chain	23.32	1.61	6.09	6.22	0.00	0.00
Tt	down	Tubulin alpha-4 chain	21.17	1.47	2.87	3.07	0.00	0.00
Tt	down	Tubulin beta chain	24.07	1.70	10.49	15.13	0.00	0.00
Tt	down	Tubulin beta-5 chain	24.07	1.72	10.62	16.21	0.00	0.00
Tt	down	Tubulin alpha-1 chain	22.73	1.68	4.30	5.22	0.00	0.00
Tt	down	Tubulin alpha-2 chain	22.60	1.89	3.60	3.18	0.00	0.00
Tt	down	Tubulin beta chain	23.15	2.03	5.34	6.96	0.00	0.00
Tt	down	Tubulin beta chain	25.23	2.22	24.66	34.55	0.00	0.00
Tt	down	Tubulin alpha-3 chain	22.44	2.01	3.20	3.52	0.00	0.00
Tt	down	Tubulin beta-2 chain	22.49	2.10	3.29	4.77	0.00	0.00
Tt	down	Tubulin alpha-2 chain	22.13	2.07	2.52	3.77	0.00	0.00
Tt	down	Tubulin beta chain	21.64	2.03	2.25	2.73	0.00	0.00
Tt	down	Tubulin beta chain	21.99	2.07	2.63	3.89	0.00	0.00
Tt	down	Tubulin beta chain	22.09	2.08	2.46	3.57	0.00	0.00
Tt	down	Tubulin alpha chain	22.11	2.13	2.49	3.53	0.00	0.00
Tt	down	Tubulin beta chain	21.98	2.26	2.28	3.51	0.00	0.00
Tt	down	Tubulin beta chain	22.29	2.63	2.96	4.17	0.00	0.00
Tt	down	Tubulin alpha chain	22.26	2.64	2.76	3.93	0.00	0.00

Supplementary table 4: Differential gene expression – continued

Sampling time	Regulation low-pH group	Gene name	log2 fold change	SE	Mean Control	SD Control	Mean low-pH	SD low-pH
Tt	down	Tubulin alpha chain	22.28	2.67	2.98	4.92	0.00	0.00
Tt	down	Tubulin beta-4 chain	24.25	2.91	11.94	13.33	0.00	0.00
Tt	down	Tubulin beta chain	22.20	2.66	2.64	4.13	0.00	0.00
Tt	down	Tubulin beta-4B chain	22.09	2.65	2.44	3.37	0.00	0.00
Tt	down	Tubulin beta-2 chain	22.42	2.69	3.21	5.70	0.00	0.00
Tt	down	Tubulin alpha-2 chain	21.97	2.64	2.23	2.58	0.00	0.00
Tt	down	Tubulin beta chain	22.03	2.69	2.42	4.02	0.00	0.00
Tt	down	Tubulin alpha chain	24.16	3.00	11.65	15.56	0.00	0.00
Tt	down	Tubulin beta chain	24.05	3.05	10.39	15.17	0.00	0.00
Tt	down	Tubulin alpha-2 chain	25.57	3.29	31.55	47.32	0.00	0.00
Tt	down	Tubulin alpha chain	23.50	3.05	6.91	10.12	0.00	0.00
Tt	down	Tubulin alpha chain	24.09	3.15	10.69	17.64	0.00	0.00
Tt	down	Tubulin beta-4B chain	23.14	3.09	5.34	8.15	0.00	0.00
Tt	down	Tubulin alpha-1 chain	23.31	3.15	6.00	8.30	0.00	0.00
Tt	down	Tubulin beta-2 chain	22.22	3.09	5.80	8.24	0.00	0.00
Tt	down	Tubulin beta-2 chain	23.99	3.38	9.97	17.19	0.00	0.00
Tt	down	Tubulin alpha chain	23.92	3.38	9.87	11.80	0.00	0.00
Tt	down	Tubulin alpha-5 chain	23.87	3.38	9.14	15.93	0.00	0.00
Tt	down	Tubulin alpha-1 chain	23.87	3.38	9.11	16.00	0.00	0.00
Tt	down	Tubulin beta chain	23.52	3.38	8.19	13.69	0.00	0.00
Tt	down	Tubulin alpha chain	23.04	3.38	4.96	7.95	0.00	0.00
Tt	down	Tubulin beta-1 chain	22.97	3.38	4.69	7.84	0.00	0.00
Tt	down	Tubulin alpha chain	22.64	3.38	3.69	5.53	0.00	0.00
Tt	down	Tubulin beta chain	22.80	3.38	4.14	7.24	0.00	0.00
Tt	down	Tubulin alpha chain	22.78	3.38	8.39	14.41	0.00	0.00
Tt	down	Tubulin alpha-2 chain	22.50	3.39	3.30	5.69	0.00	0.00
Tt	down	Tubulin beta chain	22.48	3.39	3.28	5.45	0.00	0.00
Tt	down	Tubulin beta chain	6.22	1.34	0.92	0.22	0.00	0.00
Tt	down	Tubulin alpha chain	7.12	1.53	1.74	1.51	0.00	0.00
Tt	down	Tubulin beta chain	6.85	1.48	1.48	1.12	0.00	0.00
Tt	down	Tubulin alpha-2 chain	7.41	1.65	2.17	3.01	0.00	0.00
Tt	down	Tubulin beta chain	6.97	1.56	1.59	1.18	0.00	0.00
Tt	down	Tubulin beta-4B chain;	7.46	1.67	2.23	2.66	0.00	0.00
Tt	down	Tubulin beta chain	4.76	1.10	2.37	1.74	0.09	0.11
Tt	down	Tubulin beta-5 chain	6.57	1.50	1.21	0.86	0.00	0.00
Tt	down	Tubulin alpha chain	6.26	1.49	2.78	1.97	0.05	0.09
Tt	down	Tubulin alpha chain	6.61	1.58	1.24	1.25	0.00	0.00
Tt	down	Tubulin alpha chain	6.93	1.65	1.55	1.63	0.00	0.00
Tt	down	Actin	8.06	1.46	4.72	5.80	0.03	0.06
Tt	down	Actin-11	22.48	3.39	3.29	5.56	0.00	0.00
Tt	down	Actin-1	22.62	3.38	3.59	6.43	0.00	0.00
Tt	down	Actin-1	22.92	3.38	4.53	6.95	0.00	0.00
Tt	down	Actin	23.22	3.38	5.66	9.77	0.00	0.00
Tt	down	Actin	23.11	3.38	5.22	8.93	0.00	0.00
Tt	down	Actin, non-muscle 6 2	23.48	3.38	6.74	11.99	0.00	0.00
Tt	down	Actin-1/4	23.53	3.08	7.04	11.35	0.00	0.00
Tt	down	Actin-52	23.02	3.01	4.91	7.07	0.00	0.00
Tt	down	Actin, alpha skeletal muscle	22.10	2.67	2.46	3.89	0.00	0.00
Tt	down	Actin	22.16	2.67	2.57	4.07	0.00	0.00
Tt	down	Actin	22.28	2.68	2.96	5.03	0.00	0.00
Tt	down	Actin, muscle	22.22	2.64	2.81	4.21	0.00	0.00
Tt	down	Actin, alpha skeletal muscle	20.38	2.18	3.40	5.63	0.00	0.00
Tt	down	Actin	22.03	2.16	2.34	3.11	0.00	0.00
Tt	down	Actin, alpha skeletal muscle	22.36	2.15	3.00	3.98	0.00	0.00
Tt	down	Actin	23.12	1.92	5.32	5.97	0.00	0.00
Tt	down	Actin-1	22.32	1.77	2.84	3.58	0.00	0.00
Tt	down	Actin-2	22.43	1.65	3.15	4.43	0.00	0.00
Tt	down	Actin-10	24.12	1.68	12.66	18.17	0.00	0.00
Tt	down	Actin, alpha skeletal muscle	24.34	1.66	12.83	19.41	0.00	0.00
Tt	down	Actin, muscle	24.07	1.62	11.02	14.37	0.00	0.00
Tt	down	Actin, muscle	23.03	1.47	4.89	3.83	0.00	0.00
Tt	down	Actin	22.29	1.10	4.62	0.75	0.00	0.00
Tt	down	Actin-1	22.20	1.12	5.29	1.63	0.00	0.00
Tt	down	Actin-3	23.10	1.22	5.10	2.79	0.00	0.00
Tt	down	Actin-85C	22.41	1.97	3.10	3.63	0.00	0.00
Tt	down	Actin, muscle-type	25.05	2.29	21.49	28.73	0.00	0.00

Supplementary table 4: Differential gene expression – continued

Sampling time	Regulation low-pH group	Gene name	log2 fold change	SE	Mean Control	SD Control	Mean low-pH	SD low-pH
Tt	down	Actin-5C	21.65	2.00	2.25	2.75	0.00	0.00
Tt	down	Actin-5, muscle-specific	22.52	2.10	3.37	4.71	0.00	0.00
Tt	down	Actin, muscle-type A2	22.49	2.15	3.26	4.32	0.00	0.00
Tt	down	Actin, muscle	22.24	2.13	2.74	4.31	0.00	0.00
Tt	down	Actin-1	21.63	2.11	3.37	4.32	0.00	0.00
Tt	down	Actin, alpha skeletal muscle	22.29	2.20	2.76	4.20	0.00	0.00
Tt	down	Actin-1	21.11	2.14	3.59	5.42	0.00	0.00
Tt	down	Actin, larval muscle	23.44	2.73	6.81	6.67	0.00	0.00
Tt	down	Actin, cytoplasmic	22.24	2.62	2.88	3.40	0.00	0.00
Tt	down	Actin, alpha skeletal muscle	22.05	2.69	2.46	4.02	0.00	0.00
Tt	down	Actin-1	21.79	2.70	2.80	4.91	0.00	0.00
Tt	down	Actin-1	23.32	2.91	6.04	8.73	0.00	0.00
Tt	down	Actin	24.30	3.12	12.54	20.16	0.00	0.00
Tt	down	Actin-2	22.15	2.85	5.91	7.70	0.00	0.00
Tt	down	Actin-66	24.19	3.22	11.46	16.52	0.00	0.00
Tt	down	Actin, non-muscle 6 2	24.77	3.34	17.66	25.85	0.00	0.00
Tt	down	Actin	23.29	3.18	6.09	8.59	0.00	0.00
Tt	down	Actin, non-muscle 6 2	24.65	3.38	16.12	23.16	0.00	0.00
Tt	down	Actin-1/2	23.69	3.29	25.11	40.74	0.00	0.00
Tt	down	Actin CyI, cytoplasmic	23.02	3.27	15.00	22.57	0.00	0.00
Tt	down	Actin-66	23.56	3.38	7.26	11.21	0.00	0.00
Tt	down	Actin	8.27	1.21	5.30	3.64	0.03	0.05
Tt	down	Actin CyI, cytoplasmic	22.73	3.38	3.93	6.56	0.00	0.00
Tt	down	Actin-85C	22.65	3.38	3.70	5.09	0.00	0.00
Tt	down	Actin CyI, cytoplasmic	22.81	3.38	4.17	6.08	0.00	0.00
Tt	down	Actin-11	7.20	1.38	1.86	1.30	0.00	0.00
Tt	down	Actin, non-muscle 6 2	6.29	1.24	1.62	0.71	0.02	0.05
Tt	down	Actin	7.21	1.42	1.86	1.59	0.00	0.00
Tt	down	Actin, plasmodial.isoform	6.78	1.34	1.39	0.70	0.00	0.00
Tt	down	Actin, nonmuscle	7.00	1.55	1.61	1.51	0.00	0.00
Tt	down	Actin	6.35	1.46	1.04	0.48	0.00	0.00
Tt	down	Actin, cytoskeletal 1A	5.64	1.30	19.19	27.44	0.40	0.48
Tt	down	Actin	5.78	1.39	8.32	6.54	0.16	0.32
Tt	down	Polyubiquitin	5.32	1.19	2.14	1.36	0.06	0.13
Tt	down	Ubiquitin	6.46	1.45	1.13	0.70	0.00	0.00
Tt	down	Polyubiquitin	5.11	1.15	3.16	1.79	0.10	0.20
Tt	down	Ubiquitin	6.27	1.49	1.01	0.54	0.00	0.00
Tt	down	Ubiquitin	7.17	1.48	1.83	1.50	0.00	0.00
Tt	down	Ubiquitin-40S ribosomal protein S27a	5.64	1.20	1.73	0.62	0.04	0.07
Tt	down	Polyubiquitin	7.43	1.51	2.19	2.58	0.00	0.00
Tt	down	Polyubiquitin-B	6.97	1.30	1.59	0.79	0.00	0.00
Tt	down	Polyubiquitin	4.84	0.89	2.49	0.60	0.11	0.16
Tt	down	Polyubiquitin	7.64	1.23	3.40	1.79	0.02	0.04
Tt	down	Polyubiquitin	23.07	3.38	5.06	7.50	0.00	0.00
Tt	down	Ubiquitin-60S ribosomal protein L40	23.49	3.05	6.89	10.72	0.00	0.00
Tt	down	Polyubiquitin	23.34	1.29	6.12	4.33	0.00	0.00
Tt	down	Polyubiquitin	23.89	1.40	9.14	8.85	0.00	0.00
Tt	down	Polyubiquitin	22.80	1.35	4.13	3.09	0.00	0.00
Tt	down	Ubiquitin-40S ribosomal protein S27a	22.90	1.46	4.39	3.29	0.00	0.00
Tt	down	Polyubiquitin-B	22.69	1.48	4.14	3.26	0.00	0.00
Tt	down	Polyubiquitin	24.97	1.64	20.82	29.15	0.00	0.00
Tt	down	Polyubiquitin	23.62	1.64	7.65	10.31	0.00	0.00
Tt	down	Polyubiquitin	23.40	1.69	6.45	8.11	0.00	0.00
Tt	down	Polyubiquitin	23.22	1.89	5.63	8.69	0.00	0.00
Tt	down	Ubiquitin	22.88	2.00	4.37	5.76	0.00	0.00
Tt	down	Polyubiquitin;	22.05	1.94	2.36	2.63	0.00	0.00
Tt	down	Polyubiquitin	22.48	2.01	3.28	4.59	0.00	0.00
Tt	down	Polyubiquitin	22.44	2.01	3.16	3.68	0.00	0.00
Tt	down	Polyubiquitin	22.65	2.03	3.68	4.79	0.00	0.00
Tt	down	Polyubiquitin	22.49	2.02	3.27	3.74	0.00	0.00
Tt	down	Polyubiquitin	22.83	2.11	4.25	6.19	0.00	0.00
Tt	down	Polyubiquitin	22.28	2.09	3.44	4.37	0.00	0.00
Tt	down	Polyubiquitin	22.38	2.16	3.05	4.17	0.00	0.00
Tt	down	Polyubiquitin	21.57	2.09	2.65	2.91	0.00	0.00
Tt	down	Polyubiquitin	20.43	1.99	2.76	3.25	0.00	0.00
Tt	down	Polyubiquitin-B	22.24	2.20	2.72	4.32	0.00	0.00

Supplementary table 4: Differential gene expression – continued

Sampling time	Regulation low-pH group	Gene name	log2 fold change	SE	Mean Control	SD Control	Mean low-pH	SD low-pH
Tt	down	Ubiquitin	22.43	2.61	3.17	3.69	0.00	0.00
Tt	down	Ubiquitin	22.26	2.66	2.86	4.48	0.00	0.00
Tt	down	Ubiquitin-60S ribosomal protein L40	22.01	2.68	2.29	3.51	0.00	0.00
Tt	down	Polyubiquitin-B	22.02	2.69	2.29	3.67	0.00	0.00
Tt	down	Polyubiquitin	23.93	3.04	9.48	11.96	0.00	0.00
Tt	down	Polyubiquitin	23.12	2.95	5.22	7.04	0.00	0.00
Tt	down	Polyubiquitin	23.99	3.16	9.92	12.91	0.00	0.00
Tt	down	Polyubiquitin	23.92	3.38	9.44	13.18	0.00	0.00
Tt	down	Polyubiquitin	22.96	3.38	4.64	7.49	0.00	0.00
Tt	down	Polyubiquitin-B	22.93	3.38	4.59	7.17	0.00	0.00
Tt	down	Polyubiquitin	22.83	3.38	4.21	6.67	0.00	0.00
Tt	down	Ubiquitin-60S ribosomal protein L40	22.54	3.39	3.42	6.05	0.00	0.00
Tt	down	Elongation factor 1-alpha	6.58	1.53	1.20	1.00	0.00	0.00
Tt	down	Elongation factor 1-alpha	6.75	1.54	1.37	1.34	0.00	0.00
Tt	down	Elongation factor 1-	6.73	1.46	1.33	0.96	0.00	0.00
Tt	down	Elongation factor 1-alpha	6.70	1.33	1.32	0.74	0.00	0.00
Tt	down	Elongation factor 1-alpha	6.79	1.29	1.39	0.59	0.00	0.00
Tt	down	Elongation factor 1-alpha	24.34	3.38	12.85	16.42	0.00	0.00
Tt	down	Elongation factor 1-alpha	23.76	3.08	8.40	12.90	0.00	0.00
Tt	down	Elongation factor 2	22.06	1.82	2.38	3.19	0.00	0.00
Tt	down	Elongation factor 1-alpha	22.39	1.22	3.04	1.47	0.00	0.00
Tt	down	Elongation factor 1-alpha 1	23.48	1.48	6.80	6.26	0.00	0.00
Tt	down	Elongation factor 1-alpha 2	22.33	1.49	3.18	3.29	0.00	0.00
Tt	down	Elongation factor 1-alpha;	22.17	1.68	2.72	3.84	0.00	0.00
Tt	down	Elongation factor 1-alpha	22.91	2.08	4.50	6.17	0.00	0.00
Tt	down	Elongation factor 1-alpha	22.13	2.02	2.53	3.45	0.00	0.00
Tt	down	Elongation factor 1-alpha	22.43	2.64	3.10	4.58	0.00	0.00
Tt	down	Elongation factor 1-alpha	22.07	2.66	2.39	3.45	0.00	0.00
Tt	down	Elongation factor 1-alpha, somatic form	22.20	2.70	2.68	4.66	0.00	0.00
Tt	down	Cytochrome c oxidase subunit 1	22.60	1.71	3.62	4.82	0.01	0.02
Tt	down	Cytochrome c oxidase subunit 2	22.45	1.19	3.18	1.45	0.00	0.00
Tt	down	Cytochrome c oxidase subunit 3	21.70	1.27	2.90	1.82	0.00	0.00
Tt	down	Cytochrome c oxidase subunit 2	24.22	1.54	12.28	18.37	0.00	0.00
Tt	down	Cytochrome c oxidase subunit 1	24.26	1.56	12.03	18.31	0.00	0.00
Tt	down	Cytochrome c oxidase subunit 3	22.82	1.58	4.66	6.56	0.00	0.00
Tt	down	Cytochrome c oxidase subunit 3	22.77	1.68	4.03	6.13	0.00	0.00
Tt	down	Cytochrome c oxidase subunit 2	22.61	1.78	3.62	4.99	0.00	0.00
Tt	down	Cytochrome b	22.02	1.76	2.33	2.98	0.00	0.00
Tt	down	Cytochrome b	22.24	1.80	2.82	3.77	0.00	0.00
Tt	down	Cytochrome c oxidase subunit 2	22.33	2.03	3.64	5.25	0.00	0.00
Tt	down	Cytochrome c oxidase subunit 1	22.22	2.10	2.68	4.29	0.00	0.00
Tt	down	Cytochrome c oxidase subunit 1	22.72	2.17	3.84	6.48	0.00	0.00
Tt	down	Cytochrome c oxidase subunit 2	21.97	2.23	2.24	2.85	0.00	0.00
Tt	down	Cytochrome c oxidase subunit 1	7.68	1.17	3.52	1.51	0.03	0.06
Tt	down	Cytochrome c oxidase subunit 3	6.84	1.16	6.15	4.89	0.06	0.08
Tt	down	Cytochrome b	7.42	1.36	2.17	1.66	0.00	0.00
Tt	down	Cytochrome b	7.43	1.39	2.19	1.51	0.00	0.00
Tt	down	Cytochrome c oxidase subunit 1	7.17	1.37	5.14	4.23	0.06	0.09
Tt	down	Cytochrome b	5.04	0.99	4.85	3.10	0.15	0.19
Tt	down	Cytochrome c oxidase subunit 3	5.84	1.21	4.20	3.63	0.06	0.09
Tt	down	Cytochrome c oxidase subunit 2	5.63	1.18	2.67	1.37	0.05	0.10
Tt	down	Cytochrome b	7.06	1.48	1.71	1.43	0.00	0.00
Tt	down	Cytochrome c	6.44	1.41	1.12	0.60	0.00	0.00
Tt	down	Cytochrome c oxidase subunit 3	5.42	1.21	6.27	7.80	0.15	0.12
Tt	down	Cytochrome c oxidase subunit 2	5.34	1.20	10.50	13.90	0.27	0.32
Tt	down	Cytochrome c oxidase subunit 3	5.91	1.37	2.11	1.96	0.04	0.09
Tt	down	Cytochrome c oxidase subunit 2	4.56	1.08	7.16	4.47	0.32	0.37
Tt	down	Heat shock 70 kDa protein	22.04	2.71	2.37	4.02	0.00	0.00
Tt	down	Heat shock cognate 70 kDa protein	22.99	2.12	4.77	7.00	0.00	0.00
Tt	down	Heat shock 70 kDa protein	21.68	1.40	2.84	1.95	0.00	0.00
Tt	down	Heat shock protein SSA2	22.95	1.80	4.63	6.26	0.00	0.00
Tt	down	Heat shock protein 90	22.32	1.84	3.36	4.40	0.00	0.00
Tt	down	Heat shock 70 kDa protein 12A	4.72	0.44	18.59	8.36	0.72	0.16
Tt	down	Heat shock protein 83;	22.15	2.10	2.55	3.58	0.00	0.00
Tt	down	Heat shock 70 kDa protein C	22.34	2.14	2.93	4.42	0.00	0.00
Tt	down	Heat shock protein SSA3	22.35	2.68	3.14	5.45	0.00	0.00

Supplementary table 4: Differential gene expression – continued

Sampling time	Regulation low-pH group	Gene name	log2 fold change	SE	Mean Control	SD Control	Mean low-pH	SD low-pH
Tt	down	Heat shock 70 kDa protein	23.49	3.01	6.96	9.69	0.00	0.00
Tt	down	Heat shock-related 70 kDa protein 2	23.15	3.04	5.44	8.96	0.00	0.00
Tt	down	Heat shock 70 kDa protein	22.52	3.39	3.36	5.14	0.00	0.00
Tt	down	17 6 kDa class I heat shock protein;	6.90	1.28	1.50	0.66	0.00	0.00
Tt	down	ADP-ribosylation factor 1	7.53	1.28	3.16	2.44	0.03	0.06
Tt	down	ADP-ribosylation factor 1	22.04	2.16	2.35	3.21	0.00	0.00
Tt	down	ATP synthase subunit a	22.13	1.62	2.64	3.44	0.00	0.00
Tt	down	ADP-ribosylation factor	22.23	1.96	2.71	2.96	0.00	0.00
Tt	down	ATP synthase subunit a	22.15	1.99	2.58	3.19	0.00	0.00
Tt	down	ATP synthase subunit beta	22.14	2.10	2.54	3.56	0.00	0.00
Tt	down	ADP-ribosylation factor 1	22.44	2.14	3.18	4.79	0.00	0.00
Tt	down	ATP-dependent RNA helicase eIF4A;	22.48	2.19	3.28	5.05	0.00	0.00
Tt	down	ADP,ATP carrier protein 3, mitochondrial	22.15	2.66	2.57	3.67	0.00	0.00
Tt	down	ATP synthase subunit a	5.86	1.21	4.25	3.17	0.09	0.18
Tt	down	ATP synthase gamma chain, chloroplastic	6.34	1.44	1.04	0.57	0.00	0.00
Tt	down	Transitional endoplasmic reticulum ATPase TER94	6.93	1.63	1.53	1.58	0.00	0.00
Tt	down	Actinidain	22.07	1.52	2.42	2.20	0.00	0.00
Tt	down	Actinidain	20.96	1.91	4.01	3.86	0.00	0.00
Tt	down	Actinidain	21.77	1.85	4.31	3.37	0.00	0.00
Tt	down	Oryzain alpha chain	22.94	1.91	4.54	4.31	0.00	0.00
Tt	down	Oryzain alpha chain	22.73	2.09	3.94	5.61	0.00	0.00
Tt	down	Glyceraldehyde-3-phosphate dehydrogenase, cytosolic	22.29	2.04	3.52	4.81	0.00	0.00
Tt	down	Glyceraldehyde-3-phosphate dehydrogenase 2	22.43	2.11	3.13	4.54	0.00	0.00
Tt	down	Glyceraldehyde-3-phosphate dehydrogenase	22.48	2.15	3.26	4.16	0.00	0.00
Tt	down	Glyceraldehyde-3-phosphate dehydrogenase, chloroplastic	8.16	1.15	9.74	5.54	0.02	0.03
Tt	down	Acyl-CoA-binding protein	21.98	2.16	2.28	2.99	0.00	0.00
Tt	down	Proliferating cell nuclear antigen	22.60	2.28	3.58	6.01	0.00	0.00
Tt	down	Proliferating cell nuclear antigen	22.01	2.24	2.30	3.13	0.00	0.00
Tt	down	Histone H4	22.36	2.62	3.03	4.07	0.00	0.00
Tt	down	Histone H4, major	6.95	1.47	1.55	1.39	0.00	0.00
Tt	down	Histone H4, minor	6.95	1.47	1.55	1.39	0.00	0.00
Tt	down	Digestive cysteine proteinase 1	23.42	2.77	6.49	6.93	0.00	0.00
Tt	down	Digestive cysteine proteinase 1	22.29	1.77	8.07	11.23	0.00	0.00
Tt	down	NADH-ubiquinone oxidoreductase chain 4	5.57	1.07	2.51	0.97	0.05	0.11
Tt	down	NADH-ubiquinone oxidoreductase chain 5	4.13	0.82	2.82	1.44	0.16	0.13
Tt	down	NADH-ubiquinone oxidoreductase chain 2	4.67	0.88	3.67	2.15	0.17	0.12
Tt	down	NADH-ubiquinone oxidoreductase chain 3	6.51	0.99	6.45	2.82	0.08	0.15
Tt	down	NADH-ubiquinone oxidoreductase chain 1	5.07	0.89	3.63	1.03	0.11	0.18
Tt	down	NADH-ubiquinone oxidoreductase chain 4	4.55	0.93	2.52	1.63	0.10	0.11
Tt	down	NADH-ubiquinone oxidoreductase chain 2	5.66	1.21	1.74	0.74	0.03	0.07
Tt	down	NADH-ubiquinone oxidoreductase chain 1	4.51	0.97	3.81	1.61	0.18	0.26
Tt	down	NADH-ubiquinone oxidoreductase chain 5	4.28	0.96	2.09	0.94	0.12	0.15
Tt	down	NADH-ubiquinone oxidoreductase chain 4	5.13	1.21	6.54	8.15	0.17	0.24
Tt	down	NADH-ubiquinone oxidoreductase chain 1	6.14	1.46	1.46	1.23	0.02	0.04
Tt	down	Ras-related C3 botulinum toxin substrate 1	22.31	1.71	2.89	3.72	0.00	0.00
Tt	down	Ras-related protein Rab-8A	22.12	2.08	2.53	3.53	0.00	0.00
Tt	down	Fucoxanthin-chlorophyll a-c binding protein, chloroplastic	21.58	1.20	3.55	1.47	0.00	0.00
Tt	down	Procathepsin L	22.55	1.29	3.40	2.34	0.00	0.00
Tt	down	Protein Fe65 homolo	22.89	1.36	4.44	4.41	0.00	0.00
Tt	down	Alanine--glyoxylate aminotransferase 2, mitochondrial	22.75	1.48	4.01	3.35	0.00	0.00
Tt	down	Cell division cycle protein 48 homolog	21.76	1.64	2.48	3.14	0.00	0.00
Tt	down	Zinc metalloproteinase nas-6	22.13	2.72	2.52	4.41	0.00	0.00
Tt	down	Putative uncharacterized protein ART2	22.25	1.76	2.69	3.24	0.00	0.00
Tt	down	Ribulose bisphosphate carboxylase small subunit, chloroplastic 4	22.08	1.94	2.40	2.33	0.00	0.00
Tt	down	CBL-interacting serine/threonine-protein kinase 6	21.62	1.91	2.28	3.46	0.00	0.00
Tt	down	Kielin/chordin-like protein	21.57	1.96	4.66	5.36	0.00	0.00
Tt	down	Glycine-rich protein 2	22.76	2.09	4.01	5.04	0.00	0.00
Tt	down	Adenosylhomocysteinase 1	22.39	2.09	3.04	4.07	0.00	0.00
Tt	down	S-phase kinase-associated protein 1 homolog	22.51	2.13	3.33	4.83	0.00	0.00
Tt	down	Ervatamin-B	22.53	2.15	3.39	5.60	0.00	0.00

Supplementary table 4: Differential gene expression – continued

Sampling time	Regulation low-pH group	Gene name	log2 fold change	SE	Mean Control	SD Control	Mean low-pH	SD low-pH
Tt	down	Putative NADP-dependent oxidoreductase YfmJ	22.28	2.14	2.85	4.17	0.00	0.00
Tt	down	ENTH domain-containing protein C794 11c	22.23	2.14	4.28	6.81	0.00	0.00
Tt	down	DNA-directed RNA polymerase III subunit RPC2	22.22	2.14	2.64	3.48	0.00	0.00
Tt	down	Cofilin	22.65	2.19	3.70	5.78	0.00	0.00
Tt	down	Putative actin-23	21.89	2.12	2.36	3.08	0.00	0.00
Tt	down	Peptidyl-prolyl cis-trans isomerase A2	22.26	2.17	2.78	4.00	0.00	0.00
Tt	down	Protein disulfide-isomerase	22.05	2.17	2.36	3.40	0.00	0.00
Tt	down	Eukaryotic translation elongation factor 2	21.87	2.16	2.65	3.61	0.00	0.00
Tt	down	Ribonucleoside-diphosphate reductase small chain	22.13	2.19	2.57	3.98	0.00	0.00
Tt	down	Endoplasmic reticulum chaperone BiP	22.16	2.65	2.58	3.78	0.00	0.00
Tt	down	Glycine-rich RNA-binding protein 4, mitochondrial;	22.24	2.67	2.85	4.68	0.00	0.00
Tt	down	Procathepsin L	22.00	2.66	2.23	2.67	0.00	0.00
Tt	down	Thioredoxin H-type	22.04	2.67	2.44	3.73	0.00	0.00
Tt	down	Cysteine and glycine-rich protein 1	21.59	2.64	2.48	2.88	0.00	0.00
Tt	down	Heparan sulfate glucosamine 3-O-sulfotransferase 2	22.07	2.71	2.44	4.11	0.00	0.00
Tt	down	Phosphoglycerate kinase, chloroplastic	7.67	0.97	10.50	4.28	0.05	0.07
Tt	down	Probable UDP-sugar transporter protein SLC35A4	2.03	0.27	10.83	1.57	2.67	0.62
Tt	down	Phosphatidylserine decarboxylase proenzyme	23.01	3.38	4.82	8.40	0.00	0.00
Tt	down	Putative actin-22	24.05	3.38	10.39	17.64	0.00	0.00
Tt	down	Inositol polyphosphate-4-phosphatase type I A	23.98	3.38	9.77	11.78	0.00	0.00
Tt	down	Uncharacterized protein ORF91	6.14	0.90	17.32	18.76	0.26	0.09
Tt	down	Soma ferritin	22.91	3.38	4.41	6.28	0.00	0.00
Tt	down	Peroxinectin A	22.54	3.39	3.43	5.91	0.00	0.00
Tt	down	Pancreatic secretory granule membrane major glycoprotein GP2	3.85	0.66	3.77	1.26	0.27	0.22
Tt	down	Transketolase	6.69	1.12	3.50	1.32	0.03	0.03
Tt	down	Fructose-bisphosphate aldolase	5.71	1.00	4.75	1.61	0.09	0.19
Tt	down	Cofili	6.68	1.22	1.31	0.16	0.00	0.00
Tt	down	Nucleoside diphosphate kinase B	7.07	1.31	1.70	0.91	0.00	0.00
Tt	down	Acyl carrier protein	6.86	1.28	1.45	0.57	0.00	0.00
Tt	down	Uncharacterized protein ORF91	6.84	1.28	1.45	0.60	0.00	0.00
Tt	down	Urocanate hydratase	2.03	0.39	9.84	2.88	2.46	0.87
Tt	down	Probable germin-like protein subfamily 2 member 5	6.66	1.32	1.27	0.58	0.00	0.00
Tt	down	Dephospho-CoA kinase domain-containing protein	5.90	1.17	28.49	32.08	0.48	0.20
Tt	down	Upstream activation factor subunit UAF30	6.52	1.30	1.16	0.44	0.00	0.00
Tt	down	Uncharacterized protein ORF91	5.43	1.08	15.01	15.52	0.36	0.48
Tt	down	Fucoxanthin-chlorophyll a-c binding protein E, chloroplastic	6.75	1.36	1.37	0.78	0.00	0.00
Tt	down	Protein TAR1	6.14	1.26	1.47	0.64	0.02	0.05
Tt	down	Putative uncharacterized protein ART2	5.60	1.18	2.61	1.90	0.06	0.11
Tt	down	Insoluble matrix shell protein 1	3.01	0.64	46.69	32.88	5.91	4.08
Tt	down	Delta(12)-fatty-acid desaturase FAD2	6.35	1.36	1.04	0.42	0.00	0.00
Tt	down	Light-harvesting complex stress-related protein 1, chloroplastic	6.32	1.37	1.00	0.36	0.00	0.00
Tt	down	Insoluble matrix shell protein 1	2.46	0.54	37.18	22.46	6.93	3.29
Tt	down	Putative uncharacterized protein ART2	4.28	0.94	7.77	7.27	0.41	0.37
Tt	down	Fucoxanthin-chlorophyll a-c binding protein, chloroplastic	6.49	1.42	1.13	0.72	0.00	0.00
Tt	down	Nucleoside diphosphate kinase B	6.51	1.45	1.15	0.75	0.00	0.00
Tt	down	Trichocyst matrix protein T4-A	6.42	1.45	1.09	0.65	0.00	0.00
Tt	down	Protein mono-ADP-ribosyltransferase PARP15	6.44	1.46	1.09	0.58	0.00	0.00
Tt	down	RNA-binding protein with serine-rich domain 1-A	7.24	1.64	1.93	1.89	0.00	0.00
Tt	down	Fucoxanthin-chlorophyll a-c binding protein, chloroplastic	6.33	1.44	1.03	0.50	0.00	0.00
Tt	down	Fructose-bisphosphate aldolase	6.08	1.39	1.41	1.02	0.03	0.05
Tt	down	Stearoyl-CoA desaturase 5	6.37	1.46	1.06	0.50	0.00	0.00
Tt	down	Protein disulfide-isomerase-like protein EhSep2	6.46	1.50	1.11	0.80	0.00	0.00
Tt	down	Viral protein 1	5.10	1.21	1.16	0.43	0.05	0.05

8. Acknowledgements

9. Declarations

Name: Sarina Niedzwiedz   **Enrolment number:** 4348984

Declaration of copyright

Hereby I declare that my Master's Thesis was written without external support and that I did not use any other sources and auxiliary means than those quoted. All statements which are literally or analogously taken from other publications have been identified as quotations.

Date   Signature

Declaration with regard to publishing theses

Two years after the final degree, the thesis will be submitted to the University of Bremen archive and stored there permanently. Storage includes:

1) Master's Theses with a local or regional reference, as well as 10 % of all theses from every subject and year

2) Bachelor's Theses: The first and last Bachelor degrees from every subject and year

☐ I agree that for research purposes third parties can look into my thesis stored in the University archive.

☐ I agree that for research purposes third parties can look into my thesis stored in the University archive after a period of 30 years (in line with §7 para. 2 BremArchivG).

☐ I do not agree that for research purposes third parties can look into my thesis stored in the University archive.

Date   Signature